Title
Performance Limitations of Linear Systems over Additive White Noise Channels

Author
Li, Yiqian

Publication Date
2011

Peer reviewed|Thesis/dissertation

UNIVERSITY OF CALIFORNIA
RIVERSIDE

Performance Limitations of Linear Systems over Additive White Noise Channels

A Dissertation submitted in partial satisfaction
of the requirements for the degree of

Doctor of Philosophy

in

Electrical Engineering

by

Yiqian Li

June 2011

Dissertation Committee:

Dr. Jie Chen, Co-Chairperson
Dr. Ertem Tuncel, Co-Chairperson
Dr. Jay A. Farrell
Dr. Anastasios I. Mourikis

The Dissertation of Yiqian Li is approved:

Committee Chairperson

University of California, Riverside

Acknowledgments

Mere words are not enough to express my gratitude to my two advisors. Prof. Jie Chen gave me the opportunity to pursue my PhD degree, showed me the way and led me to the area of networked control. You guided me not only in every aspect of my studies and research, but also in my daily life as an international student, helped me grow up with your continued support, and enlightened me in this critical stage of my life. Prof. Ertem Tuncel, who is always willing to listen and extremely patient, introduced me to the broad and illuminating information theory. You gave me elegant suggestions about the methodology and numerous innovative ideas of my research. Also, your lectures are great models from which I gained principles and understanding of teaching. It benefited me greatly when I was a teaching assistant.

My hearty thanks also go to Prof. Farrell and Prof. Mourikis for taking time to review the thesis and for being on the committee.

I had the chance to collaborate with Prof. Weizhou Su (South China University of Technology), whose interest on my work and insightful suggestions I am grateful to. I would also like to thank Dr. Qi Tian for the academic discussions, and for encouraging me by her consistently positive altitude.

I must acknowledge the current and past members of Lab 369: Lingfei Zhou, Dr. Yuanyuan Zhao and Dr. Lili Huang for their help and sincere suggestions along the way, and their recommendations and referrals when I was seeking a career; Anning Chen and Arvind Ramanandan for sharing the fun conversations and constructive discussions for research and various courses. Without them, my life at UCR would not be as memorable

and colorful.

I am truly indebted to my parents, Kexin Li and Yuanxiu Hao. At all times, you are a pillar of strength to me. As a token of my heartfelt gratitude, I dedicate the thesis to you.

To my parents.

ABSTRACT OF THE DISSERTATION

Performance Limitations of Linear Systems over Additive White Noise Channels

by

Yiqian Li

Doctor of Philosophy, Graduate Program in Electrical Engineering
University of California, Riverside, June 2011
Dr. Jie Chen, Co-Chairperson
Dr. Ertem Tuncel, Co-Chairperson

This thesis develops a framework to address the performance limits of feedback control systems with communication constraints modeled by additive white noise channels. By searching for the fundamental bounds on the control performance, we explore the relationship between the known limitations caused by the intrinsic properties of linear control systems and the characteristics of the communication channels. We analyze multiple-input multiple-output systems with the channel placed at either the uplink or downlink. We also study the stabilization conditions for single-input single-output systems when both channels are present in the closed loop.

For systems with uplink channels, we derive explicitly the analytical expressions for the necessary and sufficient conditions for stabilization and the best achievable performance under the channel input power constraint. The optimal tracking performance exhibits clear dependence on the power constraint and noise levels of the channel, and additionally on the unstable poles and nonminimum phase zeros of the plant. For systems with downlink channels, we derive a lower bound for the performance that incorporates the plant gain in

the entire frequency range. Moreover, we use and optimize scaling as a method of channel compensation to exploit the channel and deal with the white noise. This simple strategy is shown to significantly improve the tracking performance. Also, we attempt to discover the optimal power allocation for each of the uplink parallel channels to achieve the best tracking performance. It is shown that, the optimal strategy is to allocate more power to a more problematic channel, in contrast to the widely-known “water-filling” solution, which is to maximize the capacity. Lastly, for first-order systems controlled over both uplink and downlink channels, we analyze the achievable region of the signal-to-noise ratios of the channels for stabilizability.

Contents

List of Figures

Chapter 1

Introduction

1.1 Background

The control theory deals with how to compensate dynamical systems, so that they can generate desired response and have “self-adjustment” capability to the changes in the environment. The theory that we are most familiar with has an underlying assumption that the communications between components are ideal and synchronous. In other words, the systems are supposed to transmit as much information as they need perfectly and with a known, fixed delay. These simplifications are reasonable in most applications, allow the theory to focus on the inner structure of the systems while simplify controller synthesis, and have helped it develop, thrive, and be successfully engineered.

The assumption of perfect communication is reasonable when the real components of the systems are placed closely and connected by a dedicated network; it is usually the best choice and a must when the system demands high and precise performance. However, for large scale systems such as power systems, systems using mobile sensor networks, or remote control, the communication effects can no longer be neglected. Furthermore, as information and networking technology prevail, building *networked control systems* (NCS's) is possible and appealing, especially in some consumer or commercial applications where low cost and robustness of data networks overweigh the sacrifice of the absolute high performance.

In contrast to standard control systems, a conceptual yet typical configuration of NCS's is shown in Figure 1.1. The operations of the sensors, plants and controllers of such systems are coordinated through networks subject to various communication constraints, and they are likely to become bottlenecks in the control performance. The interplay of control and communication is the central theme of the developing theory of NCS's.

The research on NCS's has been attracting a great deal of efforts and leads to a new interdisciplinary area between control theory and information theory, as evidenced by the special issue [3]. The overview of recent development of NCS's can be found in survey papers, e.g. [30, 31], with the latter more focusing on network delay and packet dropouts.

1.1.1 Challenges

Due to the differences between control and communication/information theory, NCS's pose unique challenges unexplored in the past. In essence, communications theory aims at point-to-point reliable transmission and the control theory, in contrast, focuses on effective utilization of information: the data are to be used in a feedback loop. Also, in communication or information theory long delays are tolerable: the inequalities and tight bounds usually require coding with arbitrarily long block lengths [20]. On the other hand, time delays severely depreciate performance and stability of unstable systems in control theory. It is true that control systems can be robust to the variations modeled in the design process,

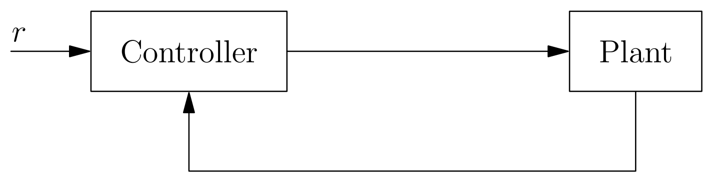

(a) Standard control systems

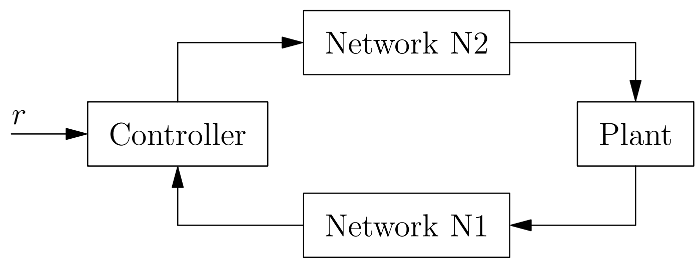

(b) Networked control systems

Figure 1.1: Key differences between generic networked control systems and standard control systems

but they cannot tolerate complex communication limitations.

First, signals sent through a digital channel must be quantized. Although under high-rate conditions, a quantizer can be modeled as additive noise channel [29], the pioneering work [21] shows that this model cannot be used to rigorously analyze feedback control systems. Quantization is inherently nonlinear and current standard control theory cannot directly address such nonlinearity. Second, the communication channels can have only limited capacity constraints, which means that only a finite alphabet of data can be transmitted. This effect limits the information available to control and thus brings about a fundamental tradeoff between the data-rate and the control performance. Thirdly, delays (possible random) always come together with data transmission. Besides the transmission delay, for example, in a packet-based data network, when packets drop happens, they are typically re-send or rerouted to their destination, causing waiting time delays. And random delays are unaccounted for in conventional control machineries. In summary, unlike standard control system, NCS's present critical challenges that will consequently necessitate an inevitable tradeoff between communication characteristics and the system's performance.

As a result, several fundamental control concepts will no longer fit in the networked environment. The most notably loss will be the theory of linear time-invariant (LTI) systems, since we consider the highly nonlinear communication channels. However, for additive noise channel, the linearity can be preserved and standard control tools can be used, base on which a line of research originates (e.g. [8]). In the thesis, we are also going to take advantage of the simplicity of this channel model. Another idea for preserving the control techniques is the "sector-bound" approach, which is used on a logarithmic quantizer [28]. A rich set of tools for robust control can make the transition to address quantization with the aid of the model, see e.g. [50].

New and daunting difficulties notwithstanding, there have been significant process in studying NCS's and we will partially review the existing results in the following section.

1.2 Literature Review

One of the goals of studying NCS's, besides search for a clear understanding of the relationship between control and communication, is to have a general design methodology which can apply to a possibly large system, with multiple sensors and agents connected through complex network topology. However, as a first step, it is best to simplify the problem as much as possible. A single plant, and a sensor and controller connected by a simple channel model has been adopted by many researches in this area, and significant progress has been witnessed in recent years. This centralized feedback control will also be our focus in this section and throughout the thesis.

1.2.1 Control with quantized feedback

We consider systems connected with digital noiseless channels in the uplink. The uplink is referred to the feedback path in the system, as "Network N1" in Figure 1.1b. Since the channel is digital, any continuous-valued measurements or signal must be first quantized. The quantization is usually included in the coding process as is shown in Figure 1.2. We shall consider in this subsection only static and memoryless quantizers, i.e., the range and levels of the quantizer is predetermined and not time-varying. Quantization inevitably causes information loss and affects the control system. Traditionally in signal-processing and some control literature, the quantizers are modeled as additive noise channels under high-rate condition. However, Delchamps [21], as one of the first researchers that rigorously analyzed quantization in control, showed that quantizers with finite quantization levels cannot asymptotically stabilize a linear system in general. Intuitively, as any two state values in the quantization block that contains the origin are indistinguishable, the unstable dynamics moves any nonzero initial state in that block away from the origin until it reaches another quantization block. Even if the control makes the state move towards the origin again, a repeated cycle will result. Thus, the state can never converge to the origin. It holds true even if the control action has memory for the past quantized state. This pioneering work implies that to achieve stability, the coding/quantizer must be more complex than a finite static and memoryless one. It thus activated a stream of work pursuing quantization/coding

Figure 1.2: Generic network model

rules that can achieve certain control objectives.

The work [23] considered logarithmic quantizers and showed that asymptotic stability could be achieved for LTI discrete time systems. Such quantizers have infinite levels and increasing density of levels toward the origin. It was also shown that it is the most efficient (coarsest partition) static memoryless quantizer to quadratically (in Lyapunov sense) stabilize a single-input single-output (SISO) unstable plant among all control laws. If we let parameter ρ denote the density of the partition of the quantizer (the smaller ρ is, the more efficient the quantizer), then it turns out the coarsest density is given by

$$\rho^* = \frac{\prod_{i=1}^{l} |p_i| - 1}{\prod_{i=1}^{l} |p_i| + 1}$$

where $p_i, i = 1, \ldots, l$ are the unstable eigenvalues of the system. Furthermore, a noticeable advantage of the logarithmic quantizer is that it can be treated non-conservatively as a sector-bound uncertainty on the input [28], and thus the quantized feedback system can be reformulated as an LTI system with a static sector-bounded uncertainty, whose bound is related to the quantization density. By showing this, not only the results can be generalized to multiple-input multiple-output (MIMO) systems (conservatively) but also tools of robust control can be applicable to quantization related networked control problems [50].

1.2.2 Control with limited data-rate

This line of research is also concerned with connecting system via digital noiseless channel, but with limited data-rate R. The data-rate is defined as

$$R \triangleq \log_2 M \text{ (bits/channel use)},$$

where M is the cardinality (number of elements) of the channel input alphabet. A significant question is: what is the lower bound on R below which it is impossible for a plant to be stabilized (in some sense), by any encoder and decoder/controller? We have seen that memoryless quantizers with finite levels cannot asymptotically stabilize a LTI system in general, hence to search for a fundamental bound on the limited data-rate, we allow the coder/quantizer to have evolving parameters and unrestricted memory, with the only constraint being causality.

Nair and Evans [45] show that a linear state-space discrete-time systems can be asymptotically stabilized if and only if the channel's data rate R satisfies the bound

$$R > H, \tag{1.1}$$

where

$$H \triangleq \sum \log_2 |\lambda_i| \tag{1.2}$$

in which λ_i is the unstable eigenvalue of the linear system. Earlier, the same authors have discovered similar bounds for noiseless autoregressive moving average systems [44]. As a generalization, the inequality (1.1) is also tight for observability, in the sense that the system's state can be reconstructed approximately based on quantized information [64]. A common technique of designing these rate-achieving quantizers is dynamic scaling/zooming used in, e.g. [10]. The range of the quantizer can adaptively zoom-in or zoom-out, according to the distance of the plant state to the target. Furthermore, the same results are shown to hold true for the mean square stability (MSS) of stochastic systems, even if the process and measurement noise have unbounded support [46]. Serving as a fundamental limit valid over any coding strategy, the bound (1.2) bears no relation to the system's input and output, depending only on the autonomous part of the system. It is named *intrinsic entropy rate* [47, 57] and represents the degree of instability of the plant, or a measure of the rate at which a unstable linear plant can generate information.

1.2.3 Control over additive white noise channels

A typical analog communication channel is the additive white noise (AWN) channel depicted in Figure 1.3. AWN channel has continuous input and output alphabet as $\mathbb{R}$. The channel output w is the sum of the input u and the noise n. The noise is drawn i.i.d. from a given distribution with zero mean and variance Φ. And the noise is independent of the input u. Without any further constraints, the capacity of this channel is infinite. The effect of the noise can be made arbitrarily small by increasing the power of the input and thus the channel practically imposes no communication constraint. To properly model an analog transmission media, it is customary to limit the channel input u to a finite instant power, $\mathcal{E}\{u^2\} \leq \Gamma$. If we assume the distribution of the noise is Gaussian and the channel operates on discrete time, then a well-known fact is that the capacity of the then called additive white Gaussian noise (AWGN) channel is [20]

$$\mathcal{C} = \frac{1}{2}\log_2\left(1 + \frac{\Gamma}{\Phi}\right).$$

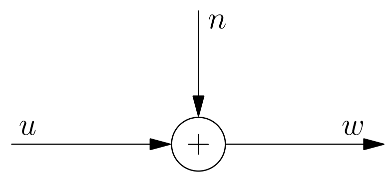

Figure 1.3: Additive white noise channel

Hence, the power constraint translates into one on the signal-to-noise ratio (SNR) and then into one on channel capacity. More importantly, the use of the AWN channel *preserves the system's linearity*, thus rendering the control analysis and design problems more amenable to conventional tools drawing upon linear systems theory. It can be further extended to accommodate colored noise and channel bandwidth, by introducing appropriate filters in the noise and signal path, respectively. Furthermore, AWGN channel model is a building block for many wireless channels [66].

We illustrate here a motivating example which is drawn from the paper [22]. The configuration is shown in Figure 1.4. A first-order scalar unstable system must be stabilized over an AWGN channel where the Gaussian noise is zero-mean and has variance Φ. We wish to find the minimum power of u over all stabilizing controllers[1]. This is a special linear quadratic Gaussian (LQG) problem which has an explicit solution [2]. In fact, the optimal feedback gain is given by $-\lambda + 1/\lambda$, and the minimal average power of u is $\Gamma = (\lambda^2 - 1)\Phi$. Therefore, the minimal channel capacity required for stabilization is

$$\mathcal{C}_{min} = \frac{1}{2}\log\left(1 + \frac{\Gamma}{\Phi}\right) = \log(\lambda) \tag{1.3}$$

where the formula of the capacity of the AWGN channel with input power constraint is applied. Thus, the channel capacity must be larger than $\log(\lambda)$ for stabilizability of the

[1]Stabilizing controllers are those that can make the closed loop system internally stable, without taking into consideration the communication channel. Internal stability is defined in Section 2.3.2

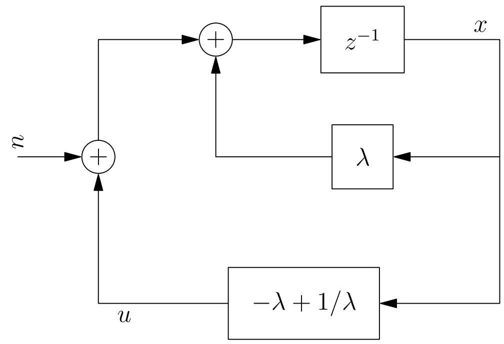

Figure 1.4: An example of stabilization over an AWGN channel

system. It coincides with (1.2) and can be considered as the rate at which the unstable system generates information.

Thus, the stabilization problem boils down to an optimal control problem, which is to search for the lowest achievable channel input power under which the closed loop system cannot be stabilized by any LTI controller. Using a similar LQG formulation, the paper [8] and its journal version [9] have shown that the bound (1.2) also holds true for stabilization of general unstable SISO linear plants over AWGN channel using state feedback. Using $\mathcal{H}_2$ optimization on the complementary sensitivity function, they also show that, however, in the case of output feedback, the bound is only tight for minimum phase plants with relative degree one. For unstable nonminimum phase plants or those with relative degree greater than one, the demand on the channel input power is strictly greater than (1.2) as an additional term must be included. The result is expected, since relative degree amounts to time delay for discrete-time systems and the negative effects of time delay and nonminimum phase zeros on control are well known. The restriction to LTI controllers also accounts for the increased SNR demand. In fact, [9] shows that, by using fast sampling and linear time-varying (LTV) control schemes, this additional cost can be made arbitrarily small.

This additional term can also be eliminated by exploring the structure of the channel with noiseless feedback [59]. The work [53, 54] extend the previous result to bandlimited AWGN channel and that with colored noise. They show that stricter stabilization requirement on the channel SNR results, which is expected. For additive Gaussian wireless fading channels, the authors of [11] use information theoretic techniques and stochastic calculus to prove a similar result for the channel capacity requirement.

Despite substantial progress on stabilization issues, research on the control performance of NCS's is only beginning to emerge. Under this topic, the authors of [26, 27] investigate the disturbance attenuation performance (measured by the variance of the plant output), which amounts to minimizing the output power of a LTI minimum phase plant in response to a Gaussian disturbance over a Gaussian communication feedback channel. The fact that the performance index is the plant output simplifies the derivations. The authors of [26] find out that pre- and post-scaling can be used effectively to compensate the channel and better the control performance. It is assumed that the channel input is a constant multiple of the plant output and so is the controller input from the channel. They derive the relation between the scaling and the best achievable performance. The scaling factor is designed such that the power constraint is fully utilized at the optimal performance, which is consistent with one's intuition. The later work by [27] studies potential improvements over [26] by allowing the channel encoder to be nonlinear and time-varying and derives the minimal variance of the plant output at a specified terminal time. Lower bound on the performance achievable is derived using information theoretic methods. To show the bound is tight, intricate coding and decoding schemes are designed, which involving noiseless feedback from the channel output with a unit time delay, and different assumptions on the information available to the encoder. In another direction of research, the authors of [40, 41] have studied the fundamental limitations that extends Bode's integral formula, for disturbance attenuation in feedback systems over noisy channel. In [41], a new type of performance bound parameterized by the channel capacity and the plant parameters is derived.

Although our main concentration is AWN channel, we provide a partial review on control over other types of noisy channels here. We have mentioned that, for AWN channels, the bound (1.2) is necessary and sufficient for MSS. However, this cannot be generalized to other noisy channels. The problem becomes dependent on the specific definitions of stability, and whether side-information on the channel errors is available [42,47,63]. In fact, Shannon capacity itself is no longer the correct figure-of-merit for stabilization over noisy channels, as transmitting at the rate close to $\mathcal{C}$ introduces long coding delay [20], which will allow the plant state to diverge further. Noiseless channels we considered in Section 1.2.2 are not exposed to this issue because we only have to investigate source coding and cast channel coding aside. The examples for the inadequacy of the Shannon capacity are provided in, e.g., [56]. In that paper, *anytime capacity* is introduced and proved to be necessary and sufficient for moment stability of stochastic feedback control system over noisy channels. However, anytime capacity is in general difficult to compute and can hardly serve as a control synthesis index.

1.3 Thesis Framework

We have reviewed the literature on NCS's. It turns out that the existing results focus mainly on stabilization and the studies on performance issues are still by and large immature. In the thesis, we shall delve into a specific performance problem of NCS's. We shall present general configurations and specific problems in this section.

1.3.1 The tracking configuration

Throughout the thesis, we shall chiefly study the fundamental limitations on *tracking performance*, for networked control systems over additive white noise channels. We shall primarily study continuous-time LTI systems and continuous-time AWN channels, while the discrete-time counterpart follows similarly. The system configuration has been shown in Figure 1.1b, in which the networks are modeled by analog AWN channel, and as we have mentioned, the linearity will be preserved. The measured signals are sent to the controller via the communication channel N1, the uplink. The control signals are transmitted via another channel N2, the downlink, to the plant. A more specific configuration is depicted in Figure 1.5. The tracking error can then be defined as

$$\boldsymbol{e} = \boldsymbol{r} - \boldsymbol{y}$$

and the stationary variance of $\boldsymbol{e}$ is the performance index. In particular, the uplink AWN channel imposes the power constraint on the plant output while the downlink imposes the constraint on the control signal.

In studying stabilization problems of SISO systems, it suffices to consider either the uplink or the downlink, as they impose the same constraint on stabilization. That is not the scenario for MIMO systems and we shall give stabilization results for both cases.

For tracking, the goal is to look for the best achievable performance through all stabilizing LTI controllers, over *either* uplink or downlink channel. The performance bound

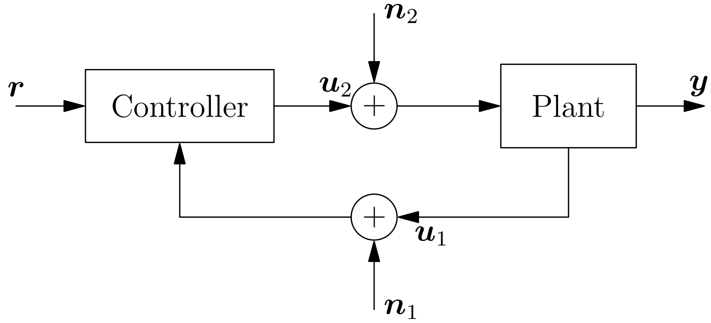

Figure 1.5: Tracking configuration over uplink and downlink AWN channels

thus is valid irrespective of the compensator. We shall analyze each case and in essence, how communication limitations affect the tracking performance.

1.3.2 Channel compensation through scaling

In conjunction with optimal tracking control, we also investigate a simple channel compensation strategy by the design of a pre- and post-processing scheme via constant scaling, which together constitute a *joint* design of the controller and the communication channel. It is a natural option to use scaling, which is the simplest coding scheme for AWN channels, to exploit the channel to the maximum extent allowable under the power constraint. We shall provide a relation between the optimal tracking performance and the corresponding optimal scaling factor. It is shown that, similar to the result in [26], the power constraint is attained via optimal scaling. Comparisons between the case with and without scaling factors show the improvement clearly.

1.3.3 Fundamental limitations on the tracking performance

Performance bounds in control engineering hold indispensable importance. It gives a separation line between what is attainable and what is not, rules out unnecessary trail and errors, and points out directions for improving the control design. It also allows us to see into what constrains the control performance fundamentally. Examples of such performance bound are the Bode and Poisson integral relations about to what extent sensitivity is reducible via feedback, including classic and recent studies [5, 6, 13, 16, 25]. It shows that, in one way or another, intrinsic plant parameter such as unstable poles or nonminimum phase zeros will impose severe limitations on the feedback system's performance.

Recent years, limitations on tracking or disturbance attenuation performance of standard linear systems have been actively investigated and seen fruitful and insightful results. A well-known characteristic is that, perfect tracking can be achieved for minimum phase systems, but this property ceases to hold if the plant is nonminimum phase [33]. Explicit expressions relating the nonminimum phase zeros to the tracking error of unit step signal for SISO systems are derived in [43, 51]. The results for MIMO systems involve directional properties and are investigated in [17], and further generalized to other standard reference inputs, such as ramp and sinusoidal signal [18], and the combination of step and several sinusoidal signals of different frequencies [62]. Also, the work [12] studies the tracking performance with structure constraint on the plant, namely the system is single-input multiple output. The seminal paper [15] has dealt with control energy constrained optimal performance using convex optimization techniques and derived analytic expressions of the performance bounds. It is among the first to study how additional constraints will affect the control performance, which our thesis is closely related to[2]. In summary, these and other works have shown that the performance generally depends on the locations of nonminimum phase zeros and unstable poles of the plant, and their directions if multivariate system is considered.

We shall investigate how tracking performance is limited by communication, primarily the power constraints modeled by AWN channels. It can then serve as a benchmark for the quality of the communication channel in designing NCS's with given performance specifications. Besides the factors we mentioned above for standard control systems, we expect that a measure of the channel quality will also limit the performance in feedback control over communication channels. We shall later see that channel capacity no longer suffices for checking performance, even for SISO systems, though channel SNR or capacity is adequate to characterize stability [9].

1.3.4 Parallel channels and power allocation

For MIMO systems, we consider multiple independent AWN channels in parallel with a common power constraint [20] in the system. The relation between performance and control systems and the channel is then more complex as spatial properties take effect. When the MIMO channel is placed in the uplink, we shall examine its power allocation strategy among individual channel to achieve the best tracking performance, which gives an essential reference on how the channel should be designed to accommodate tracking performance requirements.

[2]The techniques we use in the present thesis were mostly developed in that paper.

1.3.5 Two channel stabilization

So far most of the results on stabilization take only one channel, either uplink or downlink, into consideration. We shall study the stabilizability of the closed loop system when both channels in Figure 1.5 are present. There will be a tradeoff between the power constraints of both channels. First, the capacity or equivalently the power constraint for each channel must satisfy the fundamental bound (1.2). Then we will search for, if the power constraint for the uplink or downlink channel is limited, the bound on the power constraint for the other channel, which is in essence a constrained optimization problem. As analytical results are difficult and cumbersome to derive, we shall consider special system models, such as scalar systems as the example in Section 1.2.3 and plants with only a single real unstable pole.

1.4 Overview of Thesis Contents

The central contribution of this thesis is to discover the fundamental performance limitations for LTI control systems over power-constrained additive white noise channels. While using the tools from standard linear control theory, the thesis reveals explicitly the effect of communication constraints on the control performance and is among the first endeavors to address tracking performance problems of NCS's.

- **Chapter 2:** This chapter presents the necessary background and includes the notations, definitions, concepts, lemmas and theorems that will be used heavily in latter chapters.

- **Chapter 3:** This chapter presents the most important results of the thesis. It deals with the MIMO feedback control system with AWN channel in the uplink. First, the conditions on the channel for stabilizability of both minimum phase and nonminimum phase systems are derived. The results are generalizations of existing results on SISO systems. Then, we prove the theorems for the best achievable tracking performance over the AWN channel and investigate the optimal power allocation among the parallel channels, which is much different from the capacity-maximizing "water-filling" solution. Next we propose a simple scaling across the channel which aims to better utilize the power constraint. We derive the optimal tracking performance with scaling which shows significant performance improvement. We also consider a fully decentralized control structure and investigate its performance and power allocation when the input to each channel can be independently adjusted. Lastly we design a numerical example which agrees with the theoretical results.

The publications related to this chapter are [34, 36]. Similar results for discrete-time systems can be found in [38].

- **Chapter 4:** This chapter is devoted to the tracking performance of LTI systems with AWN channel in the downlink. As the control action is directly limited by the communication, minimum phase behavior plays a role in the tradeoff between the tracking performance and communication. We first present the stabilization results for MIMO systems, which is comparable to those in Chapter 3. Then, we decompose the tracking performance problem into a noise attenuation problem and a noise-free reference tracking problem. The lower bound on tracking performance is obtained for MIMO systems. As a special case, we show that the bound can be achieved for SISO systems.

The publication associated with this chapter is [35]. The development of the chapter is based on [15].

- **Chapter 5:** This chapter discusses a related problem of stabilization with AWN channels in both directions. Rather than focusing on the tradeoff between tracking and the AWN channel, we investigate the tradeoff between the channels themselves. We consider a special class of plants which have only one unstable pole and obtain explicit tradeoff relations. In the process, we separately look into both one-parameter and two-parameter controller. In addition, we solve the same problem for a discrete-time scalar system with state feedback. The results, although restricted to special cases, reveal interesting tradeoff relations between the channels for achieving stabilizability.

  The publication related to this chapter is [37].

- **Chapter 6:** This chapter draws conclusions and discusses possible future research directions.

Chapter 2

Preliminaries

2.1 Introduction

In this chapter, we introduce the notation, explain the general problems and then collect the technical machinery necessary for the subsequent development of the thesis.

2.2 Notations

The transpose and conjugate transpose of a matrix A are denoted by A^T and A^H, and its largest and smallest singular values are denoted by $\overline{\sigma}(A)$ and $\underline{\sigma}(A)$, respectively. In addition, let $A^{\sim}(s)$ denote $A^T(-s)$. Vectors are denoted by boldface letters. We shall assume that all the vectors and matrices have compatible dimensions, and omit the dimensions where appropriate. The field of real numbers is denoted by $\mathbb{R}$ and the field of complex numbers is denoted by $\mathbb{C}$. The open left, the open right halves of the complex plane and the imaginary axis are denoted by $\mathbb{C}_- \triangleq \{ s : \mathrm{Re}(s) < 0 \}$, $\mathbb{C}_+ \triangleq \{ s : \mathrm{Re}(s) > 0 \}$ and $\mathbb{C}_0$, respectively. The expectation operator is denoted by $\mathcal{E}$. In addition, $\| \cdot \|$ denotes the

Euclidean vector norm and $\|\cdot\|_F$ the Frobenius matrix norm. For a pair of nonzero vectors $\boldsymbol{w}$ and $\boldsymbol{v}$, we define the principal angle $\angle(\boldsymbol{w},\boldsymbol{v})$ between their directions by

$$\cos\angle(\boldsymbol{w},\boldsymbol{v}) \triangleq \frac{|\boldsymbol{w}^H\boldsymbol{v}|}{\|\boldsymbol{w}\|\|\boldsymbol{v}\|}.$$

We shall consider the Hilbert space

$$\mathcal{L}_2 \triangleq \left\{ G : G(s) \text{ measurable in } \mathbb{C}_0, \|G\|_2^2 \triangleq \frac{1}{2\pi}\int_{-\infty}^{\infty} \|G(j\omega)\|_F^2 \,\mathrm{d}\omega < \infty \right\},$$

in which the inner product is defined as

$$\langle F, G\rangle \triangleq \frac{1}{2\pi}\int_{-\infty}^{\infty} \mathrm{Trace}\left\{F(j\omega)G^H(j\omega)\right\} \mathrm{d}\omega.$$

It is known that $\mathcal{L}_2$ admits an orthogonal decomposition into the (closed) subspaces $\mathcal{H}_2$ and $\mathcal{H}_2^\perp$, where

$$\mathcal{H}_2 \triangleq \left\{ G : G(s) \text{ analytic in } \mathbb{C}_+,\ \|G\|_2^2 \triangleq \sup_{\epsilon>0} \frac{1}{2\pi}\int_{-\infty}^{\infty} \|G(\epsilon+j\omega)\|_F^2 \,\mathrm{d}\omega < \infty \right\} \tag{2.1}$$

and its complement is

$$\mathcal{H}_2^\perp \triangleq \left\{ G : G(s) \text{ analytic in } \mathbb{C}_-,\ \|G\|_2^2 \triangleq \sup_{\epsilon<0} \frac{1}{2\pi}\int_{-\infty}^{\infty} \|G(\epsilon+j\omega)\|_F^2 \,\mathrm{d}\omega < \infty \right\}.$$

It follows that for any $F \in \mathcal{H}_2$ and $G \in \mathcal{H}_2^\perp$, we have $\langle F, G\rangle = 0$. Thus, for any $F \in \mathcal{L}_2$, we can decompose it into part in $\mathcal{H}_2$, denoted by $[F]_{\mathcal{H}_2}$, and part in $\mathcal{H}_2^\perp$, denoted by $[F]_{\mathcal{H}_2^\perp}$, as

$$F = [F]_{\mathcal{H}_2} + [F]_{\mathcal{H}_2^\perp}. \tag{2.2}$$

Then, because of the orthogonality

$$\|F\|_2^2 = \|[F]_{\mathcal{H}_2}\|_2^2 + \|[F]_{\mathcal{H}_2^\perp}\|_2^2.$$

Finally, let $\mathbf{R}\mathcal{H}_\infty$ denote the set of all stable, proper, rational transfer function matrices. If the norm is defined as

$$\|F\|_\infty \triangleq \sup_{\mathrm{Re}(s)>0} \overline{\sigma}\left(F(s)\right),$$

then $\mathbf{R}\mathcal{H}_\infty$ is a Banach space.

2.3 Stability and Performance of Feedback Systems

2.3.1 Linear dynamical systems

The introduction of linear dynamical systems follows [70]. We can represent a continuous-time finite dimensional, linear time invariant system in state space by the following constant coefficient differential equations:

$$\begin{aligned} \dot{x} &= Ax + Bu, \qquad x(t_0) = x_0, \\ y &= Cx + Du \end{aligned}$$

where $\boldsymbol{x}(t) \in \mathbb{R}^n$ is called the system state, $x(t_0)$ is called the initial condition of the system, $\boldsymbol{u}(t) \in \mathbb{R}^k$ is called the system input, and $\boldsymbol{y}(t) \in \mathbb{R}^m$ is the system output. A system with $k = 1$ and $m = 1$ is called SISO, otherwise it is called MIMO. The transfer function from $\boldsymbol{u}$ to $\boldsymbol{y}$ is defined as

$$\hat{\boldsymbol{y}}(s) = G(s)\hat{\boldsymbol{u}}(s)$$

where $\hat{\boldsymbol{u}}(s)$ and $\hat{\boldsymbol{y}}(s)$ are the Laplace transform of $\boldsymbol{u}(t)$ and $\boldsymbol{y}(t)$ with zero initial condition, respectively. The frequency variable s shall be omitted whenever convenient. We shall assume that all transfer functions are real-rational. For a causal system, its transfer function $G(s)$ must be proper, which means $\lim_{s\to\infty} G(s)$ exists and is finite. A transfer function

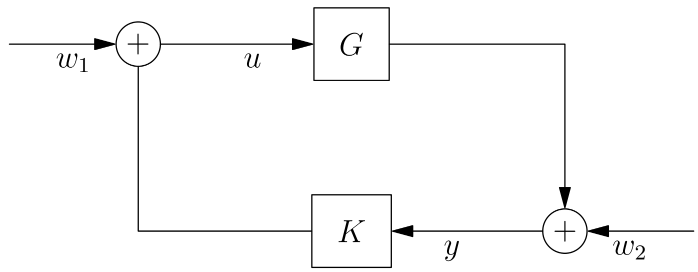

Figure 2.1: Block diagram for stability definition

$G(s)$ is strictly proper if and only if $\lim_{s\to\infty} G(s) = 0$. It is well-known that a transfer function in $\mathcal{L}_2$ must be strictly proper.

A pole p is said to be stable if and only if $p \in \mathbb{C}_-$, unstable if and only if $p \in \mathbb{C}_+$ and marginally stable if and only if $p \in \mathbb{C}_0$. Then, we say that a proper transfer function G is stable if and only if all of its poles are stable, unstable if and only if it has poles that are unstable, and marginally stable if and only if it has marginally stable poles besides stable poles.

Similarly, a zero z is said to be minimum phase if and only if $z \in \mathbb{C}_-$, nonminimum phase if and only if $z \in \mathbb{C}_+$ and marginally minimum phase if and only if $z \in \mathbb{C}_0$. Then, we say that a proper transfer function G is minimum phase if and only if all of its zeros are minimum phase, nonminimum phase if and only if it has zeros that are nonminimum phase, and marginally minimum phase if and only if it has marginally minimum phase zeros besides minimum phase zeros.

2.3.2 Internal stability

Consider the feedback system depicted in Figure 2.1. To guarantee that a block diagram of a system is physically realizable, we need the following definition.

Definition 2.1 (Well-posedness of feedback loop [70]) *A feedback system is said to be* well-posed *if all closed-loop transfer matrices are well-defined and proper.*

A necessary and sufficient condition for well-posedness is

$$I - K(\infty)P(\infty)$$

is invertible, which will be assumed throughout the thesis.

Definition 2.2 (Internal stability [70]) *The system is said to be internally stable if and only if the state vectors of G and K converge to zero from all initial conditions when $(w_1, w_2) = 0$.*

The system in Figure 2.1 is internally stable if and only if the transfer function matrix from (w_1, w_2) to (u, y) belongs to $\mathbf{R}\mathcal{H}_\infty$. We use "stability" as a synonym for "internal stability".

Definition 2.3 (Stabilizable plant) *A plant G is said to be* stabilizable *if and only if there exists a system $K(s)$, which is proper, such that the interconnected system in Figure 2.1 is internally stable and well-posed.*

2.3.3 Coprime factorization over R$\mathcal{H}_\infty$

Definition 2.4 (Coprime matrices, see, e.g. [24])

1. *Two matrices F and G in $\mathbf{R}\mathcal{H}_\infty$ are* right-coprime *(over $\mathbf{R}\mathcal{H}_\infty$) if they have equal number of columns and there exist matrices X and Y in $\mathbf{R}\mathcal{H}_\infty$ such that*

$$\begin{bmatrix} X & Y \end{bmatrix} \begin{bmatrix} F \\ G \end{bmatrix} = I,$$

or, equivalently, $\begin{bmatrix} F \\ G \end{bmatrix}$ *is left-invertible in* $\mathbf{R}\mathcal{H}_\infty$.

2. *Two matrices* F *and* G *in* $\mathbf{R}\mathcal{H}_\infty$ *are* left-coprime *(over* $\mathbf{R}\mathcal{H}_\infty$*) if* $\begin{bmatrix} F & G \end{bmatrix}$ *is right-invertible in* $\mathbf{R}\mathcal{H}_\infty$.

We shall need a *doubly-coprime* factorization of a transfer function matrix G [24].

Lemma 2.5 *For each proper real-rational transfer function matrix* G*, there exist matrices satisfying the following equation*

$$G = NM^{-1} = \tilde{M}^{-1}\tilde{N} \tag{2.3}$$

where $N, M, \tilde{N}, \tilde{M} \in \mathbf{R}\mathcal{H}_\infty$ *and satisfy the double Bezout identity*

$$\begin{bmatrix} \tilde{X} & -\tilde{Y} \\ -\tilde{N} & \tilde{M} \end{bmatrix} \begin{bmatrix} M & Y \\ N & X \end{bmatrix} = I \tag{2.4}$$

for some $X, Y, \tilde{X}, \tilde{Y} \in \mathbf{R}\mathcal{H}_\infty$.

A system configuration with a two-parameter controller is depicted in Figure 2.2. The two-parameter controller operates on $r(t)$ and $y(t)$ obeying the equation in frequency domain as

$$\hat{u} = K_1\hat{r} + K_2\hat{y}.$$

It has two degrees of freedom and represents the most general linear feedback structure. In the thesis we shall frequently use the following Youla parameterization [67] of stabilizing two-parameter controllers:

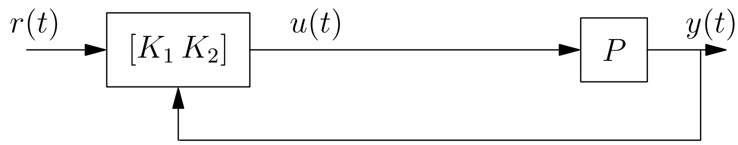

Figure 2.2: Tracking via a two-parameter controller

Theorem 2.6 *Consider the system in Figure 2.2. Assume the plant G is stabilizable. The set of all stabilizing two-parameter compensators is characterized by*

$$\mathcal{K} = \left\{ K : K = \begin{bmatrix} K_1 & K_2 \end{bmatrix} = (\tilde{X} - R\tilde{N})^{-1} \times \begin{bmatrix} Q & \tilde{Y} - R\tilde{M} \end{bmatrix}, Q, R \in \mathbf{R}\mathcal{H}_\infty \right\}. \tag{2.5}$$

The one-parameter controller, being a special case, is equivalent to the two-parameter controller with $K_1 = -K_2 = K$, in which case we have the following theorem:

Theorem 2.7 *The set of all stabilizing compensator K is characterized by*

$$\mathcal{K} = \left\{ K : K = -(Y - MQ)(X - NQ)^{-1} = (\tilde{X} - Q\tilde{N})^{-1}(\tilde{Y} - Q\tilde{M}), Q \in \mathbf{R}\mathcal{H}_\infty \right\}. \tag{2.6}$$

2.3.4 Zeros and poles

The zeros and poles for a SISO transfer function are the roots of its numerator and denominator polynomials. For multivariable systems, the zeros and poles are similar but have directional properties involved. We introduce the notion of *transmission zeros* here, which are the only type of zeros we will deal with. They are often defined via the *Smith-McMillan form* [52] and can be characterized using state space representations [13, 14, 58]. In particular, let (A, B, C, D) be a minimal realization of a proper, left-invertible transfer function matrix $G(s)$, then a point $z \in \mathbb{C}_+$ is called a nonminimum phase zero of G if there exist vectors $\boldsymbol{\chi}$ and $\boldsymbol{\omega}$ such that the equation

$$\begin{bmatrix} zI - A & -B \\ -C & -D \end{bmatrix} \begin{bmatrix} \boldsymbol{\chi} \\ \boldsymbol{\omega} \end{bmatrix} = 0$$

holds, where $\boldsymbol{\omega}$ with $\|\boldsymbol{\omega}\| = 1$ is called the input zero direction vector associated with z. Alternatively, a nonminimum phase zero z of a right-invertible $G(s)$ satisfies the relation

$$\begin{bmatrix} \boldsymbol{\zeta}^H & \boldsymbol{\eta}^H \end{bmatrix} \begin{bmatrix} zI - A & -B \\ -C & -D \end{bmatrix} = 0$$

where $\boldsymbol{\zeta}$ is some vector and $\|\boldsymbol{\eta}\| = 1$. The vector $\boldsymbol{\eta}$ is called the output zero direction associated with z. It follows immediately from these definitions that $G(z)\boldsymbol{\omega} = 0$ or $\boldsymbol{\eta}^H G(z) = 0$, respectively. Thus, the matrix $G(s)$ drops in rank at z. There may exist multiple independent input (or output) directions associated with z, the number of those directions is equal to the rank deficiency of $G(z)$ and is defined as the *geometric multiplicity* of the zero.

In our later development we shall primarily be interested in the characterization of the nonminimum phase zeros and unstable poles via the doubly coprime factorization (2.3). In this vein, a complex number $z \in \mathbb{C}_+$ is said to be a nonminimum phase zero of G with an output direction vector $\boldsymbol{\eta}$ if and only if $\boldsymbol{\eta}^H N(z) = 0$, where $\|\boldsymbol{\eta}\| = 1$ and that it is a nonminimum phase zero with an input direction vector $\boldsymbol{\omega}$ if and only if $\tilde{N}(z)\boldsymbol{\omega} = 0$. On the other hand, since the unstable poles of G coincide with the nonminimum phase zeros of M and $\tilde{M}$, the poles of G can also be characterized analogously using the doubly coprime factorizations. We shall call $p \in \mathbb{C}_+$ a unstable pole of G with a left pole direction vector $\boldsymbol{\eta}$ if $\boldsymbol{\eta}^H M(p) = 0$, where $\|\boldsymbol{\eta}\| = 1$. Accordingly, p is an unstable pole of G with right direction vector $\boldsymbol{\omega}$, if $\tilde{M}(p)\boldsymbol{\omega} = 0$. We shall assume throughout this thesis that a zero and a pole can not be at the same location and hence preclude the possibility of hidden unstable pole-zero cancelation. Furthermore, we shall also assume that the plant transfer function has only *simple* (i.e. single multiplicity) poles and zeros in $\mathbb{C}_+$.

2.3.5 Allpass factorization

We shall assume that the plant transfer function $G(s)$ is right-invertible. Then it is well-known that a nonminimum phase system G can be factorized into a minimum phase factor and an allpass part by an iterative procedure. Here, we shall be particular interested in the similar factorizations on coprime factors.

Suppose that the nonminimum phase zeros of the plant are ordered as $z_i \in \mathbb{C}_+$, $i = 1, \ldots, k$, which coincide with zeros of $N(s)$. Let $\boldsymbol{\eta}_1$ be the output direction vector associated with z_1 and define

$$L_1(s) \triangleq I - \frac{2\mathrm{Re}\{z_1\}}{s + \bar{z}_1} \boldsymbol{\eta}_1 \boldsymbol{\eta}_1^H.$$

Note that L_1 is constructed such that it is unitary, has only one zero at z_1 with $\boldsymbol{\eta}_1$ as a zero vector. Upon this factorization, the transfer function $L_1^{-1}N$ has zeros z_i, $i = 2, \ldots, k$. Then, for the zero z_2 we can find the associated vector $\boldsymbol{\eta}_2$ for $L_1^{-1}N$ and construct

$$L_2(s) \triangleq I - \frac{2\mathrm{Re}\{z_2\}}{s + \bar{z}_2} \boldsymbol{\eta}_2 \boldsymbol{\eta}_2^H.$$

Then, the transfer function $L_2^{-1}L_1^{-1}N$ has zeros z_i, $i = 3, \ldots, k$. Continue this procedure until we have collected all nonminimum phase zeros, then the part left is minimum phase.

Lemma 2.8 *Suppose that the plant P is right invertible and admits the coprime factorization 2.3. Order the nonminimum phase zeros as $z_i \in \mathbb{C}_+$, $i = 1, \ldots, k$ such that conjugate pairs are placed adjacently. Then, it is possible to factorize the coprime factor N as*

$$N(s) = L(s)N_m(s) \tag{2.7}$$

where $L(s)$ *can be constructed as*

$$L(s) \triangleq \prod_{i=1}^{k} L_i(s) \tag{2.8}$$

with

$$L_i(s) \triangleq I - \frac{2\mathrm{Re}\{z_i\}}{s + \bar{z}_i} \boldsymbol{\eta}_i \boldsymbol{\eta}_i^H \tag{2.9}$$

where the unitary vector $\boldsymbol{\eta}_i$ *associated with* z_i *is determined sequentially. The factor* N_m *is minimum phase.*

Alternatively, if the plant is left-invertible, we may factorize $\tilde{N}$ in the same way, as state in the following lemma:

Lemma 2.9 *Suppose that the plant* P *is left invertible and has the nonminimum phase zeros ordered as* $z_i \in \mathbb{C}_+$, $i = 1, \ldots, k$. *Then, it is possible to factorize the coprime factor* $\tilde{N}$ *as*

$$\tilde{N}(s) = \tilde{N_m}(s)\tilde{L}(s) \tag{2.10}$$

where $\tilde{L}(s)$ *can be constructed as*

$$\tilde{L}(s) \triangleq \tilde{L}_k \tilde{L}_{k-1} \cdots \tilde{L}_1 \tag{2.11}$$

with

$$\tilde{L}_i(s) \triangleq I - \frac{2\mathrm{Re}\{z_i\}}{s + \bar{z}_i} \tilde{\boldsymbol{\eta}}_i \tilde{\boldsymbol{\eta}}_i^H \tag{2.12}$$

and $\tilde{N_m}$ *is minimum phase.*

Additionally, it is possible to factorize M and $\tilde{M}$ analogously.

Lemma 2.10 *If the unstable poles of P are ordered as $p_i \in \mathbb{C}_+$, $i = 1, \ldots, l$. Then*

$$M(s) = B(s)M_m(s), \tag{2.13}$$

$$\tilde{M}(s) = \tilde{M}_m(s)\tilde{B}(s), \tag{2.14}$$

and $B(s)$, $\tilde{B}(s)$ can be constructed as,

$$B(s) \triangleq \prod_{i=1}^{l} B_i(s) \tag{2.15}$$

and

$$\tilde{B}(s) \triangleq \tilde{B}_l(s)\tilde{B}_{l-1}(s)\cdots\tilde{B}_1(s) \tag{2.16}$$

with

$$B_i(s) \triangleq I - \frac{2\mathrm{Re}\{p_i\}}{s+\bar{p}_i}\boldsymbol{\omega}_i\boldsymbol{\omega}_i^H,$$
$$\tilde{B}_i(s) \triangleq I - \frac{2\mathrm{Re}\{p_i\}}{s+\bar{p}_i}\tilde{\boldsymbol{\omega}}_i\tilde{\boldsymbol{\omega}}_i^H.$$

The factors M_m and $\tilde{M}_m$ are minimum phase.

While these factorizations can be explicitly constructed, they are not unique and depend on the specific order of the zeros or poles. It is also worth noting that, the allpass factors satisfy $B_i(0) = \tilde{B}_i(0) = L_i(0) = \tilde{L}_i(0) = I$.

2.3.6 Inner-outer factorization

Definition 2.11 (Inner and outer matrices in $\mathbf{R}\mathcal{H}_\infty$ [24])

1. *A matrix G in $\mathbf{R}\mathcal{H}_\infty$ is inner if and only if $G^{\sim}G = I$.*

2. *A matrix G in $\mathbf{R}\mathcal{H}_\infty$ is outer if and only if G has full row-rank for every $s \in \mathbb{C}_+$.*

An inner matrix must be tall and pre-multiplication by an inner matrix is $\mathcal{L}_2$ norm preserving. Likewise, an outer matrix must be wide and has a right inverse which is analytic in $\mathbb{C}_+$.

Theorem 2.12 (Inner-outer factorization) *If $G \in \mathbf{R}\mathcal{H}_\infty$, then there exists the inner-outer factorization*

$$G = G_i G_o, \tag{2.17}$$

in which the matrix G_i is inner and G_o is outer.

Definition 2.13 *A matrix G is called* co-inner *or* co-outer *if and only if G^T is inner or outer.*

A inner outer factorization of G^T yields the co-inner-outer factorization, which has the form

$$G = G_{co} G_{ci}. \tag{2.18}$$

2.3.7 Optimization in $\mathcal{H}_2$

For $F, G, Q, H \in \mathbf{R}\mathcal{H}_\infty$, define

$$J(Q) = \|F - GQH\|_2 .$$

In the thesis, we shall repeatedly encounter the $\mathcal{H}_2$ optimization problem

$$J^* \triangleq \inf_{Q \in \mathbf{R}\mathcal{H}_\infty} J(Q) \tag{2.19}$$

under the conditions that

Assumption 2.14

1. *F is strictly proper,*

2. *$G(\mathrm{j}\omega)$ has full row rank for all $0 \leq \omega \leq \infty$,*

3. *$H(\mathrm{j}\omega)$ is square and nonsingular for all $0 \leq \omega \leq \infty$.*

Because of the fact that $F - GQH$ is affine in Q and the property of the $\mathcal{H}_2$ norm, the functional $J(Q)$ is convex in Q. The optimization problem can be solved by using the decomposition (2.2) and the inner-outer factorization. To be more specific, factorize G and H as

$$G = G_i G_o,$$

$$H = H_{co} H_{ci}.$$

Then we have the following result

Theorem 2.15 *Under Assumption 2.14, the solution to (2.19) is given by*

$$J^* = \|I - G_i G\|_2^2 + \left\| [G_i^{\sim} F H_{ci}^{\sim}]_{\mathcal{H}_2^{\perp}} \right\|_2^2, \tag{2.20}$$

and the optimal $Q \in \mathbf{R}\mathcal{H}_\infty$ satisfies

$$G_o Q H_{co} = [G_i^{\sim} F H_{ci}^{\sim}]_{\mathcal{H}_2} \tag{2.21}$$

The proof of the theorem relies on the following lemma about a $\mathcal{L}_2$-norm preserving matrix [15, 24]

Lemma 2.16 *Let U be an inner matrix and define the matrix*

$$E \triangleq \begin{bmatrix} U^{\sim} \\ I - UU^{\sim} \end{bmatrix}. \tag{2.22}$$

Then, $E^{\sim} E = I$ and thus $\|EG\|_2^2 = \|G\|_2^2$.

Proof. This can be easily verified by basic algebraic manipulation. ■

Proof of Theorem 2.15. Since H is nonsingular, the co-inner factor H_{ci} is also square and nonsingular. Then we have

$$\begin{aligned} J &= \|F - G_i G_o Q H_{co} H_{ci}\|_2^2 \\ &= \|F H_{ci}^{\sim} - G_i G_o Q H_{co}\|_2^2 . \end{aligned}$$

Introduce the matrix

$$E = \begin{bmatrix} G_i^{\sim} \\ I - G_i G_i^{\sim} \end{bmatrix}.$$

It follows that

$$\begin{bmatrix} G_i^{\sim} \\ I - G_i G_i^{\sim} \end{bmatrix} G_i G_o Q H_{co} = \begin{bmatrix} G_o Q H_{co} \\ 0 \end{bmatrix}.$$

Pre-multiplying $F H_{ci}^{\sim} - G_i G_o Q H_{co}$ by E, we arrive at

$$J = \|G_i^{\sim} F H_{ci}^{\sim} - G_o Q H_{co}\|_2^2 + \|(I - G_i G_i^{\sim})\, F\|_2^2$$

since $\left\| \begin{bmatrix} A \\ B \end{bmatrix} \right\|_2^2 = \|A\|_2^2 + \|B\|_2^2$. Then, applying the decomposition (2.2) on $G_i^{\sim} F H_{ci}^{\sim}$, we have

$$\begin{aligned} J &= \left\| [G_i^{\sim} F H_{ci}^{\sim}]_{\mathcal{H}_2} - G_o Q H_{co} \right\|_2^2 + \left\| [G_i^{\sim} F H_{ci}^{\sim}]_{\mathcal{H}_2^{\perp}} \right\|_2^2 + \|(I - G_i G_i^{\sim})\, F\|_2^2 \\ &\geq \left\| [G_i^{\sim} F H_{ci}^{\sim}]_{\mathcal{H}_2^{\perp}} \right\|_2^2 + \|(I - G_i G_i^{\sim})\, F\|_2^2 \\ &= J^* \end{aligned}$$

and the theorem is proved. ■

Remark 2.17 *The second or third condition on Assumption 2.14 may not always hold. In the thesis, we shall run into the problem that G is strictly proper and in this case,* *the parameter Q^* that satisfies* (2.21) *does not belong to* $\mathbf{R}\mathcal{H}_\infty$. *However, we can always construct a suboptimal parameter (see, e.g. [67])*

$$Q_\epsilon \triangleq \frac{1}{(\epsilon s+1)^l} Q^* \tag{2.23}$$

where l is selected such that $Q_\epsilon \in \mathbf{R}\mathcal{H}_\infty$. It can be proven that

$$\lim_{\epsilon \rightarrow 0} J(Q_\epsilon) = J^*.$$

Therefore, (2.20) *still holds true.*

2.3.8 Partial fraction expansion

To yield possible explicit decomposition (2.2) and expressions for $\mathcal{H}_2$ optimization, we resort to the well-known partial fraction expansion technique. Here we develop a matrix variation of the partial fraction expansion, which will find applications in Chapter 3. The result is summarized in the following lemma:

Lemma 2.18 *Consider a matrix function $R \in \mathbf{R}\mathcal{H}_\infty$ and a collection of points $z_i \in \mathbb{C}_+$, $i = 1, \ldots, k$. Define allpass matrix functions $L(s)$ and $F(s)$ as*

$$L(s) = \prod_{i=1}^{k} L_i(s),$$

$$F(s) = L_k(s) L_{k-1}(s) \cdots L_1(s),$$

with

$$L_i(s) = I - \frac{2\mathrm{Re}\{z_i\}}{s+\bar{z}_i} \boldsymbol{\eta}_i \boldsymbol{\eta}_i^H$$

where $\|\boldsymbol{\eta}_i\| = 1$. Then the following equality holds for some $Y \in \mathbf{R}\mathcal{H}_\infty$:

$$L^{-1} R = Y + \sum_{i=1}^{k} L_k^{-1}(z_i) \cdots L_{i+1}^{-1}(z_i) L_i^{-1} L_{i-1}^{-1}(z_i) \cdots L_1^{-1}(z_i) R(z_i). \tag{2.24}$$

It is also true that for some $Z \in \mathbf{R}\mathcal{H}_\infty$,

$$RF^{-1} = Z + \sum_{i=1}^{k} R(z_i)L_1^{-1}(z_i)\cdots L_{i-1}^{-1}(z_i)L_i^{-1}L_{i+1}^{-1}(z_i)\cdots L_k^{-1}(z_i). \tag{2.25}$$

In addition, if R is a constant matrix, then Y and Z are also constant matrices.

Proof. We shall only prove (2.24). The second part (2.25) follows analogously. For $k = 1$, the lemma clearly holds and $L_1^{-1}(R - R(z_1)) = Y \in \mathbf{R}\mathcal{H}_\infty$. More generally, for any $i \in [1, k]$, and any constant matrices Z_1 and Z_2, it is true that

$$Z_1 L_i^{-1} Z_2 R = Y + Z_1 L_i^{-1} Z_2 R(z_i) \tag{2.26}$$

with $Y \in \mathbf{R}\mathcal{H}_\infty$.

Now for any $k > 1$, consider the case $i, j \in [1, k]$, $i \neq j$. Using the Sherman-Morrison formula, we have

$$L_i^{-1}(s) = I + \frac{2\mathrm{Re}\{z_i\}}{s - z_i}\boldsymbol{\eta}_i\boldsymbol{\eta}_i^H. \tag{2.27}$$

In light of (A.4), it is easy to verify that for any constant matrix Z we can construct a *constant* matrix Y_{ij} such that

$$\left(L_i^{-1} - L_i^{-1}(z_j)\right) Z \left(L_j^{-1} - L_j^{-1}(z_i)\right) = Y_{ij}.$$

If we define $Y = Y_{ij} - L_i^{-1}(z_j)ZL_j^{-1}(z_i)$, which is also constant, then

$$L_i^{-1}ZL_j^{-1} = Y + L_i^{-1}ZL_j^{-1}(z_i) + L_i^{-1}(z_j)ZL_j^{-1}. \tag{2.28}$$

Then, we can complete the proof by induction. To this end, suppose that the lemma is true for $k = n - 1$. There exists $Y_{n-1} \in \mathbf{R}\mathcal{H}_\infty$, such that

$$L_{n-1}^{-1}\cdots L_1^{-1}R = Y_{n-1} + \sum_{i=1}^{n-1} L_{n-1}^{-1}(z_i)\cdots L_{i+1}^{-1}(z_i)L_i^{-1}L_{i-1}^{-1}(z_i)\cdots L_1^{-1}(z_i)R(z_i). \tag{2.29}$$

It follows that for $k = n$,

$$L_n^{-1} \cdots L_1^{-1} R = L_n^{-1} Y_{n-1} + L_n^{-1} \sum_{i=1}^{n-1} L_{n-1}^{-1}(z_i) \cdots L_{i+1}^{-1}(z_i) L_i^{-1} L_{i-1}^{-1}(z_i) \cdots L_1^{-1}(z_i) R(z_i).$$

From (2.26), we obtain

$$L_n^{-1} Y_{n-1} = Y' + L_n^{-1} Y_{n-1}(z_n)$$

where $Y' \in \mathbf{R}\mathcal{H}_\infty$. Then, applying (2.28) to the second term of the equation, and making use of the equation (2.29) at $s = z_n$, we obtain that

$$L_n^{-1} \cdots L_1^{-1} R = Y_n + \sum_{i=1}^{n} L_n^{-1}(z_i) \cdots L_{i+1}^{-1}(z_i) L_i^{-1} L_{i-1}^{-1}(z_i) \cdots L_1^{-1}(z_i) R(z_i).$$

The matrix $Y_n \in \mathbf{R}\mathcal{H}_\infty$ is thus given by

$$Y_n = L_n^{-1}(Y_{n-1} - Y_{n-1}(z_n)) + \sum_{i=1}^{n-1} Y^{(i)},$$

where $Y^{(i)} \in \mathbf{R}\mathcal{H}_\infty$ is the remainder of the partial fraction expansion of

$$L_n^{-1} L_{n-1}^{-1}(z_i) \cdots L_{i+1}^{-1}(z_i) L_i^{-1} L_{i-1}^{-1}(z_i) \cdots L_1^{-1}(z_i) R(z_i)$$

by applying (2.28). The matrix $Y^{(i)}$ is a *constant* matrix if R is constant. Hence, if R is a constant matrix, then Y_n is also constant. ■

2.4 Convex Optimization

As the AWN channel is power constrained, we rely on constrained convex optimization to derive several main results of the thesis. Excellent materials on convex optimization are [7, 39]. In this section we shall give two fundamental results of the subjects.

The first is a general principle. It shows that minimization of a function of two variables can be performed one at a time [7].

$$\inf_{x,y} f(x,y) = \inf_{x} \tilde{f}(x) \tag{2.30}$$

where $\tilde{f}(x) = \inf_y f(x,y)$.

The second result is concerned with constrained optimization. The basic problem is:

$$\begin{aligned} \text{minimize} \quad & f(x), \\ \text{subject to} \quad & x \in \Omega,\ G(x) \leq 0, \end{aligned} \tag{2.31}$$

where Ω is a convex subset of a vector space X, f and G are real-valued convex functional on Ω. As we consider values in $\mathbb{R}$, the ordering is well-defined. Problem (2.31) is referred to as the general convex programming problem.

Introduce the *dual function* φ on $\mathbb{R}$ corresponding to (2.31) as

$$\varphi(v) = \inf_{x \in \Omega} [\, f(x) + vG(x)\,]\,.$$

It is easy to verify that $\varphi(v)$ is concave. The problem (2.31) can then be studied through *duality principle* by way of the *Lagrange multiplier* v. The following theorem, adopted as a special case of [39, section 8.6, Theorem 1], demonstrates the equivalence between the minimization of a convex function and the maximization of a concave function.

Theorem 2.19 (Lagrange duality [39]) *Let f be a real-valued convex function defined on a convex subset Ω of a vector space X, and let G be a convex mapping of X into $\mathbb{R}$. Suppose there exists an x_1 such that $G(x_1) < 0$ and the optimal value* $\inf\{\, f(x) : G(x) \leq 0,\, x \in \Omega\,\}$ *is finite. Then*

$$\inf_{\substack{G(x)\leq 0 \\ x\in\Omega}} f(x) = \max_{v \geq 0} \varphi(v) \tag{2.32}$$

and the maximum on the right is achieved by some $v^* \geq 0$

2.5 Stochastic Processes

As the communication channel we deal with is AWN channel, we need the framework of stochastic control system. Rather than examining precisely the transient behavior of stochastic control through stochastic calculus, we focus on and analyze only stationary characteristics using control system theory. In this section, we introduce the basic concepts (see, e.g. [4, 49]) pertaining to stochastic processes that will be referred to in the coming chapters.

A stochastic process (random process) is a family of (vector valued) random variables $\{\boldsymbol{x}(t) \in \mathbb{R}^n, t \in T\}$. The index t is often interpreted as time and belongs the the index set T. When $T = \{\ldots, -1, 0, 1, \ldots\}$ or $\{0, 1, 2, \ldots\}$, the stochastic process is referred to as discrete-time process; when $T = \{t : 0 \leq t < \infty\}$ or $\{t : -\infty < t < \infty\}$, the stochastic process is referred to as continuous-time process.

The complete description of $\boldsymbol{x}(t)$ requires the joint cumulative distribution function (CDF) of $\boldsymbol{x}(t_1), \boldsymbol{x}(t_2), \ldots, \boldsymbol{x}(t_k)$ for any k and arbitrary $t_i \in T$[1]. However, it suffices to consider the first and second moment statistics of the random process for the purpose of this thesis.

We assume the random process $\boldsymbol{x}(t)$ is real-valued.

Definition 2.20 *The mean of a random process $\boldsymbol{x}(t)$ is defined as $\mathcal{E}\{\boldsymbol{x}(t)\}$, which is denoted by $\boldsymbol{\mu}_{\boldsymbol{x}}(t)$.*

Higher moments of the random process are defined similarly.

[1] An exception is the Gaussian process, which is completely determined by its mean and covariance function.

Definition 2.21 *The covariance matrix of* $\boldsymbol{x}(t)$ *is denoted by* $R_x(t, t+\tau)$*, which is defined as*

$$R_x(t, t+\tau) \triangleq \mathcal{E}\left\{ (\boldsymbol{x}(t) - \boldsymbol{\mu}_{\boldsymbol{x}}(t)) (\boldsymbol{x}(t+\tau) - \boldsymbol{\mu}_{\boldsymbol{x}}(t+\tau))^T \right\}$$

for all t *and* $t+\tau$ *such that* $\boldsymbol{x}(t)$ *and* $\boldsymbol{x}(t+\tau)$ *are defined.*

The variance of $\boldsymbol{x}(t)$, denoted by $\sigma^2_{\boldsymbol{x}}(t)$, is thus given by

$$\sigma^2_{\boldsymbol{x}}(t) = \mathrm{Trace}\{R_x(t, t)\}. \tag{2.33}$$

Definition 2.22 *A pair of stochastic processes* $\boldsymbol{x}(t)$ *and* $\boldsymbol{y}(t)$ *are* uncorrelated *if their cross-covariance*

$$R_{xy} \triangleq \mathcal{E}\left\{ (\boldsymbol{x}(s) - \boldsymbol{\mu}_{\boldsymbol{x}}(s)) (\boldsymbol{y}(t) - \boldsymbol{\mu}_{\boldsymbol{y}}(t))^T \right\}$$

is 0 *for all* $s, t \in T$.

Given the above definitions, we will discuss some special stochastic processes that are of particular interest to the ensuing chapters.

Definition 2.23 (Stationary processes [1, 49])

1. *A stochastic process* $\boldsymbol{x}(t)$ *is* strict-sense stationary*, or simply* stationary *if any of its associated joint CDF's are unaffected by time translation.*

2. *A stochastic process* $\boldsymbol{x}(t)$ *is* wide-sense stationary *if the first and second moments of the distributions are invariant under time translation. In this case, the mean* $\boldsymbol{\mu}_{\boldsymbol{x}}(t)$ *is constant and the covariance* $R_x(t, t+\tau) = R_x(\tau)$*, and thus only depends on the time difference.*

Definition 2.24 (Second order) *A process $\boldsymbol{x}(t)$ is of second order if the second moment $\mathcal{E}\left\{ \boldsymbol{x}^T(t)\boldsymbol{x}(t) \right\} < \infty$ for all $t \in T$.*

For a process of second order the mean $\boldsymbol{\mu_x}(t)$ and the covariance function $R_x(t, t+\tau)$ exist.

Definition 2.25 (Power spectrum [49]) *The power spectrum matrix $G_x(s)$ for a wide-sense stationary stochastic process $\boldsymbol{x}(t)$ is the (bilateral) Laplace transform of the covariance matrix $R_x(\tau)$, as*

$$G_x(s) \triangleq \int_{-\infty}^{\infty} R_x(\tau)e^{-s\tau}\,\mathrm{d}\tau.$$

Remark 2.26 *The Wiener-Khinchin theorem states that the region of convergence of the above Laplace transform will at least include the imaginary axis $\mathbb{C}_0$, on which it yields $G_x(\mathrm{j}\omega)$, the* power spectral density *of $\boldsymbol{x}(t)$.*

It is worth noting that the variance of $\boldsymbol{x}(t)$

$$\sigma_{\boldsymbol{x}}^2(t) = \mathrm{Trace}\{R_x(0)\} = \int_{-\infty}^{\infty} \mathrm{Trace}\{G_x(\mathrm{j}\omega)\}\,\mathrm{d}\omega. \tag{2.34}$$

The covariance matrix of a wide-sense stationary stochastic process $\boldsymbol{x}(t)$ has the property that $R_x^T(\tau) = R_x(-\tau)$, therefore its power spectrum matrix satisfies $G_x^H(s) = G_x(-\bar{s})$. If we further assume that G_x is rational, it admits the *spectral factorization*

$$G_x = \Psi_x^{\sim}\Psi_x \tag{2.35}$$

and the spectral factor Ψ_x and its inverse Ψ_x^{-1} are both analytic in $\mathbb{C}_+$ [1, 68]. It then follows from (2.34) and the definition of the $\mathcal{H}_2$ norm that the variance of a second order stochastic process can be expressed as,

$$\sigma_{\boldsymbol{x}}^2 = \|\Psi_x(s)\|_2^2. \tag{2.36}$$

Definition 2.27 (White noise) *A process $\boldsymbol{x}(t)$ is referred to as a white noise process if it is zero mean, wide-sense stationary and has constant power spectral density.*

This is equivalent to

$$R_x(\tau) = C\delta(\tau)$$

for some constant matrix C, where $\delta(t)$ is the dirac delta function.

2.5.1 Stochastic process as input to LTI systems

Stability of LTI systems in the deterministic sense suggests bounded behavior of stochastic systems. In particular, if a LTI system is asymptotically stable[2], then the mean and the second moment of the state of the corresponding stochastic system converge and are finite[3], provided that the initial state random variable and the input process are both of second order (see [61, Section 4.4.5] or [4, Section 3.6]). If a wide-sense stationary random process $\boldsymbol{x}(t)$ passes through an asymptotically stable, LTI system described by the transfer function matrix $P(s)$, then the power spectrum of the output process $\boldsymbol{y}(t)$ (which is also wide-sense stationary) is given by [4, 49, 61]

$$G_y(s) = P(s)G_x(s)P^{\sim}(s).$$

A simple derivation shows an important fact about the variance of $\boldsymbol{y}(t)$:

Lemma 2.28 *Assume that $\boldsymbol{y}(t)$ is the output process of an internally stable LTI system $P(s)$ driven by a wide-sense stationary input process $\boldsymbol{x}(t)$ commencing in the infinitely remote past. Then $\boldsymbol{y}(t)$ is also wide-sense stationary and its variance is calculated as*

$$\sigma_{\boldsymbol{y}}^2 = \|P\Psi_x\|_2^2\,, \tag{2.37}$$

[2]The eigenvalues of the autonomous matrix A lie in $\mathcal{C}_-$.

[3]This is called the mean square stability of a stochastic system.

where Ψ_x is the power spectral factor of $\boldsymbol{x}(t)$.

This lemma serves as a cornerstone of the subsequent development of the thesis.

2.6 Summary

In this chapter, we have provided relevant concepts, definitions and technical tools that will be used repeatedly throughout the thesis. Specifically, as for LTI systems, we have introduced the notion of internal stability, coprime factorization, definitions of zeros and poles in multivariate systems and inner-outer factorizations. We have also presented the general procedures for $\mathcal{H}_2$ optimization and proved a form of matrix partial fraction expansion. Also, we have listed results in convex optimization. As we shall deal with communication channels, we have provided relevant results of stochastic processes and control.

Chapter 3

Tracking Performance over Uplink Channel

3.1 Introduction

In this chapter, we delve into the problem of the fundamental constraints that the uplink AWN channels impose on the tracking performance. First and foremost, we investigate the stabilization of MIMO systems over the parallel AWN channels. Although the stabilization results for SISO systems are available [9], as well as a stream of ensuing work such as [53,54], the more general MIMO configuration generates more complex results that have interesting properties we have not observed for single variable systems.

For standard control systems, the tracking performance depends solely on nonminimum phase zeros for SISO stable plants [43]. For MIMO unstable systems, the tracking capability is determined by the location and directional properties of the unstable poles and nonminimum phase zeros of the plant [19, 51, 65]. We show that these factors continue to play important roles in networked configurations, though in a much different way. This is expected since standard control systems can be considered as special cases of NCS's with communication channels being ideal. Furthermore, unique characteristics pertaining to networked configuration such as the spectral factor of the reference process, the power constraint and the noise levels, constrain the performance as well, which we have not seen previously.

It is expected that the best tracking performance is achieved when the channel input power constraint is fully utilized. Among various channel compensation/coding mechanisms, the simplest method, a pre- and post-scaling, can effectively adjust the power to its upper bound. This simple strategy is optimally designed and is shown to significantly improve the tracking performance.

It is well-known that for parallel AWGN channels sharing a total power constraint, the maximal capacity is achieved through allocating power using Shannon's classical "water-filling" solution. However, the solution maximizes the capacity without considering system specifications and thus is in general not adequate to characterize performance. As another important result in this chapter, we derive the optimal power allocation policy for tracking performance of MIMO systems.

The rest of the chapter is organized as follows: Section 3.2 introduces the problem and its mathematical formulation. In Section 3.3 we derive the conditions for stabilization of MIMO LTI systems over parallel AWN channels. Section 3.4 presents the results for the optimal tracking performance for both minimum phase and nonminimum phase MIMO systems, without considering scaling. Section 3.5 develops in parallel with Section 3.4 but investigates optimized scaling across the channel. Both sections present optimal power allocation strategies for the parallel channels. Section 3.6 numerically validates and demonstrates the previous results by examples of SISO plants.

3.2 Problem Formulation

We consider the specific configuration shown in Figure 3.1. The plant output is to track the reference input and the channel constrains the power of the feedback signal. That the channel input power is finite indicates that the system can only track reference process of second order. It then necessitates the following assumption:

Assumption 3.1 *The reference stochastic process $\boldsymbol{r}(t)$ is real, zero-mean, of second order and has a rational power spectrum matrix.*

It follows from (2.36) that the power of the reference input $\sigma_{\boldsymbol{r}}^2 = \|\Psi_r\|_2^2$.

A standard assumption in tracking problems is that the plant transfer function matrix is right-invertible (see, e.g., [19, 51]). Consequently, we shall impose the following assumption in this chapter.

Assumption 3.2 *The plant transfer function matrix $P(s)$ has full row rank for some $s \in \mathbb{C}$.*

We can then characterize the zeros and poles of the plant by way of the doubly coprime factorization (Lemma 2.5). Furthermore, suppose that the nonminimum phase zeros of the plant are ordered as $z_i \in \mathbb{C}_+$, $i = 1, \ldots, k$ and the unstable poles are ordered as $p_i \in \mathbb{C}_+$, $i = 1, \ldots, l$. Then we may apply the allpass factorizations illustrated in Section 2.3.5. The sequentially determined direction vectors associated with zero z_i and pole p_i are denoted by $\boldsymbol{\eta}_i$ and $\boldsymbol{\omega}_i$, respectively. We shall be particular interested in the factorizations (2.7) and (2.14).

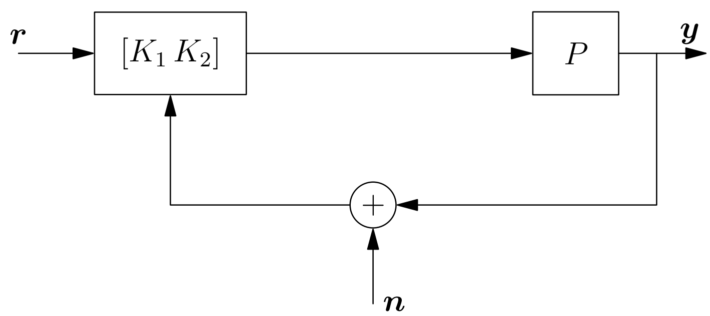

Figure 3.1: Tracking configuration over uplink AWN channel

The collection of *zero-mean* white noise of the parallel AWN channels is represented by the vector $\boldsymbol{n} = (n_1, \ldots, n_m)^T$ and Φ_i, $1 \leq i \leq m$ denote the power spectral density of the corresponding white noise process. It has power spectral factor $\Psi_n \triangleq \mathrm{diag}\{\sqrt{\Phi_1}, \ldots, \sqrt{\Phi_m}\}$ as we assume that the noise processes for two different channels n_i and n_j are uncorrelated for any $i \neq j$, $1 \leq i, j \leq m$. The channel input $\boldsymbol{u}$ is equal to the plant output $\boldsymbol{y}$. The tracking error is $\boldsymbol{e} = \boldsymbol{r} - \boldsymbol{y}$.

The performance problem of interest is that, under a given power constraint on the uplink channel, the smallest tracking error the system can achieve over all stabilizing LTI controllers $K = [K_1\ K_2]$. It can be formulated as

$$\begin{aligned} &\text{minimize} \quad \mathcal{E}\{\|\boldsymbol{e}\|^2\} \\ &\text{subject to} \quad \mathcal{E}\{\|\boldsymbol{u}\|^2\} \leq \Gamma,\ K \in \mathcal{K} \end{aligned} \tag{3.1}$$

where $\mathcal{K}$ is the parameterized set of all stabilizing controllers defined in (2.5). The problem (3.1) is a special case of the multiple objective optimal control problem [32].

Define $T^e_{r,n}$ and $T^u_{r,n}$ as the closed-loop transfer function from $\boldsymbol{r}$, $\boldsymbol{n}$ to $\boldsymbol{e}$ and $\boldsymbol{u}$, respectively. Then, it is straightforward to write

$$T^e_{r,n} = \Big[I - (I - PK_2)^{-1} PK_1, \quad -(I - PK_2)^{-1} PK_2 \Big],$$

$$T^u_{r,n} = \Big[(I - PK_2)^{-1} PK_1, \quad (I - PK_2)^{-1} PK_2 \Big].$$

Given the Youla parametrization (2.5), the optimization problem (3.1) is then equivalent to

$$\text{minimize} \quad \|T^e_{r,n}\Psi_{r,n}\|_2^2 \tag{3.2a}$$

$$\text{subject to} \quad \|T^u_{r,n}\Psi_{r,n}\|_2^2 \leq \Gamma, \quad Q, R \in \mathbf{R}\mathcal{H}_\infty \tag{3.2b}$$

where $\Psi_{r,n} \triangleq \text{diag}\{\Psi_r, \Psi_n\}$. The following lemma shows that (3.2) is a convex optimization problem.

Lemma 3.3 *Both* $\|T^e_{r,n}\Psi_{r,n}\|_2^2$ *and* $\|T^u_{r,n}\Psi_{r,n}\|_2^2$ *are convex functionals of* $(Q, R) \in \mathbf{R}\mathcal{H}_\infty \times \mathbf{R}\mathcal{H}_\infty$.

Proof. With the aid of Youla parametrization (2.5), the transfer matrices can be expressed as

$$T^e_{r,n} = \Big[I - NQ, \quad -N(\tilde{Y} - R\tilde{M}) \Big],$$

$$T^u_{r,n} = \Big[NQ, \quad N(\tilde{Y} - R\tilde{M}) \Big],$$

and each of the above entries is an affine function of Q or R. From the assumption that $\boldsymbol{r}$ and $\boldsymbol{n}$ are uncorrelated, we have

$$\|T^e_{r,n}\Psi_{r,n}\|_2^2 = \|(I - NQ)\Psi_r\|_2^2 + \|N(\tilde{Y} - R\tilde{M})\Psi_n\|_2^2, \tag{3.3a}$$

$$\|T^u_{r,n}\Psi_{r,n}\|_2^2 = \|NQ\Psi_r\|_2^2 + \|N(\tilde{Y} - R\tilde{M})\Psi_n\|_2^2. \tag{3.3b}$$

And they are convex functionals of $(Q, R) \in \mathbf{R}\mathcal{H}_\infty \times \mathbf{R}\mathcal{H}_\infty$ since the $\mathcal{L}_2$-norm functional is convex (cf. Section 2.3.7). ■

Definition 3.4 *The* feasibility set *of problem* (3.1) *is defined as*

$$\digamma \triangleq \left\{ \Gamma : \textit{There exists } K \in \mathcal{K} \textit{ with } \mathcal{E}\{\|\boldsymbol{u}\|^2\} \leq \Gamma \right\}. \tag{3.4}$$

On the set $\digamma$*, we define the* primal function *as*

$$H_e^*(\Gamma) \triangleq \inf \left\{ \mathcal{E}\{\|\boldsymbol{e}\|^2\} : K \in \mathcal{K},\ \mathcal{E}\{\|\boldsymbol{u}\|^2\} \leq \Gamma \right\}. \tag{3.5}$$

We have the following characterization of the primal function:

Lemma 3.5 *Let* $\epsilon \in [0, 1]$*, and define the following functional:*

$$H(\epsilon, Q, R, \Gamma) \triangleq (1-\epsilon)\|T_{r,n}^e \Psi_{r,n}\|_2^2 + \epsilon \left(\|T_{r,n}^u \Psi_{r,n}\|_2^2 - \Gamma \right). \tag{3.6}$$

If there exists $Q, R \in \mathbf{R}\mathcal{H}_\infty$ *such that*

$$\|T_{r,n}^u \Psi_{r,n}\|_2^2 < \Gamma, \tag{3.7}$$

then

$$H_e^*(\Gamma) = \sup_{0 \leq \epsilon \leq 1} \frac{1}{1-\epsilon} \left(\inf_{Q,R \in \mathbf{R}\mathcal{H}_\infty} H(\epsilon, Q, R, \Gamma) \right). \tag{3.8}$$

Proof. The lemma follows from Theorem 2.19 if we take $\mathbf{R}\mathcal{H}_\infty \times \mathbf{R}\mathcal{H}_\infty$ as Ω, and the dual function as $\frac{1}{1-\epsilon}\left(\inf_{Q,R \in \mathbf{R}\mathcal{H}_\infty} H(\epsilon, Q, R, \Gamma)\right)$.

The dual function gives a lower bound of $H_e^*(\Gamma)$ as

$$\frac{1}{1-\epsilon} \left(\inf_{Q,R \in \mathbf{R}\mathcal{H}_\infty} H(\epsilon, Q, R, \Gamma) \right) \leq H_e^*(\Gamma).$$

Then Lemma 3.3 and the condition (3.7) guarantee that the bound is tight and the equality is achieved by the right-hand side of (3.8). ■

Remark 3.6 *Define*

$$H^*(\epsilon) \triangleq \inf_{Q,R\in\mathbf{R}\mathcal{H}_\infty} H(\epsilon, Q, R, \Gamma).$$

There may not exist a pair $Q, R \in \mathbf{R}\mathcal{H}_\infty$ *to achieve* $H^*(\epsilon)$. *However, as discussed in Remark 2.17, the value of the functional* $H(\epsilon, Q, R, \Gamma)$ *can be made arbitrarily close to* $H^*(\epsilon)$ *by suitable choice of* $Q_\epsilon, R_\epsilon \in \mathbf{R}\mathcal{H}_\infty$ *as* $\epsilon \to 0$.

In later derivations, we shall need the allpass factorization (cf. Section 2.3.5) of the transfer function matrix $\tilde{M}\Psi_n$, which shares the same nonminimum phase zeros as $\tilde{M}$, but their input directions are altered by the different noise levels (cf. (2.14)). Specifically, the factorization takes the form

$$\tilde{M}(s)\Psi_n = \tilde{M}_m^{(n)}(s)F(s) \tag{3.9}$$

where the matrix $\tilde{M}_m^{(n)}(s)$ is minimum phase and $F(s)$ is the allpass factor. Following the same iterative procedure in constructing (2.13), we have

$$F(s) \triangleq F_l(s)F_{l-1}(s)\cdots F_1(s) \tag{3.10}$$

with

$$F_i(s) \triangleq I - \frac{2\mathrm{Re}\{p_i\}}{s+\bar{p}_i}\boldsymbol{\zeta}_i\boldsymbol{\zeta}_i^H. \tag{3.11}$$

The unitary vector $\boldsymbol{\zeta}_i$ is a zero direction vector of $\tilde{M}_m^{(n)}(s)F_l(s)\cdots F_i(s)$ and we explicitly express the vector as $\left(\zeta_i^1, \ldots, \zeta_i^m\right)^T$.

3.3 Stabilization

The power constraint of the parallel AWN channels determines the capacity and the limitation they impose on the system. What is the lower bound on the power constraint that ensures the stabilizability? The problem is mathematically equivalent to the feasibility of (3.1) when the reference is zero, or the minimal Γ such that the feasibility set $\mathcal{F}$ is nonempty. Thus, the necessary and sufficient condition on the power constraint for stabilizability is given by

$$\Gamma > \mu \triangleq \inf_{K\in\mathcal{K}} \mathcal{E}\{\|\boldsymbol{u}\|^2\}. \tag{3.12}$$

From (3.2b) and (3.3b), we have

$$\mu = \inf_{R\in\mathbf{R}\mathcal{H}_\infty} \left\| N(\tilde{Y} - R\tilde{M})\Psi_n \right\|_2^2. \tag{3.13}$$

As stabilization bears no relations to the reference input, it suffices to consider only one-parameter controller, which has another form of parametrization given by $K_2 = (Y - MR)(X - NR)^{-1}$ (see (2.6)). Then, after a simple calculation of the parameterized transfer function T_n^u, we have

$$\mu = \inf_{R\in\mathbf{R}\mathcal{H}_\infty} \left\| \left[-I + (X - NR)\tilde{M} \right] \Psi_n \right\|_2^2. \tag{3.14}$$

3.3.1 Minimum phase plants

The following result gives an explicit expression of μ for minimum phase plants.

Theorem 3.7 *Suppose P is right-invertible and has unstable poles p_i, $i = 1, \ldots, l$. Suppose further that $\tilde{M}(s)\Psi_n$ is factorized as in* (3.9). *Then the feedback system is stabilizable if and only if $\Gamma > \mu_m$, where*

$$\mu_m = 2\sum_{i=1}^{l} p_i \sum_{j=1}^{m} |\zeta_i^j|^2 \Phi_j. \tag{3.15}$$

The requirement on the channel input for stabilizability depends not only on the unstable poles, but their input directions which is altered by the noise levels Ψ_n.

Proof. The proof is concerned with the calculation of (3.13). For notation simplicity, we define

$$H_2 \triangleq \left\| N(\tilde{Y} - R\tilde{M})\Psi_n \right\|_2^2.$$

Then, a simple algebraic manipulation yields

$$H_2 = \left\| \left(-I + \left((N\tilde{Y} + I)\tilde{M}^{-1} - NR \right) \tilde{M} \right) \Psi_n \right\|_2^2.$$

If we let $Z = (N\tilde{Y} + I)\tilde{M}^{-1}$, it is true that $Z \in \mathbf{R}\mathcal{H}_\infty$. In fact, from the Bezout identity $\tilde{X}M - \tilde{Y}N = I$, we obtain $N\tilde{X} - N\tilde{Y}P = P$, which implies

$$N\tilde{X} = (N\tilde{Y} + I)\tilde{M}^{-1}\tilde{N}.$$

Since $N\tilde{X} \in \mathbf{R}\mathcal{H}_\infty$ and $\tilde{N} \in \mathbf{R}\mathcal{H}_\infty$ and is minimum phase, it follows that $Z \in \mathbf{R}\mathcal{H}_\infty$. We then make use of the factorization (3.9) and the fact $(F^{-1} - I) \in \mathcal{H}_2^\perp$ to arrive at

$$\mu = \left\| \Psi_n(F^{-1} - I) \right\|_2^2 + \inf_{R \in \mathbf{R}\mathcal{H}_\infty} \left\| \Psi_n - (Z - NR)\, \tilde{M}_m^{(n)} \right\|_2^2,$$

and

$$\inf_{R \in \mathbf{R}\mathcal{H}_\infty} \left\| \Psi_n - (Z - NR)\, \tilde{M}_m^{(n)} \right\|_2^2 = 0.$$

Then,

$$\begin{aligned}
\mu &= \left\| \Psi_n(F^{-1} - I) \right\|_2^2 \\
&= \sum_{i=1}^{l} \left\| \frac{2\mathrm{Re}\{p_i\}}{s - p_i} \Psi_n \zeta_i \right\|_2^2 \\
&= \sum_{i=1}^{l} \left\| \frac{2\mathrm{Re}\{p_i\}}{s - p_i} \right\|_2^2 \left\| \Psi_n \zeta_i \right\|^2.
\end{aligned}$$

Lastly, by applying the residue theorem [48], we have

$$\left\| \frac{2\mathrm{Re}\{p_i\}}{s - p_i} \right\|_2^2 = 2\mathrm{Re}\{p_i\},$$

and the theorem is proved. ■

3.3.2 Nonminimum phase plants

The stabilization bound for Γ for nonminimum phase plants over uplink AWN channel is given by the following theorem:

Theorem 3.8 *Let P be right-invertible and have unstable poles p_i, $i = 1, \ldots, l$ and nonminimum phase zeros z_i, $i = 1, \ldots, k$. Then the feedback system is stabilizable if and only if $\Gamma > \mu_n$, and*

$$\mu_n = \mu_m + \sum_{i,j=1}^{k} \frac{4\mathrm{Re}\{z_i\}\mathrm{Re}\{z_j\}}{\bar{z}_i + z_j} \boldsymbol{v}_i^H \boldsymbol{v}_j \boldsymbol{w}_j^H \boldsymbol{w}_i, \tag{3.16}$$

where

$$\boldsymbol{v}_i \triangleq \left(\prod_{j=i+1}^{k} L_j(z_i) \right)^{-1} \boldsymbol{\eta}_i,$$
$$\boldsymbol{w}_i \triangleq \left(I - F^{-H}(z_i)\right) \Psi_n \left(\prod_{j=1}^{i-1} L_j(z_i) \right)^{-H} \boldsymbol{\eta}_i.$$

Proof. See Appendix A.1. ■

As expected, the presence of nonminimum phase zeros causes steeper requirement on the power constraint of the AWN channel, especially when they are close to the unstable poles, as captured by the term $\boldsymbol{w}_i$. It is conceivable that the tracking performance will be affected in the same way as we show that it depends directly on μ_n.

We analyze the theorems by solving a few special cases. For SISO systems, Theorem 3.7 reduces to

$$\Gamma > \mu_m = 2\Phi \sum_{i=1}^{l} p_i \tag{3.17}$$

With regard to SISO nonminimum phase systems and Theorem 3.8, we have the following simplifications:

$$L_i(s) = \frac{s - z_i}{s + \bar{z}_i} \qquad F(s) = \prod_{i=1}^{l} \frac{s - p_i}{s + \bar{p}_i}$$

$$v_i \bar{w}_i = \sqrt{\Phi}\left(1 - F^{-1}(z_i)\right) \prod_{\substack{j=1 \\ j \neq i}}^{k} \frac{z_j + \bar{z}_i}{z_j - z_i}.$$

Thus the stabilization condition reduces to

$$\Gamma > \mu_n = \Phi \left(2 \sum_{i=1}^{l} p_i + \sum_{i,j=1}^{k} \frac{\bar{\nu}_i \nu_j}{\bar{z}_i + z_j} \right) \tag{3.18}$$

where

$$\nu_i \triangleq 2\mathrm{Re}\{z_i\}(1 - F^{-1}(z_i)) \prod_{\substack{j=1 \\ j \neq i}}^{k} \frac{z_j + \bar{z}_i}{z_j - z_i}.$$

Thus, for SISO systems the SNR of the channel suffices to be an essential figure of merit. Both results agree with those for continuous time systems in [9].

For MIMO systems, we assume that the plant has only one (real) pole, p with a right pole direction $\boldsymbol{\omega}$. In this case, the direction vector $\boldsymbol{\zeta}$ in (3.11) has a simple expression given as

$$\boldsymbol{\zeta} = \frac{\Psi_n^{-1}\boldsymbol{\omega}}{\|\Psi_n^{-1}\boldsymbol{\omega}\|}.$$

It follows that

$$\mu_m = \frac{2p}{\left\|\Psi_n^{-1}\boldsymbol{\omega}\right\|^2}.$$

Furthermore, if the plant has a single zero z along with its direction vector $\boldsymbol{\eta}$, we have

$$\boldsymbol{v} = \boldsymbol{\eta} \qquad \boldsymbol{w} = \frac{2p}{p - z} \boldsymbol{\zeta}\boldsymbol{\zeta}^H \Psi_n \boldsymbol{\eta}.$$

The stabilization condition reduces to

$$\Gamma > \frac{2p}{\left\|\Psi_n^{-1}\boldsymbol{\omega}\right\|^2} \left[1 + \left(\left(\frac{z + p}{z - p} \right)^2 - 1 \right) \cos^2 \angle(\boldsymbol{\eta}, \boldsymbol{\omega}) \right].$$

It is clear that the proximity of zero and pole location is detrimental and causes large response at the channel input, thus a large channel input power is needed for stabilization. Also, the power of channel input behaves differently depending on the alignment of zero and pole directions. An orthogonal pair of directions completely eliminates the effect of the real nonminimum phase zero on stabilization. Another interesting observation is that, when the noise at any of the channel Φ_i is 0, then the total power of the channel input for stabilization is also 0 because of the term $\left\|\Psi_n^{-1}\boldsymbol{\omega}\right\|^2$. The direction $\boldsymbol{\zeta}$ is optimized to be an Euclidean vector with 1 at the i-th element. Along this direction, the controller can suppress the effect of the pole on all noise inputs except the i-th channel and thus zero the plant output. However, this property does not carry over to plants with multiple poles.

If the plant contains multiple zeros, the expression of μ becomes cumbersome. But if we follow (3.13) instead of (3.14), we obtain another equivalent form of μ_n which allows us to derive the following result:

$$\Gamma > \frac{2p}{\left\|\Psi_n^{-1}\boldsymbol{\omega}\right\|^2}\left\|L^{-1}(p)\boldsymbol{\omega}\right\|^2.$$

3.4 Optimal Tracking Performance

In this section, we shall look into the tracking performance under the AWN channel constraints (3.1) provided that the problem is feasible or, equivalently, the system is stabilizable. It appears that the less noisy the channel is, the better performance the system can achieve. However, we will show that, sending the signal to the channel without processing, the performance cannot be adequately improved by increasing the channel SNR.

In general, the power spectrum of the reference process has direct impact on the tracking performance. For minimum phase plants, however, optimal tracking performance only depends on the power of the reference.

3.4.1 Minimum phase plants

The following theorem characterizes the best tracking performance of the system depicted in Figure 3.1

Theorem 3.9 *If P is minimum phase and has poles $p_i \in \mathbb{C}_+$, $i = 1, \dots, l$. The power of the reference process is $\sigma_{\boldsymbol{r}}^2$. Then, under the condition $\Gamma > \mu_m$ where μ_m is defined in* (3.15), *the best tracking performance is given by*

$$H_e^*(\Gamma) = \begin{cases} \left(\sqrt{\sigma_{\boldsymbol{r}}^2} - \sqrt{\Gamma - \mu_m}\right)^2 + \mu_m, & \text{if } \mu_m < \Gamma < \Gamma_{max}, \\ \mu_m, & \text{if } \Gamma \geq \Gamma_{max}, \end{cases} \tag{3.19}$$

where $\Gamma_{max} \triangleq \mu_m + \sigma_{\boldsymbol{r}}^2$.

Proof. See Appendix A.2. ■

It is well known that for minimum phase systems in the absence of communication channels, perfect tracking can be achieved [19]. However, in a networked control setting, the AWN channel imposes additional constraint. Indeed, when $\Gamma \geq \Gamma_{max}$, the tracking error cannot be made smaller than μ_m. Thus it is no longer possible to recover perfect tracking even when the channel power constraint goes to infinity. This performance downgrade is due to the channel's restriction on the feedback, since to track the reference input, the power of the plant output cannot be allowed arbitrarily large and the channel may not be efficiently utilized. To see it more clearly, we derive the channel input power under the optimal control scheme:

$$\mathcal{E}\{\|\boldsymbol{u}\|^2\} = \begin{cases} \Gamma, & \text{if } \mu_m < \Gamma < \Gamma_{max}, \\ \Gamma_{max}, & \text{if } \Gamma \geq \Gamma_{max}. \end{cases}$$

Therefore, the maximum channel input power consumed for optimal tracking is Γ_{max} even when $\Gamma > \Gamma_{max}$. In the next subsection, we introduce and design scaling across the channel to address the saturation of the channel input power.

3.4.1.1 Power allocation

The parallel AWN channels, as depicted in Figure 3.2, share a common input power constraint and we examine how the power is allocated among each channel under the optimal tracking scheme.

Corollary 3.10 *Under the assumptions in Theorem 3.9, to achieve the best tracking performance, the power distributed to the k-th AWN channel out of the total power Γ is given by*

$$\mathcal{E}\{u_k^2\} = \begin{cases} \frac{\Gamma-\mu_m}{\sigma_r^2}\sigma_{rk}^2 + 2\sum\limits_{i=1}^{l} p_i|\zeta_i^k|^2\Phi_k, & \textit{if } \mu_m < \Gamma < \Gamma_{max}, \\ \sigma_{rk}^2 + 2\sum\limits_{i=1}^{l} p_i|\zeta_i^k|^2\Phi_k, & \textit{if } \Gamma \geq \Gamma_{max}. \end{cases}$$

Proof. Define the Euclidean vector $\boldsymbol{e}_k \triangleq (0,\ldots,0,\underset{k}{1},0,\ldots,0)^T$. The power allocated to the k-th channel can be evaluated using

$$\begin{aligned} \mathcal{E}\{u_k^2\} &= \|\boldsymbol{e}_k^T T_{r,n}^u \Psi_{r,n}\|_2^2 \\ &= \|\boldsymbol{e}_k^T N Q^* \Psi_r\|_2^2 + \|e_k^T N(\tilde{Y} - R^*\tilde{M})\Psi_n\|_2^2. \end{aligned}$$

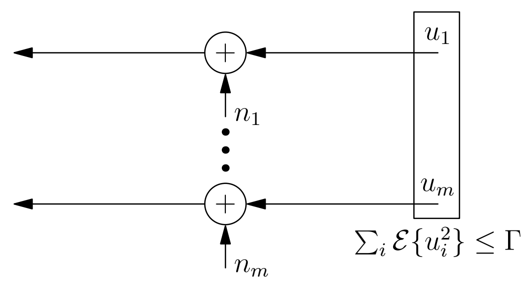

Figure 3.2: Parallel AWN channel

For the first term, using the optimal parameters Q^* as found in (A.9), we obtain that

$$\begin{aligned}\|\boldsymbol{e}_k^T N Q^* \Psi_r\|_2^2 &= \|\,(1-\epsilon^*)\,\boldsymbol{e}_k^T \Psi_r\|_2^2\\ &= (1-\epsilon^*)^2\,\sigma_{rk}^2.\end{aligned}$$

But $(1-\epsilon^*) = 1/(1+\alpha^*)$ and it can be derived using (A.12).

For the second term, we make use of R^* found in the proof of Theorem 3.7 and have

$$\|\boldsymbol{e}_k^T N(\tilde{Y} - R^*\tilde{M})\Psi_n\|_2^2 = \left\|\boldsymbol{e}_k^T \Psi_n (F^{-1} - I)\right\|_2^2.$$

Then we can prove the corollary after straightforward calculations. ■

We shall postpone the discussion of the power allocation result until after Corollary 3.13.

3.4.2 Nonminimum phase plants

For general MIMO nonminimum phase plants, the power spectrum of the reference signal together with nonminimum phase zeros incur additional penalties. We explicitly characterize the optimal tracking performance (3.1) in the following theorem.

Theorem 3.11 *Let the reference signal be specified as in Assumption 3.1 and have power spectral factor Ψ_r. Suppose the plant P is right-invertible and has unstable poles p_i, $i =$*

$1, \ldots, l$ *and nonminimum phase zeros* z_i, $i = 1, \ldots, k$. *Let* $N(s)$ *and* $\tilde{M}(s)\Psi_n$ *be factorized as in* (2.7) *and* (3.9)*, respectively. The AWN channel has input power constraint* $\mathcal{E}\{\|\boldsymbol{u}\|^2\} \leq \Gamma$. *Define*

$$Z \triangleq L^{-1}\Psi_r - \sum_{i=1}^{k} \frac{2\mathrm{Re}\{z_i\}}{s - z_i} \boldsymbol{a}_i \boldsymbol{b}_i^H,$$

where

$$\boldsymbol{a}_i \triangleq L_k^{-1}(z_i) \cdots L_{i+1}^{-1}(z_i)\boldsymbol{\eta}_i,$$
$$\boldsymbol{b}_i \triangleq \Psi_r^H(z_i) \left(\prod_{j=1}^{i-1} L_j^{-H}(z_i) \right) \boldsymbol{\eta}_i.$$

The best tracking performance is given by

$$H_e^* = \begin{cases} \left(\|Z\|_2 - \sqrt{\Gamma - \mu_n}\right)^2 + \mu_n + \delta, & \text{if } \mu_n < \Gamma < \Gamma'_{max}, \\ \mu_n + \delta, & \text{if } \Gamma \geq \Gamma'_{max}, \end{cases} \tag{3.20}$$

where $\Gamma'_{max} \triangleq \mu_n + \|Z\|_2^2$ *and*

$$\delta \triangleq \sum_{i,j=1}^{k} \frac{4\mathrm{Re}\{z_i\}\mathrm{Re}\{z_j\}}{\bar{z}_i + z_j} \boldsymbol{a}_i^H \boldsymbol{a}_j \boldsymbol{b}_j^H \boldsymbol{b}_i.$$

Proof. See Appendix A.3. ■

If the plant output is sent directly to the channel, the smallest tracking performance achievable is $\mu_n + \delta$, which happens as Γ exceeds Γ'_{max}. The term μ_n is due to the requirement for stabilization on the channel, whereas δ is independent of the channel and marks the effect of nonminimum phase zeros coupled with the reference input process. The result is consistent with and similar to the additional constraint caused by nonminimum phase zeros in standard control systems (cf. [15, 19, 62]). The theorem also shows explicitly how the performance is limited when the channel power constraint is not adequate to cope with the adverse effect of the reference input (characterized by $\|Z\|_2^2$).

3.5 Optimal Tracking Performance with Scaling

As shown in Figure 3.3, we introduce a channel compensation strategy consisting of a pre- and post-processing scheme via constant scaling. The scaling factor is defined by $\Lambda \triangleq \mathrm{diag}\{\lambda_1, \ldots, \lambda_m\}$, with $\lambda_i \in \mathbf{R}^+$, $1 \leq i \leq m$. The idea lies in how to exploit the channel to the maximum extent allowable under the power constraint, and at the same time reduce the noise effect. We show explicitly how this simple or even naive scheme may improve tracking performance, and how the scheme should be optimally designed.

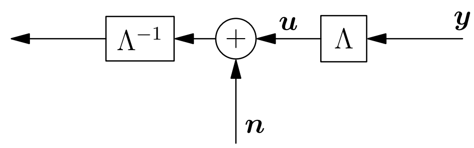

Figure 3.3: Scaling for the AWN channel

For a general scaling factor Λ, we have the freedom to tune the input power for each channel; however, it also rotates the direction of the vector signals in the system. Thus, the scaling around the channel cannot be canceled for MIMO systems by completing the closed loop. For this reason, it complicates the stabilization result as well as optimization. For consistency with the stabilization results that should be a system property and for simplicity, we shall consider the case $\Lambda = \lambda I$, i.e. a uniform scaling factor λ that acts on each channel. The optimal tracking problem can then be formulated as

$$\text{minimize} \quad \mathcal{E}\{\|\boldsymbol{e}\|^2\} \tag{3.21a}$$

$$\text{subject to} \quad \mathcal{E}\{\|\boldsymbol{u}\|^2\} \leq \Gamma, \tag{3.21b}$$

$$K \in \mathcal{K}, \quad \lambda \in \mathbf{R}^+. \tag{3.21c}$$

In this case, the transfer function matrices are given by

$$T^e_{r,n} = \begin{bmatrix} I - NQ, & -\frac{1}{\lambda}N(\tilde{Y} - R\tilde{M}) \end{bmatrix},$$

$$T^u_{r,n} = \begin{bmatrix} \lambda NQ, & N(\tilde{Y} - R\tilde{M}) \end{bmatrix}.$$

And we note that Lemma 3.5 still holds with a simple modification that includes the scaling factor. We define the same functional as (3.6), which depends on λ and can be expressed as

$$H(\epsilon, Q, R, \lambda, \Gamma) = \left\| \begin{bmatrix} \sqrt{1-\epsilon}(I - NQ) \\ \lambda\sqrt{\epsilon}NQ \end{bmatrix} \Psi_r \right\|_2^2 + \left(\frac{1-\epsilon}{\lambda^2} + \epsilon \right) \left\| N(\tilde{Y} - R\tilde{M})\Psi_n \right\|_2^2 - \epsilon\Gamma. \tag{3.22}$$

If there exists an interior point of (Q, R) such that (3.7) holds, then from the principle (2.30) the optimal tracking performance is specified by

$$H_e^*(\Gamma) = \inf_{\lambda > 0} H_e(\Gamma, \lambda), \tag{3.23}$$

where

$$H_e(\Gamma, \lambda) = \sup_{0 \le \epsilon \le 1} \frac{1}{1-\epsilon} \left(\inf_{Q, R \in \mathbf{R}\mathcal{H}_\infty} H(\epsilon, Q, R, \lambda, \Gamma) \right).$$

3.5.1 Minimum phase plants

It is shown in the following theorem that the tracking performance is inversely proportional to the power constraint.

Theorem 3.12 *Suppose that the plant, reference process and the channel satisfy the same assumptions in Theorem 3.9. Consider the scaling depicted in Figure 3.3 with $\Lambda = \lambda I$. The best tracking performance is given by*

$$H_e^*(\Gamma) = \sigma_{\boldsymbol{r}}^2 \frac{\mu_m}{\Gamma}, \tag{3.24}$$

which is achieved when the optimal scaling factor is

$$\lambda^* = \frac{\Gamma}{\sqrt{\sigma_{\boldsymbol{r}}^2(\Gamma - \mu_m)}}. \tag{3.25}$$

Proof. The first part of the proof is similar to that of Theorem 3.9, only that we need to consider λ as a design variable. We start with (3.22) and follow similar steps. The inner matrix corresponding to (A.6) is given by

$$\Delta = \frac{1}{\sqrt{\lambda^2\epsilon + 1 - \epsilon}} \begin{bmatrix} -\sqrt{1-\epsilon} I \\ \\ \lambda\sqrt{\epsilon} I \end{bmatrix}$$

and we can proceed following similar steps.

Define

$$H^*(\epsilon, \lambda, \Gamma) \triangleq \inf_{Q,R \in \mathbf{R}\mathcal{H}_\infty} H(\epsilon, Q, R, \lambda, \Gamma).$$

Then,

$$H^*(\epsilon, \lambda, \Gamma) = \frac{\lambda^2\epsilon(1-\epsilon)}{\lambda^2\epsilon + 1 - \epsilon}\sigma_{\boldsymbol{r}}^2 + \left(\frac{1-\epsilon}{\lambda^2} + \epsilon\right)\mu_m - \epsilon\Gamma.$$

Also define the Lagrange multiplier as $\alpha = \epsilon/(1-\epsilon)$, then

$$H_e(\Gamma, \lambda) = \sup_{\alpha > 0}\left(\frac{\alpha\lambda^2}{1 + \alpha\lambda^2}\sigma_{\boldsymbol{r}}^2 + \frac{1}{\lambda^2}\mu_m + \alpha(\mu_m - \Gamma)\right).$$

The optimal α is given by

$$\alpha^* = \frac{\sqrt{\sigma_{\boldsymbol{r}}^2}}{\lambda\sqrt{\Gamma - \mu_m}} - \frac{1}{\lambda^2} \tag{3.26}$$

and it follows that

$$H_e(\Gamma, \lambda) = \frac{\Gamma}{\lambda^2} - \frac{2\sqrt{(\Gamma - \mu_m)\sigma_{\boldsymbol{r}}^2}}{\lambda} + \sigma_{\boldsymbol{r}}^2,$$

which achieves its minimum at (3.25). ∎

Not surprisingly, by optimally designing the scaling factor, the power of the channel input is active at Γ and the noise effect on the system is suppressed. The tracking performance is improved, more significantly when $\Gamma > \Gamma_{max}$, by this simple scaling scheme. Only in the limit when $\Gamma \to \infty$, i.e., the channel has no input power constraint, the system can achieve zero tracking error that is comparable with the perfect tracking of step signal for standard minimum phase control systems [19]. Therefore for feedback control over AWN channels, an additional limitation on the tracking performance results, which persists even when an extra design freedom is made available in selecting the scaling factor.

3.5.1.1 Power allocation

The power allocation is similar to Corollary 3.10 except that the saturation case when $\Gamma > \Gamma_{max}$ is eliminated by the design of the scaling.

Corollary 3.13 *Under the optimal scaling and control scheme in Theorem 3.12. The power allotment for the k-th channel out of the total power constraint Γ is*

$$\frac{\Gamma - \mu_m}{\sigma_{\boldsymbol{r}}^2}\sigma_{rk}^2 + 2\sum_{i=1}^{l} p_i|\zeta_i^k|^2\Phi_k.$$

For achieving the optimal tracking performance, the power allocation policy essentially resembles "fire-quenching" as Corollary 3.10 and 3.13 demonstrate that the controller allocates more power to more problematic channels, i.e. the channel that has a greater noise power or has to deal with a stronger reference input. This strategy departs fundamentally from Shannon's classical "water-filling" solution [20, 66], which gives more power to better channels and aims at maximizing channel capacity. This deviation reflects from another perspective that channel capacity is generally not suitable for the characterization of feedback control over communication channels.

3.5.1.2 SISO systems

There are no spatial properties involved for SISO systems and the result for tracking will be further simplified as a function of the SNR.

Corollary 3.14 *Let P be a scalar transfer function, minimum phase and have unstable poles p_i, $i = 1, \ldots, l$. Also, let Φ denote the power spectral density of n. Then the system is stabilizable if and only if*

$$\frac{\Gamma}{\Phi} > 2 \sum_{i=1}^{l} p_i.$$

Under this condition, the best tracking performance is

$$H_e^* = \sigma_r^2 \left(2 \sum_{i=1}^{l} p_i \right) \frac{\Phi}{\Gamma}.$$

3.5.1.3 Fully decentralized structure

Here we consider the general scaling Λ around the AWN parallel channels as shown in Figure 3.4. We shall, however, impose constraints on the structure of the system. To be more specific, we assume that it is fully decentralized: the controller and the plant have the same number of input as the output and they are completely decoupled, i.e. $P(s) = \mathbf{diag}\{P_1(s), \ldots, P_m(s)\}$. Then it is equivalent to considering separately different SISO systems/agents except that the output of the plant is fed back via parallel AWN channels sharing a common power constraint, Γ. This scenario is applicable when we have a few independently controlled systems, but the measured outputs are sent jointly through an MIMO communication channel to the controllers.

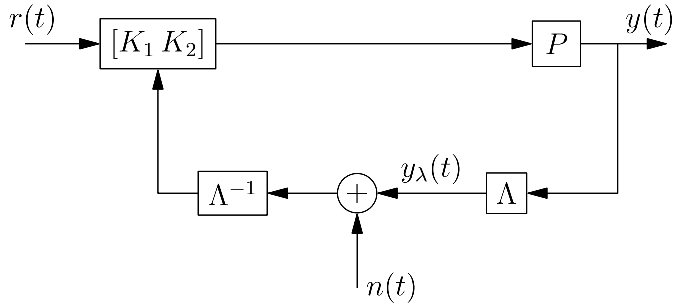

Figure 3.4: Tracking over parallel AWN channel with scaling

We assume that each SISO plant P_i is minimum phase[1]. Further assume that the stabilization threshold for P_i over an AWN channel is μ_i. As we have individual scaling factor for each SISO system, we may apply Corollary 3.14 and have the tracking performance for the i-th agent as

$$J_i^* = \sigma_{ri}^2 \frac{\mu_i}{\gamma_i},$$

under the condition $\gamma_i \geq \mu_i$, where γ_i is the input power allocated for the i-th channel. We shall study the best achievable tracking performance and power allocation problem of such systems under the total power constraint Γ. The problem can be formulated as a convex optimization problem:

$$\begin{array}{ll} \text{minimize} & \displaystyle\sum_{i=1}^{m} \sigma_{ri}^2 \frac{\mu_i}{\gamma_i} \\ \text{subject to} & \gamma_i \geq \mu_i,\ 1 \leq i \leq m, \quad \displaystyle\sum_{i=1}^{m} \gamma_i = \Gamma. \end{array}$$

The solution is summarized in the following corollary:

Corollary 3.15 *Assume that the control system in Figure 3.4 is decoupled and have m*

[1]This assumption is for the simplicity of the result. The nonminimum phase case can be derived similarly, with assumptions on the reference input and an additional term caused by the nonminimum phase zeros. (See the theorems of the next section.)

inputs and outputs. If $\Gamma > \sum_{i=1}^{m} \mu_i$*, then the optimal tracking performance is given by*

$$\sum_{i=1}^{m} \sigma_{ri}^2 \frac{\mu_i}{\gamma_i^*},$$

where

$$\gamma_i^* = \max\left\{\mu_i, \sigma_{ri}\sqrt{\frac{\mu_i}{\nu^*}}\right\}$$

with ν^* *determined from*

$$\sum_{i=1}^{m} \max\left\{\mu_i, \sigma_{ri}\sqrt{\frac{\mu_i}{\nu^*}}\right\} = \Gamma.$$

Proof. This problem can be solved using Lagrange multipliers. Introducing Lagrange multipliers $\boldsymbol{\lambda}^* \in \mathbb{R}^m$ for the inequality constraints and a multiplier $\nu^* \in \mathbb{R}$ for the equality constraint, we obtain the Kuhn-Tucker conditions [7]

$$\begin{aligned}
&\gamma_i^* - \mu_i \geq 0, \quad 1 \leq i \leq m, \qquad \sum_{i=1}^{m} \gamma_i^* = \Gamma,\\
&\boldsymbol{\lambda}^* \geq 0 \qquad \lambda_i^*(\gamma_i^* - \mu_i) = 0,\\
&-\frac{\sigma_{ri}^2 \mu_i}{\gamma_i^{*2}} - \lambda_i^* + \nu^* = 0, \quad 1 \leq i \leq m.
\end{aligned}$$

By eliminating λ^*, we obtain

$$\begin{aligned}
&\gamma_i^* - \mu_i \geq 0, \quad 1 \leq i \leq m, \qquad \sum_{i=1}^{m} \gamma_i^* = \Gamma, \qquad \lambda^* \geq 0\\
&(\nu^* - \frac{\sigma_{ri}^2 \mu_i}{\gamma_i^{*2}})(\gamma_i^* - \mu_i) = 0, \qquad \nu^* \geq \frac{\sigma_{ri}^2 \mu_i}{\gamma_i^{*2}}, \quad 1 \leq i \leq m.
\end{aligned}$$

If $\nu^* < \sigma_{ri}^2/\mu_i$, the last condition can only hold if $\gamma_i^* > \mu_i$, but it implies $\nu^* = \frac{\sigma_{ri}^2 \mu_i}{\gamma_i^{*2}}$. The optimal γ_i is given by

$$\gamma_i^* = \sigma_{ri}\sqrt{\frac{\mu_i}{\nu^*}}, \quad \text{if } \nu^* < \sigma_{ri}^2/\mu_i.$$

On the other hand, if $\nu^* \geq \sigma_{ri}^2/\mu_i$, we have $\nu^* > \sigma_{ri}^2 \mu_i/\gamma_i^{*2}$, which implies

$$\gamma_i^* = \mu_i, \quad \text{if } \nu^* \geq \sigma_{ri}^2/\mu_i.$$

Therefore, we have

$$\gamma_i^* = \begin{cases} \sigma_{ri}\sqrt{\frac{\mu_i}{\nu^*}} & \text{if } \nu^* < \sigma_{ri}^2/\mu_i, \\ \mu_i & \text{if } \nu^* \geq \sigma_{ri}^2/\mu_i. \end{cases}$$

or $\gamma_i^* = \max\{\mu_i, \sigma_{ri}\sqrt{\mu_i/\nu^*}\}$. Substituting this expression for γ_i^* into $\sum_{i=1}^m \gamma_i^* = \Gamma$ we obtain

$$\sum_{i=1}^m \max\{\mu_i, \sigma_{ri}\sqrt{\frac{\mu_i}{\nu^*}}\} = \Gamma.$$

Then ν^* can be determined from the above equation, and the optimization problem is solved. ■

Corollary 3.15 shows a seemingly different but fundamentally similar result as Corollary 3.10 and 3.13. It agrees with the "fire-quenching" rules: allocating more power to a more demanding or problematic channel, which corresponds to a system with higher degree of instability μ_i, or a system to track a more dynamic reference process with bigger variance σ_{ri}^2. In contrast, the classic "water-filling" strategy takes advantage of stronger channels and cares less or even none about weaker channels [66]. This strategy, when assessing the tracking performance, will cause unacceptably tracking error on the weaker channel and the system utilizing it.

3.5.2 Nonminimum phase plants

Comparing with Theorem 3.11, the tracking performance with scaling is improved in the same way as the minimum phase systems depicted above. As expected, the nonminimum phase zeros cause an additional performance constraint δ that cannot be rectified by the scaling.

Theorem 3.16 *Let the plant satisfy the assumptions in Theorem 3.11. Consider the scaling around the channel depicted in Figure 3.3 with $\Lambda = \lambda I$. Then the best tracking performance is*

$$H_e^*(\Gamma) = \|Z\|_2^2 \frac{\mu_n}{\Gamma} + \delta, \tag{3.27}$$

which is achieved when the optimal scaling factor is

$$\lambda^* = \frac{\Gamma}{\|Z\|_2 \sqrt{(\Gamma - \mu_n)}}.$$

Proof. The proof combines the steps in Theorem 3.11 and Theorem 3.12. The intermediate steps, which are omitted here, lead to

$$H^*(\epsilon, \lambda, \Gamma) = (1-\epsilon)\delta + \frac{\lambda^2 \epsilon (1-\epsilon)}{\lambda^2 \epsilon + 1 - \epsilon} \|Z\|_2^2 + \left(\frac{1-\epsilon}{\lambda^2} + \epsilon \right) \mu_m - \epsilon \Gamma.$$

It follows that

$$H_e(\Gamma, \lambda) = \sup_{\alpha > 0} \left(\delta + \frac{\alpha \lambda^2}{1 + \alpha \lambda^2} \|Z\|_2^2 + \frac{1}{\lambda^2} \mu_m + \alpha(\mu_m - \Gamma) \right).$$

The result can then be proved by proceeding identically as the proof of Theorem 3.12. ■

3.6 Examples

In this section, we use an SISO plant model to calculate and illustrate the preceding results. We detail the reference signal first. We assume that the power spectral factor of the reference signal $r(t)$ is given by

$$\Psi_r(s) = c \frac{\sqrt{-2p_r}}{s - p_r}$$

where $p_r < 0$ is the stable pole and $c > 0$ is the amplitude. Defined in this way, $r(t)$ is a special type of random telegraph signal [49]. In particular, $r(t)$ assumes the values $\pm c$,

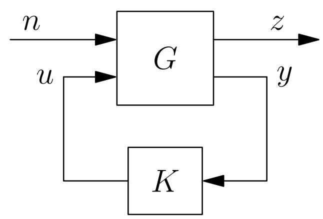

Figure 3.5: Standard block diagram of interconnecting the systems G and K

$r(0) = c$ or $-c$ with probability 1/2 and it switches polarity with each occurrence of an event in a Poisson process of rate $-p_r/2$.

In light of (3.17), the tracking performance in Theorem 3.9 is (3.19) with $\mu_m = \Phi 2 \sum_{i=1}^{l} p_i$ and $\sigma_r = c$.

On the other hand, for plants with a real nonminimum phase zero z, we consider Theorem 3.11. Then, according to (3.18), we have

$$\mu_n = \Phi \left(2 \sum_{i=1}^{l} p_i + 2z \left| 1 - F^{-1}(z) \right|^2 \right). \tag{3.28}$$

The quantity Z reduces to $L^{-1}(p_r)\Psi_r(s)$ and therefore

$$\|Z\|_2^2 = c^2 \left(\frac{p_r + z}{p_r - z} \right)^2. \tag{3.29}$$

Finally, the extra term δ is given by

$$c^2 \frac{-4zp_r}{(z - p_r)^2}. \tag{3.30}$$

Then we are able to calculate the tracking performance (3.20).

We compare the theoretical results with numerical results calculated by the robust control toolbox of MATLAB. For the latter purpose it is possible to formulate and numerically derive the optimal tracking performance as a form of general $\mathcal{H}_2$ optimal control problem for a specified ϵ. In this case the generalized plant G, as depicted in Figure 3.5, contains the plant model, the interconnection structure and the weighting factors [60]. Specifically, we have

$$\left[\begin{array}{cc|c} 0 & \sqrt{1-\epsilon}\Psi_r & -\sqrt{1-\epsilon}P \\ 0 & 0 & \lambda\sqrt{\epsilon}P \\ \hline 0 & \Psi_r & 0 \\ \frac{1}{\lambda} & 0 & P \end{array}\right] \left[\begin{array}{c} n \\ w \\ \hline u \end{array}\right] = \left[\begin{array}{c} \sqrt{1-\epsilon}e \\ \lambda\sqrt{\epsilon}y \\ \hline r \\ y + \frac{1}{\lambda}n \end{array}\right]$$

where n and w are the white noise input, u the controller output, λy is the channel input and $y + \frac{1}{\lambda}n$ is the channel output. The perturbation method [55] is applied to circumvent singular $\mathcal{H}_2$ control formulation. Then, we seek the performance by linearly searching for ϵ, and λ if scaling factor is utilized.

We are about to study the plant

$$P_1(s) = \frac{s - z_1}{s^2 - 2s + 4}$$

which has a zero z_1 and a conjugate pair of unstable poles $1 \pm \mathrm{j}\sqrt{3}$. We fix the amplitude of the reference signal $c = 2$ and the pole $p_r = -2$. The power spectral density Φ of the white noise is 1.

3.6.1 Weighted performance and the effect of nonminimum phase zeros

We shall consider two cases: $z_1 = -1/2$ and $z_1 = 1/2$. For each case we let ϵ very from 0 to 1 and compute $H^*(\epsilon)$ (defined in Remark 3.6) when $\Gamma = 0$. The result represents the weighted power of tracking error and channel input. We compare the optimal solution by using MATLAB and the expression (A.10). Figure 3.6 shows these two computations match exactly. For the following figures we omit the comparisons for clearness, with the understanding that they match very well.

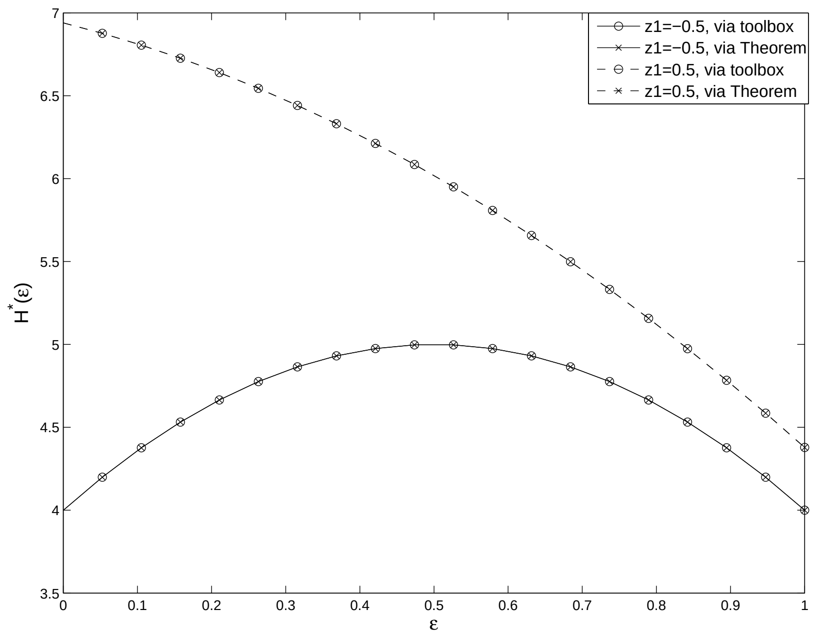

Figure 3.6: $H^*(\epsilon)$ for plant P_1, for $z_1 = -0.5$ and 0.5. The amplitude of the reference is $c = 2$ and its pole is $p_r = -2$.

Also from the figure we can see that the presence of a nonminimum phase zero worsens the performance. To illustrate this point, we plot μ_n as in (3.28), δ as in (3.30), $\|Z\|_2^2$ as in (3.29) and the weighted performance at $\epsilon = 0.5$ versus z_1 in Figure 3.7. Derived from (3.28), the expression for μ_n in Figure 3.7 is

$$\mu_m + 2z_1 \left(1 - \left|\frac{z_1 + p_1}{z_1 - p_1}\right|^2\right)^2$$

where $p_1 = 1 + \mathrm{j}\sqrt{3}$. It can be seen that the nonminimum phase behavior of the plant, which is characterized by μ_n, dominates. At the peak of μ_n, which is achieved at about $z_1 = 2.6$, the systems has very steep stabilization requirement and thus the performance is poor.

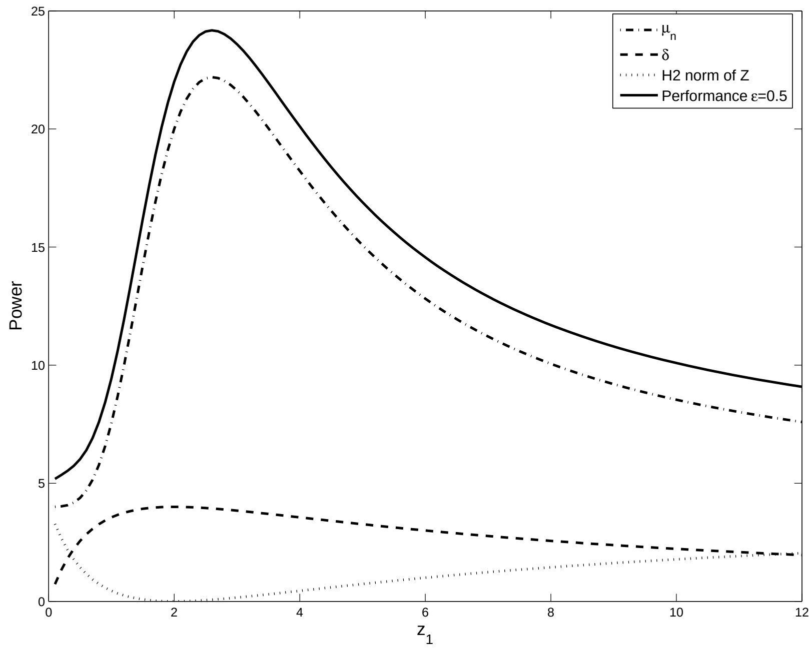

Figure 3.7: The effect of nonminimum phase behavior on the performance with respect to the location of z_1.

3.6.2 Lagrangian and the optimal tracking performance for different power constraints

We first investigate minimum phase systems and set $z_1 = -1/2$. The Lagrangian $\phi(\epsilon) \triangleq H^*(\epsilon)/(1-\epsilon)$, is plotted against ϵ for a few values of Γ using Robust Control Toolbox. The maximum values of $\phi(\epsilon)$, indicated as stars, are the optimal tracking performance H_e^*. In Figure 3.8, the optimal tracking error decreases as Γ goes up until $\Gamma_{max} = \mu_m + \sigma_r^2$ which is 8. After this point, the best performance we can achieve is $\mu_m = 4$. The optimal values admit a quadratic relationship with $\sqrt{\Gamma}$ and are in agreement with (3.19).

The performance for nonminimum phase systems with $z_1 = 1/2$ is depicted in Figure 3.9. The Lagrangian behaves similarly with ϵ and Γ. As expected, the performance is

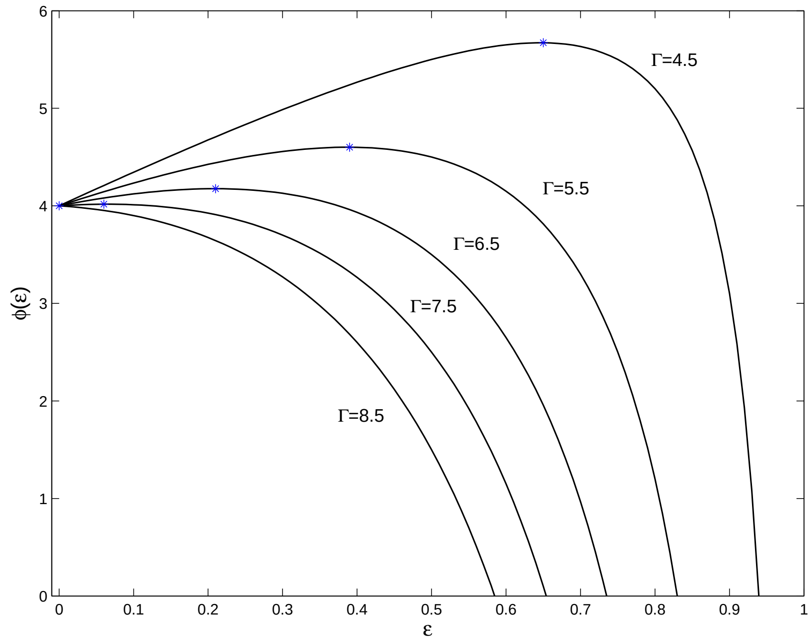

Figure 3.8: $\phi(\epsilon)$ against ϵ for Γ from 4.5 to 8.5. The stars represent H_e^*.

worse. The range of the effective power constraint is from $\mu_n = 4.38$ to $\Gamma'_{max} = \mu_n + \|Z\|_2^2 = 5.82$. Hence $\Gamma = 6$ and $\Gamma = 6.4$ have the same value for H_e^*. The best achievable performance is $\mu_n + \delta = 6.94$. The figure is consistent with (3.20).

3.6.3 Optimal tracking performance against power constraint

We plot the optimal tracking performance against the power constraint in Figure 3.11a. We vary the nonminimum phase zero in a small range but it affects the performance greatly. It is consistent with the nonminimum phase effect depicted in Figure 3.7.

The values of Γ'_{max} for the nonminimum phase zero at 0.5, 0.7 and 0.9 are 5.82, 6.08 and 7.15, respectively. From the tips in the figure we can see that, when Γ goes beyond the corresponding values above, the performance will stay at 6.94, 8.22 and 10.00, respectively. It thus confirms that the performance cannot go below $\mu_n + \delta$, as indicated in (3.20).

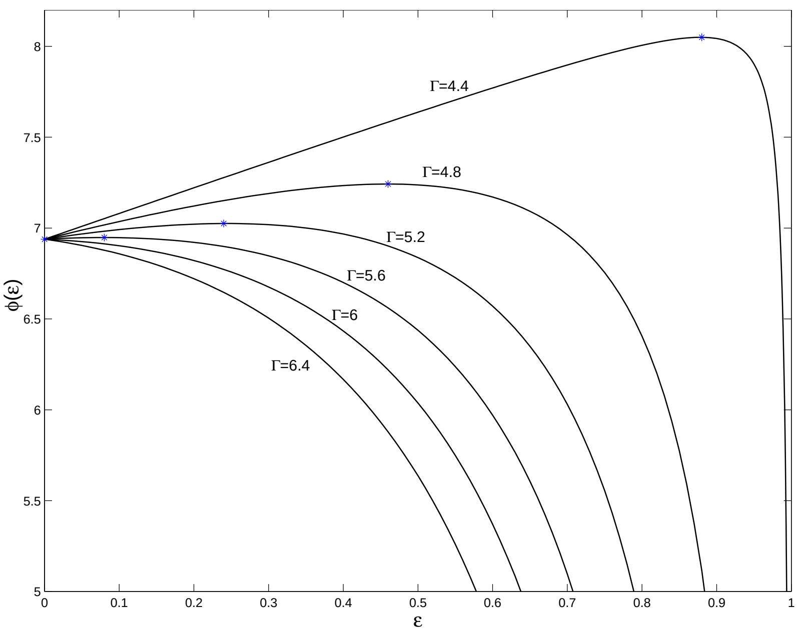

Figure 3.9: $\phi(\epsilon)$ against ϵ for $P_1(s)$ with a nonminimum phase zero at 0.5 and Γ from 4.4 to 6.4. The stars represent H_e^*.

3.6.4 Optimal tracking performance with scaling

Finally we examine the effect of scaling on the optimal tracking performance, as depicted in Figure 3.10. With optimal design of the scaling factor, as the power constraint increases, the optimal tracking error decreases but it will converge to $\delta = 2.56$ and cannot go below it. The values of H_e^* at $\lambda = 1$, which gather around 6.9 except the $\Gamma = 4.4$ curve, correspond to the optimal values in Figure 3.9. Direct comparisons among these two figures and the $z1 = 0.5$ curve in Figure 3.11a show significant performance improvement by adding one degree of freedom in selecting the scaling factor. The figure matches the result in (3.27) exactly.

We also plot the tracking performance versus the power constraint with optimized scaling in Figure 3.11b. The comparison in Figure 3.11 proves the obvious advantage of

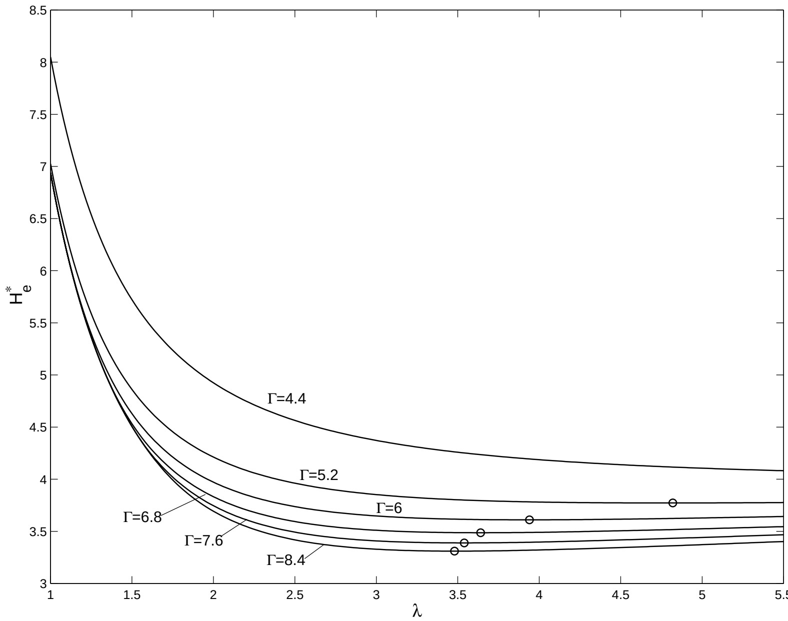

Figure 3.10: $H_e^*(\lambda)$ against the scaling factor λ for plant P_1 with $z_1 = 0.5$. The circles represent the best tracking performance with optimal scaling. For the curve $\Gamma = 4.4$, the optimal λ is 21.

using the scaling: not only that as Γ increases, the smallest tracking error will inverse-proportionally tend to δ, but when Γ is arbitrarily close to the stabilization threshold μ_n from above, the worst tracking error $\|Z\|_2^2 + \delta = \sigma_r^2 = 4$ is still below the optimal performance without the scaling.

3.7 Summary

In this chapter, we study the $\mathcal{H}_2$ optimal tracking performance of LTI feedback systems over uplink AWN channels. Our work explores the area of performance characterizations of NCS's; our primary objective is to explore the relation between the known limitations caused by the interaction of control systems and the characteristics of the communication

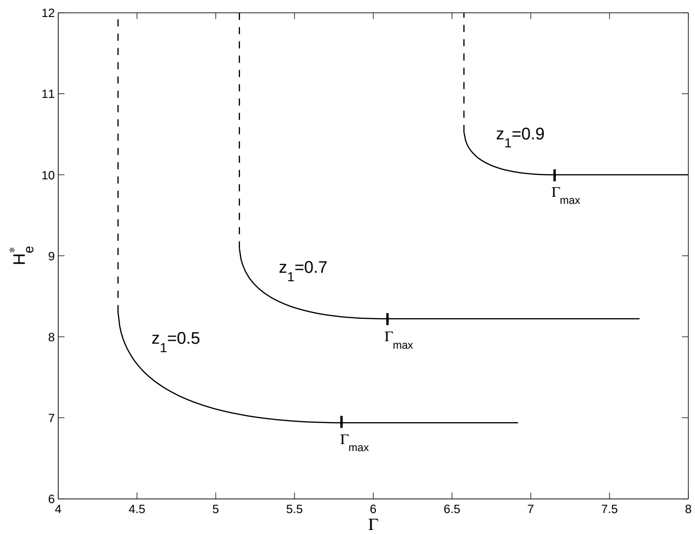

(a)

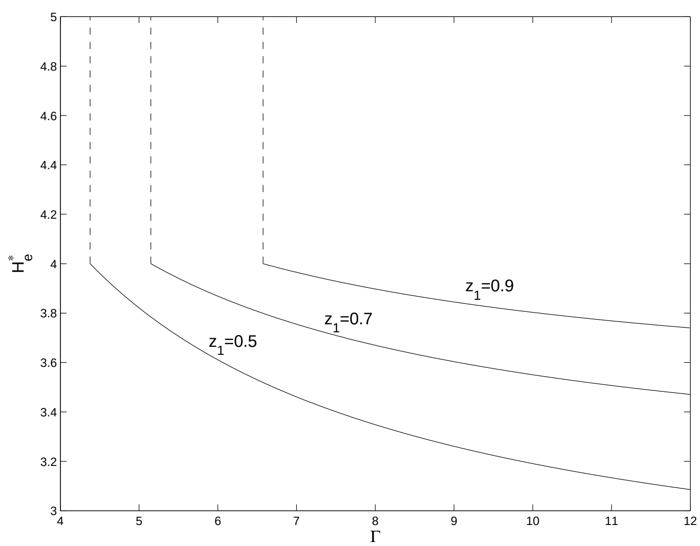

(b)

Figure 3.11: Comparison between the performance with and without scaling. (a) H_e^* against Γ for three values of z_1. The ticks represent the values of Γ'_{max} (b) H_e^* against Γ with scaling. For both cases, the power constraint Γ must be greater than the stabilization requirement, otherwise the tracking error is infinite.

channel for MIMO systems.

Analytical solutions show that the tracking performance is a quadratic function with respect to the square root of the power constraint before it stays at the vertex. The unstable poles and nonminimum phase zeros, together with the strength of noise and reference signal affect mostly the stabilization requirement for the channel, which also determine the vertex of the tracking performance. The proximity of the nonminimum phase zeros and the unstable poles are most harmful, which is similar to tracking in standard control systems. We have also considered a simple scaling scheme, through which the channel is better utilized. The tracking performance with optimized scaling is inversely proportional to the power constraint and can reach zero in limiting case. Moreover, we have derived the optimal power allocation policy, which exhibits a "fire-quenching" strategy, allocating more power to more problematic channels, as opposed of Shannon's classical "water-filling" solution.

Chapter 4

Tracking Performance over Downlink Channel

4.1 Introduction

In this chapter, we formulate and study another tracking problem with a different configuration: we assume that the communication is placed at the downlink. In this scenario, the controller output to the plant is corrupted by the additive white noise and subject to the power constraint. The results for stabilization are analogous to that of the uplink case. We shall show, however, that the best tracking performance depends on not only unstable poles and noise strength, but the plant's minimum phase behavior and gain in the entire frequency range, which has not been observed previously.

The rest of the chapter is organized as follows: Section 4.2 defines the problem mathematically and makes assumptions. Section 4.3 investigates the stabilization problem for MIMO systems over the downlink channel. Section 4.4 derives lower bounds of the optimal tracking performance for minimum phase MIMO systems by decomposing the problem into noise attenuation and noise-free reference tracking.

4.2 Problem formulation

The configuration is depicted in Figure 4.1. The optimal tracking problem of interest is still given by (3.21) and is equivalent to

$$\begin{aligned} \text{minimize} \quad & \|T^e_{r,n}\Psi_{r,n}\|_2^2 \\ \text{subject to} \quad & \|T^u_{r,n}\Psi_{r,n}\|_2^2 \le \Gamma, \quad Q, R \in \mathbf{R}\mathcal{H}_\infty, \quad \lambda > 0. \end{aligned} \tag{4.1}$$

The transfer functions are given by

$$\begin{aligned} T^e_{r,n} &= \left[I - (I - PK_2)^{-1} PK_1, \quad -\tfrac{1}{\lambda} (I - PK_2)^{-1} P \right], \\ T^u_{r,n} &= \left[\lambda (I - K_2 P)^{-1} K_1, \quad (I - K_2 P)^{-1} K_2 P \right]. \end{aligned}$$

We can parameterize the transfer functions via the Youla parametrization (2.5) and obtain

$$\begin{aligned} T^e_{r,n} &= \left[I - NQ, \quad -\tfrac{1}{\lambda} N(\tilde{X} - R\tilde{N}) \right], \\ T^u_{r,n} &= \left[\lambda MQ, \quad -I + M(\tilde{X} - R\tilde{N}) \right]. \end{aligned} \tag{4.2}$$

Assumption 4.1 *The plant transfer function matrix $P(s)$ is invertible for some $s \in \mathbb{C}$.*

The assumption is stronger than Assumption 3.2. It is needed since to counter the channel noise at the plant input, the plant also needs to be of full column rank. Suppose that the plant has simple nonminimum phase zeros $z_i \in \mathbb{C}_+$, $i = 1, \ldots, k$ and unstable poles $p_i \in \mathbb{C}_+$,

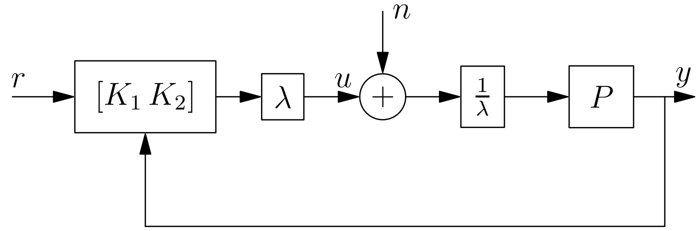

Figure 4.1: Tracking with AWN channel in the downlink

$i = 1, \ldots, l$. We shall need the following factorizations (cf. (2.13) and (3.9)) as

$$\tilde{N}(s)\Psi_n = \tilde{N}_m^{(n)}(s)G(s), \tag{4.3}$$

$$M(s) = B(s)M_m(s), \tag{4.4}$$

where the all-pass factor $G(s)$ can be constructed as

$$G(s) \triangleq G_k(s)G_{k-1}(s)\cdots G_1(s). \tag{4.5}$$

with

$$G_i(s) \triangleq I - \frac{2\mathrm{Re}\{z_i\}}{s + \bar{z}_i}\boldsymbol{\rho}_i\boldsymbol{\rho}_i^H \tag{4.6}$$

where $\|\boldsymbol{\rho}_i\|^2 = 1$.

Likewise, as shown in Lemma 2.10, the all-pass factor $B(s)$ is given by

$$B(s) \triangleq \prod_{i=1}^{l} B_i(s). \tag{4.7}$$

with

$$B_i(s) \triangleq I - \frac{2\mathrm{Re}\{p_i\}}{s + \bar{p}_i}\boldsymbol{\omega}_i\boldsymbol{\omega}_i^H, \tag{4.8}$$

and we spell out the vector $\boldsymbol{\omega}$ as $\left(\omega_i^1, \ldots, \omega_i^l\right)^T$. In addition, the factors $\tilde{N}_m^{(n)}$ and M_m are minimum phase.

4.3 Stabilization

For MIMO systems, the stabilization result is slightly different from that of the uplink case. The necessary and sufficient condition on the power constraint for stabilizability is given by (cf. Section 3.3)

$$\Gamma > \mu,$$

where, in light of the factorization (4.4),

$$\begin{aligned}\mu &= \inf_{R\in\mathbf{R}\mathcal{H}_\infty} \left\| \left(I - M\left(\tilde{X} - R\tilde{N}\right)\right)\Psi_n \right\|_2^2 \\ &= \left\| \left(B^{-1} - I\right)\Psi_n \right\|_2^2 + \inf_{R\in\mathbf{R}\mathcal{H}_\infty} \left\| \left(I - M_m\left(\tilde{X} - R\tilde{N}\right)\right)\Psi_n \right\|_2^2 .\end{aligned}$$

4.3.1 Minimum Phase Plants

As the plant is of full column rank, so is $\tilde{N}$. It is thus possible to define a free parameter in $\mathbf{R}\mathcal{H}_\infty$ as $R_0 \triangleq \tilde{X} - R\tilde{N}$. It follows that

$$\begin{aligned}\mu &= \left\| \left(B^{-1} - I\right)\Psi_n \right\|_2^2 + \inf_{R_0\in\mathbf{R}\mathcal{H}_\infty} \left\| \left(I - M_m R_0\right)\Psi_n \right\|_2^2 \\ &= \left\| \left(B^{-1} - I\right)\Psi_n \right\|_2^2 ,\end{aligned}$$

since $\left\| \left(I - M_m R_0\right)\Psi_n \right\|_2^2$ is 0 by appropriately choosing R_0.

Theorem 4.2 *Suppose the plant transfer function matrix is left-invertible, minimum phase and has unstable poles p_i, $i = 1, \ldots, l$. Then the closed-loop system over the AWN channel shown in Figure. 4.1 is stabilizable if and only if*

$$\Gamma > \mu_m$$

where

$$\mu_m = 2\sum_{i=1}^{l} p_i \sum_{j=1}^{m} |\omega_i^j|^2 \Phi_j.$$

4.3.2 Nonminimum Phase Plants

The derivations of stabilization requirement of the downlink channel bears a similar fashion to Theorem 3.8. We make use of the factorization (4.5) to derive

$$\mu = \mu_m + \inf_{R\in\mathbf{R}\mathcal{H}_\infty} \left\| \left(I - M_m\tilde{X}\right)\Psi_n G^{-1} - M_m R\tilde{N}_m^{(n)} \right\|_2^2.$$

Then we may apply Lemma 2.18 as in the proof of Theorem 3.8 and prove the following theorem.

Theorem 4.3 *Suppose the plant transfer function matrix is left-invertible and has both unstable poles p_i, $i = 1, \ldots, l$ and nonminimum phase zeros z_i, $i = 1, \ldots, k$. Then the feedback system shown in Figure 4.1 is stabilizable if and only if*

$$\Gamma > \mu_m + \sum_{i,j=1}^{k} \frac{4\mathrm{Re}\{z_i\}\mathrm{Re}\{z_j\}}{\bar{z}_i + z_j} \boldsymbol{c}_i^H \boldsymbol{c}_j \boldsymbol{d}_j^H \boldsymbol{d}_i,$$

where

$$\boldsymbol{c}_i \triangleq \left(I - B^{-1}(z_i)\right)\Psi_n \left(\prod_{j=1}^{i-1} G_j^{-1}(z_i)\right)\boldsymbol{\rho}_i,$$

$$\boldsymbol{d}_i \triangleq \left(\prod_{j=i+1}^{k} G_j^{-1}(z_i)\right)^H \boldsymbol{\rho}_i.$$

Both theorems are similar to those for the uplink case. The difference stems from the spatial properties of MIMO systems. It is obvious that for SISO systems they share the same result as the uplink case.

4.4 Performance

To evaluate the tracking performance (4.1), we define the functional

$$J(\epsilon, \lambda, Q, R) \triangleq (1-\epsilon)\|T^e_{r,n}\Psi_{r,n}\|_2^2 + \epsilon\left(\|T^u_{r,n}\Psi_{r,n}\|_2^2 - \Gamma\right)$$

$$= J_1(Q) + J_2(R) - \epsilon\Gamma$$

for $\epsilon \in [0,1]$, where

$$J_1(Q) \triangleq \left\| \begin{bmatrix} \sqrt{1-\epsilon}(I - NQ) \\ \lambda\sqrt{\epsilon} MQ \end{bmatrix} \Psi_r \right\|_2^2,$$

and

$$J_2(R) \triangleq \left\| \frac{1}{\lambda} \begin{bmatrix} \sqrt{1-\epsilon} N\left(\tilde{X} - R\tilde{N}\right) \\ \lambda\sqrt{\epsilon}\left(I - M\left(\tilde{X} - R\tilde{N}\right)\right) \end{bmatrix} \Psi_n \right\|_2^2.$$

Since Lemma 3.3 and 3.5 hold for the transfer functions (4.2), the optimal tracking performance can be specified by

$$J_e^* = \inf_{\lambda > 0} J_e(\lambda), \tag{4.9}$$

where

$$J_e(\lambda) = \sup_{0 \le \epsilon \le 1} \frac{1}{1-\epsilon} J^*, \tag{4.10}$$

and

$$J^* \triangleq \inf_{Q, R \in \mathbf{R}\mathcal{H}_\infty} J(\epsilon, \lambda, Q, R).$$

The functional J exhibits a separation property between Q and R, and r and n, respectively, due to the two-parameter controller and that r and n are uncorrelated. We thus break down the problem into two parts. We begin with the evaluation of $J_2^* \triangleq \inf_{R \in \mathbf{R}\mathcal{H}_\infty} J_2(R)$, which amounts to a noise attenuation problem. Then, we analyze the tracking performance with power constraint in a noise-free setting. The combination of the two yields J.

4.4.1 Noise attenuation

When the reference input is zero, (4.1) becomes a problem of minimizing the power of the plant output with channel input power constraint. It follows that the functional $J_2(R)$ is the performance measure, which induces a two-block $\mathcal{H}_2$ control problem. The following assumption is necessary for J_2 to be finite.

Assumption 4.4 *The plant transfer function matrix P is strictly proper.*

The following lemma gives an analytical expression for the optimal performance J_2^* for minimum phase plants.

Lemma 4.5 *Suppose that P is strictly proper, minimum phase and it has poles $p_i \in \mathbb{C}_+$, $i = 1, \ldots, l$. Introduce the inner-outer factorization*

$$\begin{bmatrix} \sqrt{1-\epsilon}N \\ -\lambda\sqrt{\epsilon}M_m \end{bmatrix} = \Theta_i \Theta_o. \tag{4.11}$$

With $\boldsymbol{e}_i$ denoting the Euclidean vector, define the functions

$$g_i(s) \triangleq \lambda^2 \epsilon \boldsymbol{e}_i^T M_m(s) \Theta_o^{-1}(s) \Theta_o^{-T}(\infty) M_m^T(\infty) \boldsymbol{e}_i$$

for $1 \le i \le m$, which are diagonal terms of the matrix. Then

$$J_2^* = \epsilon \mu_m + \hat{J}_2 \tag{4.12}$$

where

$$\hat{J}_2 \triangleq \frac{\epsilon}{\pi} \int_{-\infty}^{\infty} \sum_{i=1}^{m} \Phi_i \left(1 - \mathrm{Re}\{g_i(\mathrm{j}\omega)\}\right) \mathrm{d}\omega \tag{4.13a}$$

$$\ge J_{2L} \triangleq \frac{\epsilon}{\pi} \left(\sum_{i=1}^{m} \Phi_i \right) \int_0^{\infty} \log \left(1 + \frac{1-\epsilon}{\lambda^2 \epsilon} \underline{\sigma}^2 \left[P(\mathrm{j}\omega) \right] \right) \mathrm{d}\omega \tag{4.13b}$$

Furthermore, for SISO systems, the optimal noise attenuation performance is

$$J_2^* = \epsilon\Phi\left(2\sum_{i=1}^{l} p_i + \frac{1}{\pi}\int_0^{\infty} \log\left(1 + \frac{1-\epsilon}{\lambda^2\epsilon}\left|P(\mathrm{j}\omega)\right|^2\right) \mathrm{d}\omega\right).$$

Proof. See Appendix A.4. ■

4.4.2 Tracking

Because of the power constraint on the control signal, the tracking performance $J_1^* \triangleq \inf_{Q\in\mathbf{R}\mathcal{H}_\infty} J_1(Q)$ depends on the spectral factor of the reference process. As the derivation for general reference input processes is difficult, in subsequent developments, we shall consider a specific reference input process that resembles a deterministic step signal. Specifically, the reference $\boldsymbol{r}(t)$ is a vector of zero-mean processes and each component is the output of the integrator system $1/s$ with its input as a white noise process with variance σ_{ri}^2. The power spectral factor of $\boldsymbol{r}(t)$ is thus given by $\Psi_r(s) = \frac{1}{s}\mathrm{diag}\{\sigma_{r1}, \ldots, \sigma_{rn}\}$. The process can be used to model a slowly varying random variable [52].

We consider the problem of tracking the reference with power constraint in a noise-free setting, and $J_1(Q)$ serves as the performance measure. It requires the plant contains integrators for the tracking performance to be bounded due to the special form for Ψ_r, thus

Assumption 4.6 *The plant P has a pole at $s = 0$.*

The following lemma characterize an analytical expression for the optimal performance J_1^* for minimum phase plants.

Lemma 4.7 *Suppose that Assumption 4.6 holds. Also suppose P is minimum phase and has poles $p_i \in \mathbb{C}_+$, $i = 1, \ldots, l$. The inner-outer factorization is given by* (4.11)*. Define the* *functions*

$$f_i(s) \triangleq (1-\epsilon)\boldsymbol{e}_i^T N(s)\Theta_o^{-1}(s)\Theta_o^{-T}(0)N^T(0)\boldsymbol{e}_i \tag{4.14}$$

for $1 \le i \le n$. *Then*

$$J_1^* = \frac{1-\epsilon}{\pi}\int_{-\infty}^{\infty}\sum_{i=1}^{n}\sigma_{ri}^2\frac{1-\mathrm{Re}\{f_i(\mathrm{j}\omega)\}}{\omega^2}\,\mathrm{d}\omega \tag{4.15a}$$

$$\ge J_{1L} \triangleq \frac{1-\epsilon}{\pi}\sigma_{\boldsymbol{r}}^2\int_0^{\infty}\frac{1}{\omega^2}\log\left(1+\frac{\lambda^2\epsilon}{(1-\epsilon)\bar{\sigma}^2\left[P(\mathrm{j}\omega)\right]}\right)\mathrm{d}\omega \tag{4.15b}$$

Furthermore, for SISO systems, the optimal tracking performance is

$$J_1^* = \frac{(1-\epsilon)\sigma_r^2}{\pi}\int_0^{\infty}\frac{1}{\omega^2}\log\left(1+\frac{\lambda^2\epsilon}{(1-\epsilon)\left|P(\mathrm{j}\omega)\right|^2}\right)\mathrm{d}\omega.$$

Proof. See Appendix A.5. ■

4.4.3 Tracking over downlink channel

The following theorem gives an analytical characterization of J^* and is an immediate consequence of Lemma 4.5 and Lemma 4.7.

Theorem 4.8 *Suppose that P is strictly proper, contains an integrator, minimum phase and it has poles $p_i \in \mathbb{C}^+$, $i = 1, \ldots, l$. Define $\Phi_s = \sum_i \Phi_i$. Then*

$$J^* = J_1^* + J_2^* - \epsilon\Gamma \tag{4.16}$$

$$\ge \epsilon\left(\mu_m - \Gamma\right) + J_{1L} + J_{2L}. \tag{4.17}$$

The lower bound for the best tracking performance is given by

$$J_e(\lambda) \ge J_R + J_N + \alpha^*\left(\mu_m - \Gamma\right) \tag{4.18}$$

where

$$J_R \triangleq \frac{1}{\pi}\sigma_{\boldsymbol{r}}^2 \int_0^\infty \frac{1}{\omega^2} \log\left(1 + \frac{\lambda^2\alpha^*}{\bar{\sigma}^2\left[P(\mathrm{j}\omega)\right]}\right) \mathrm{d}\omega$$

$$J_N \triangleq \frac{\alpha^*}{\pi}\Phi_s \int_0^\infty \log\left(1 + \frac{\underline{\sigma}^2\left[P(\mathrm{j}\omega)\right]}{\lambda^2\alpha^*}\right) \mathrm{d}\omega,$$

and α^* *is the positive solution to the following equation*

$$\pi(\Gamma - \mu_m) = \sigma_{\boldsymbol{r}}^2 \int_0^\infty \frac{1}{\omega^2} \frac{1}{\bar{\sigma}^2\left[P(\mathrm{j}\omega)\right]/\lambda^2 + \alpha^*} \mathrm{d}\omega + \Phi_s \int_0^\infty \left[\log\left(1 + \frac{\underline{\sigma}^2\left[P(\mathrm{j}\omega)\right]}{\lambda^2\alpha^*}\right) - \frac{\underline{\sigma}^2\left[P(\mathrm{j}\omega)\right]}{\lambda^2\alpha^* + \underline{\sigma}^2\left[P(\mathrm{j}\omega)\right]}\right] \mathrm{d}\omega. \quad (4.19)$$

Furthermore, for SISO systems, we have $\sigma_{\boldsymbol{r}}^2 = \sigma_r^2$, $\Phi_s = \Phi$ *and* $\underline{\sigma}^2\left[P(\mathrm{j}\omega)\right] = \bar{\sigma}^2\left[P(\mathrm{j}\omega)\right] = |P(\mathrm{j}\omega)|^2$, *and the lower bound is attained.*

With the communication constraint at the downlink, the tracking performance not only depends on the unstable poles for stabilization, but also exhibits competing objectives related to the plant gain at entire frequency range and minimum phase zeros close to the imaginary axis. The latter is true because in the vicinity of such zeros, the term $|P(\mathrm{j}\omega)|$ is small, which commands a large value for the integral in J_R. Theorem 4.8 incorporate these factors among unstable poles, power constraint and noise level; and the optimal tracking performance reconciles all the tradeoffs.

The AWN channel in the downlink imposes additional constraints that we have not seen in tracking in a standard control system or over uplink AWN channels. It is a result of directly limiting the control action with the channel input power constraint.

We have not derived an analytical expression for the optimal scaling, but a numerical result can always be found via Theorem 4.8. For SISO systems, we examine two special cases when the channel SNR goes to infinity, and show the roles played by scaling. On one hand, if the power constraint $\Gamma \to \infty$, from (4.19) we have $\alpha^* = 0$. It then implies that $J_e^* = 0$, the zero tracking error. On the other hand, if the noise power is 0, then $\mu_m = 0$ and $J_N = 0$. The optimal Lagrangian multiplier $\alpha^*(\lambda)$ (nonzero if Γ is finite) can be obtained from the equation

$$\sigma_r^2 \int_0^\infty \frac{1}{\omega^2} \frac{1}{|P(\mathrm{j}\omega)|^2 / \lambda^2 + \alpha^*} \, \mathrm{d}\omega = \pi\Gamma. \tag{4.20}$$

Then, the optimal λ is selected such that $\alpha^*(\lambda) = 0$, which implies $\alpha^*\lambda^2 = 0$. Therefore, the tracking performance $J_e^* = 0$. However, it is achieved through controlling the channel input power by scaling. Hence, perfect tracking can be achieved when the AWN channel is ideal, for either non power-constrained or noise-free channel.

4.5 Summary

In this chapter, we investigate the limitations on the tracking performance of LTI feedback systems over downlink AWN channels. Although the system configuration and problem formulation are similar to the previous chapter, the results incorporate new and previously unobserved perspectives, the most important of which is the minimum phase behavior. In fact, the tracking performance over downlink, in addition to unstable poles and power constraint, depends on the plant gain over the entire frequency range. In this case, certain minimum phase zeros, especially ones that are close to the imaginary axis, will greatly worsen the performance. Hence, perfect tracking is not possible even if the plant is both minimum phase and stable. For MIMO plants, the performance bound is related to the largest and smallest singular value of the plant transfer function matrix at the entire frequency range.

Chapter 5

Limitations on Stabilization over Both Uplink and Downlink Channels

5.1 Introduction

As we have discussed in Section 1.2.2 and Section 1.2.3, there have been actively-studied and well-developed results on stabilization of feedback control systems over either the uplink or downlink communication channel while assuming the other direction is noiseless. However, few efforts have been made towards analysis of control systems with channels in both directions. An exception is the recent paper [69]. That paper considers stochastic but scalar LTI systems driven by Brownian motion process and uses the notion of stochastic stability of Markov chain to study the necessary and sufficient conditions on the channels and controllers for stabilizability. In this chapter, we address the stabilizability problem of LTI systems over both uplink and downlink AWN channels while staying in the framework we established in previous chapters. Thus, we only consider LTI control laws and scaling of the channels, rather than complicated coding/decoding schemes with memory. The systems we study include discrete-time scalar unstable system and continuous time systems with only a single unstable pole.

The remainder of the chapter is organized as follows. Section 5.2 formulates the problem. Section 5.3 discusses the stabilization of discrete-time scalar systems via state feedback over the uplink and downlink channels. As state feedback cannot stabilize the continuous-time scalar systems, we employ one- and two-parameter dynamic controller on the output feedback to achieve stabilizability, as discussed in Section 5.4.

5.2 Problem Formulation

The system configuration is depicted in Figure 5.1. The AWN channels have power constraints $\mathcal{E}\{u_1^2\} \leq \Gamma_1$ and $\mathcal{E}\{u_2^2\} \leq \Gamma_2$, respectively. The constant scaling is represented by λ_1 and λ_2. The noise n_1 and n_2 are uncorrelated zero-mean white noise processes.

The problem is to search for the lower bound on the input power of the uplink channel over stabilizing controllers when the input power of the downlink channel is constrained:

$$\begin{aligned} &\text{minimize} \quad \mathcal{E}\{u_1^2\} \\ &\text{subject to} \quad \mathcal{E}\{u_2^2\} \leq \Gamma_2, \quad K \in \mathcal{K}, \quad \lambda_1, \lambda_2 > 0. \end{aligned} \tag{5.1}$$

The solution gives a separation line between what is achievable and what is not for stability, and the region of SNR pairs that guarantees it.

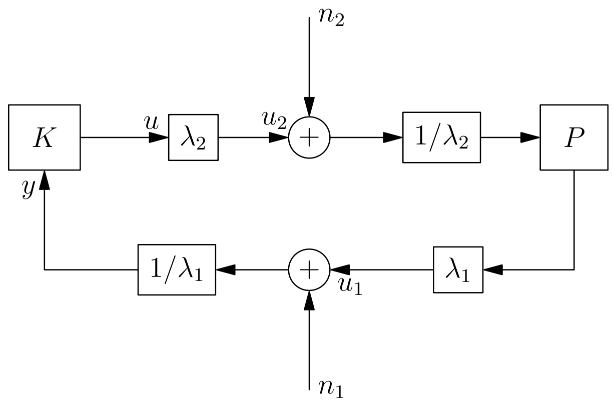

Figure 5.1: Stabilization over two AWN channels

5.3 Stabilization of discrete-time scalar systems

In this section, we consider the stabilization of a discrete-time scalar system, as depicted in Figure 5.2. The controller amounts to the state feedback gain k and accesses the state information through the uplink channel (hence we do not have the exact state information) and the controller output is sent to the plant through the downlink channel.

Accordingly, we consider the LTI systems described in state-space by

$$x[t+1] = \alpha x[t] + u[t]$$

where t is the discrete-time variable, $x[t] \in \mathbb{R}$ is the plant state, and $|\alpha| > 1$. The plant input is thus $u[t] = k(x[t] + n_1[t]/\lambda_1) + n_2[t]/\lambda_2$. The feedback gain must satisfy $|\alpha + k| < 1$ to internally stabilize the system. With a slight abuse of notation, we denote the variance of the white noise processes n_1 and n_2 by Φ_1 and Φ_2, respectively.

Recall from Section 1.2.3 that if there is only a single channel at either uplink or downlink while the other one is noise-free, the fundamental lower bound on channel capacity (assuming the noise is Gaussian distributed) for stabilization is $\mathcal{C} > \log_2(|\alpha|)$. This leads us to the following necessary condition:

Theorem 5.1 *A necessary condition for the stabilizability of the system depicted in Figure 5.2 is*

$$\min\{\mathcal{C}_1, \mathcal{C}_2\} > \log_2(|\alpha|)$$

where $\mathcal{C}_1$ and $\mathcal{C}_2$ denote the channel capacities of the uplink and downlink, respectively.

To prove the sufficient condition, we follow a similar approach in Chapter 3 and Chapter 4 and directly deal with the input power at both channels. First, we write the input-output relation as

$$\begin{aligned} \mathcal{E}\{u_1^2\} &= \frac{k^2\Phi_1 + (\lambda)^2\,\Phi_2}{1-(\alpha+k)^2}, \\ \mathcal{E}\{u_2^2\} &= \frac{\left(\frac{1}{\lambda}\right)^2\left(1-\alpha^2-2\alpha k\right)k^2\Phi_1 + k^2\Phi_2}{1-(\alpha+k)^2}, \end{aligned} \tag{5.2}$$

where $\lambda \triangleq \lambda_1/\lambda_2$. Then, the stabilization problem 5.1 is translated to

$$\begin{aligned} \text{minimize} \quad & \mathcal{E}\{u_1^2\} \\ \text{subject to} \quad & \mathcal{E}\{u_2^2\} \leq \Gamma_2,\ |\alpha+k| < 1, \quad \lambda > 0. \end{aligned} \tag{5.3}$$

The necessary and sufficient condition for stabilizabilty over both channels is summarized in the following theorem:

Theorem 5.2 *The system depicted in Figure 5.2 is stabilizable if and only if the inequalities*

$$\frac{\Gamma_2}{\Phi_2} > \left(\alpha^2-1\right) \tag{5.4}$$

$$\frac{\Gamma_1}{\Phi_1} > \frac{(\alpha^2-1)(\frac{\Gamma_2}{\Phi_2}+1)}{\frac{\Gamma_2}{\Phi_2}-(\alpha^2-1)} \tag{5.5}$$

are both satisfied.

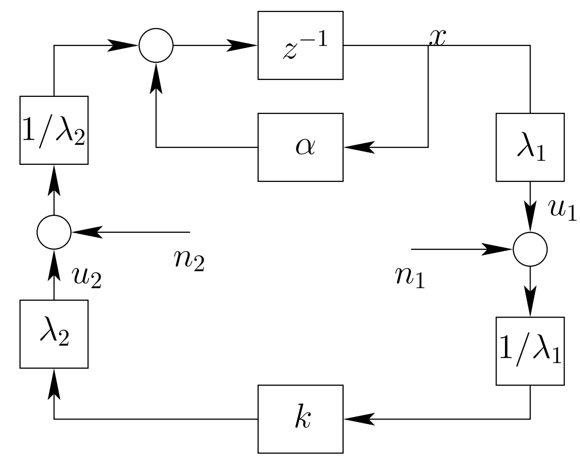

Figure 5.2: State feedback stabilization over two channels for a unstable scalar plant

Proof. See appendix A.6. ■

Assume that the noise processes are Gaussian distributed. The following corollary, which reveals the case when one of the channels is extremely reliable, is immediate.

Corollary 5.3 *If the capacity of the downlink channel $\mathcal{C}_2 \to \infty$, then the condition on the uplink channel becomes $\mathcal{C}_1 > \log_2(|\alpha|)$.*

Alternatively, the inequality (5.5) can be expressed as

$$\left[\frac{\Gamma_1}{\Phi_1} - (\alpha^2 - 1)\right]\left[\frac{\Gamma_2}{\Phi_2} - (\alpha^2 - 1)\right] > \alpha^2(\alpha^2 - 1).$$

It demonstrates by how much the channel SNR should exceed the quantity $\alpha^2 - 1$, the degree of instability.

Furthermore, after some algebraic manipulation on (5.5) and taking logarithm on both sides of the inequality, we may obtain yet another form of the conditions in Theorem 5.2, in terms of channel capacity, as

$$\mathcal{C}_1 + \mathcal{C}_2 - \frac{1}{2}\log_2\left(1 + \frac{\Gamma_1}{\Phi_1} + \frac{\Gamma_2}{\Phi_2}\right) > \log_2|\alpha|.$$

The term

$$\frac{1}{2}\log_2\left(1+\frac{\Gamma_1}{\Phi_1}+\frac{\Gamma_2}{\Phi_2}\right)$$

may be considered as the capacity of a “pseudo AWN channel” with SNR

$$\left(\Gamma_1\Phi_2+\Gamma_2\Phi_1\right)/(\Phi_1\Phi_2).$$

It is a penalty of stabilizing a unstable LTI plant over two AWN channels and restricting to state feedback control strategy. The capacity of the two channels must overcome the negative effect of this “pseudo channel” and the degree of the instability of the plant to ensure the stabilizability of the system.

We plot the tradeoff in Figure 5.3. The region above the convex curve represents the SNR pairs that can ensure the stabilizability of the system. The region below the curve represents what is not achievable via state feedback. The origin of the figure is at (2, 2) and the rectangular region above the axes strictly contains the region for the achievable SNR pairs. It represents the necessary condition of the stabilization over a single channel

$$\left[\frac{\Gamma_1}{\Phi_1}-(\alpha^2-1)\right]\left[\frac{\Gamma_2}{\Phi_2}-(\alpha^2-1)\right]>0.$$

5.4 Stabilization of continuous-time scalar systems

5.4.1 State feedback

We consider continuous time systems with the setup of Figure 5.1. With state feedback, the stabilization of scalar continuous-time systems over AWN channels is not manageable. In fact, as the state signal is corrupted by the white noise n_1, the input power at the downlink

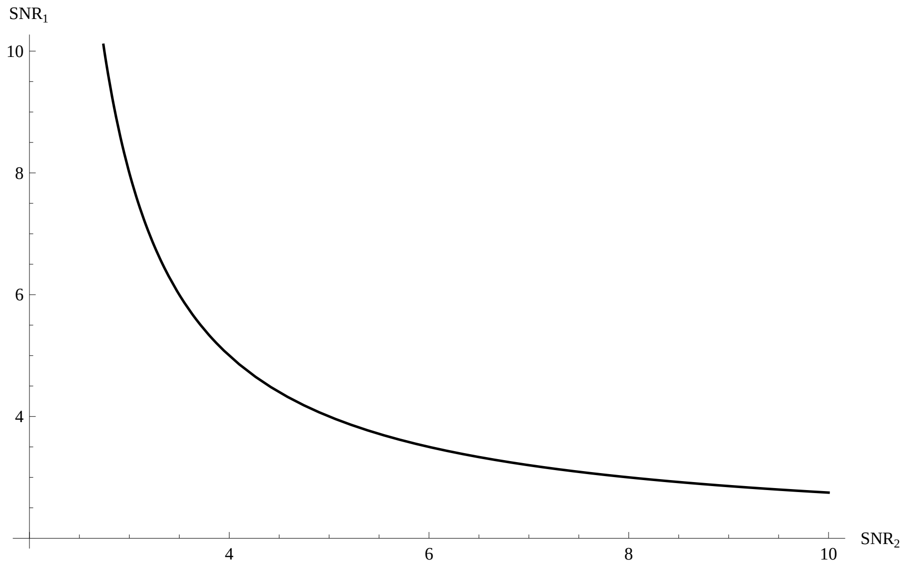

Figure 5.3: Tradeoff between the SNR of the uplink and downlink channels in the case of $\alpha = \sqrt{3}$.

channel is unbounded and thus any practical channels cannot transmit the control signal needed.

5.4.2 Output feedback

Although we consider first order scalar systems, we may treat the state information as plant output and thus utilize more general controllers. The problem is formulated in (5.1), and with a slight abuse of notation, the transfer functions are given by

$$
\begin{aligned}
u_1 &= \frac{PK}{1-PK} n_1 + \frac{1}{\lambda} \frac{P}{1-PK} n_2, \\
u_2 &= \lambda \frac{K}{1-PK} n_1 + \frac{PK}{1-PK} n_2.
\end{aligned}
$$

We tackle this optimization problem using the same approaches as the previous two chapters. As special instances of Section 2.3.3, we introduce the coprime factorization

$$P = NM^{-1}$$

in which $N, M \in \mathbf{R}\mathcal{H}_\infty$ and satisfy the Bezout identity $MX - NY = 1$. The parametrization of all stabilizing controllers is

$$\mathcal{K} = \{K : K = -(Y - MQ)(X - NQ)^{-1}, Q \in \mathbf{R}\mathcal{H}_\infty\}.$$

We can then characterize input power at the two channels as

$$\mathcal{E}\{u_1^2\} = \|(Y - MQ)N\|_2^2 \, \Phi_1 + \frac{1}{\lambda^2} \|(X - NQ)N\|_2^2 \, \Phi_2,$$
$$\mathcal{E}\{u_2^2\} = \lambda^2 \|(Y - MQ)M\|_2^2 \, \Phi_1 + \|(Y - MQ)N\|_2^2 \, \Phi_2.$$

where $\lambda \triangleq \lambda_2/\lambda_1$. The optimization over stabilizing controller is then equivalent to that over $Q \in \mathbf{R}\mathcal{H}_\infty$. It is easy to verify that the problem is convex (see Lemma 3.3) and we define the Lagrangian functional J as

$$J(Q, \epsilon, \lambda) \triangleq (1 - \epsilon)\mathcal{E}\{u_1^2\} + \epsilon(\mathcal{E}\{u_2^2\} - \Gamma_2),$$

where $0 \le \epsilon \le 1$.

As a related problem, we first fix a stabilizing controller K and seek for a tradeoff relationship between the SNR of the two channels for optimized λ. The scaling factors are optimal, when they are designed to guarantee the input powers at the channels match the constraints. Specifically, we obtain

$$\inf_{\lambda > 0} J(Q, \epsilon, \lambda) = \|(Y - MQ)N\|_2^2 \left((1 - \epsilon)\Phi_1 + \epsilon\Phi_2\right)$$
$$+ 2\sqrt{\epsilon(1 - \epsilon)\Phi_1\Phi_2} \, \|(X - NQ)N\|_2 \, \|(Y - MQ)M\|_2 - \epsilon\Gamma_2.$$

Define $J_\lambda^* \triangleq \inf_{\lambda>0} J(Q,\epsilon,\lambda)$. By the duality principle Theorem 2.19, it follows that

$$\Gamma_1 \geq \mathcal{E}\{u_1^2\} = \max_{\epsilon>0} \frac{1}{1-\epsilon} J_\lambda^*$$

With some elementary calculus, we obtain the following theorem:

Theorem 5.4 *Consider the system shown in Figure 5.1. For a fixed $Q \in \mathbf{R}\mathcal{H}_\infty$ or stabilizing controller K, a necessary and sufficient condition on the SNR of the two channels for stabilization is*

$$\left(\frac{\Gamma_1}{\Phi_1} - \left\|\frac{PK}{1-PK}\right\|_2^2\right)\left(\frac{\Gamma_2}{\Phi_2} - \left\|\frac{PK}{1-PK}\right\|_2^2\right) \geq \left\|\frac{P}{1-PK}\right\|_2^2 \left\|\frac{K}{1-PK}\right\|_2^2.$$

or equivalently,

$$\left(\frac{\Gamma_1}{\Phi_1} - \|(Y-MQ)N\|_2^2\right)\left(\frac{\Gamma_2}{\Phi_2} - \|(Y-MQ)N\|_2^2\right) \geq \|(X-NQ)N\|_2^2 \|(Y-MQ)M\|_2^2.$$

If one of the channels becomes noise-free and very reliable, for example as $\Gamma_2/\Phi_2 \to \infty$, then the condition in the theorem boils downs to

$$\frac{\Gamma_1}{\Phi_1} \geq \|(Y-MQ)N\|_2^2.$$

After optimization on $Q \in \mathbf{R}\mathcal{H}_\infty$, the right hand side equals $2\sum p_i$ (for minimum phase plants), which agrees with the results obtained for a single channel [8].

To accurately quantify a fundamental bound on Γ_1 and Γ_2, we need optimization of K or Q over all proper real-rational functions. Thus, it is notably difficult to arrive at an exact analytical characterization for a general plant transfer function. However, we can show a similar result as the discrete-time case if we consider only scalar systems. Suppose that the plant is described by

$$\dot{x}(t) = px(t) + u(t) \tag{5.6}$$

where t is the time variable, $x(t) \in \mathbb{R}$ is the plant state and $u(t)$ is the control input. We assume that the pole $p > 0$ and therefore the plant is unstable. The following theorem gives stabilization conditions for the two channels:

Theorem 5.5 *Consider the system configuration in Figure 5.1. The power constraints of the uplink and downlink channels are Γ_1 and Γ_2, respectively. Assume that the power spectral densities of the noise processes n_1 and n_2 are Φ_1 and Φ_2, respectively. If the plant is given by* (5.6) *with $p > 0$, then it is stabilizable over the channels if and only if the following conditions hold:*

$$\frac{\Gamma_2}{\Phi_2} > 2p \tag{5.7}$$

$$\frac{\Gamma_1}{\Phi_1} > \frac{p}{2}\left(\frac{2\sqrt{\frac{\Gamma_2}{\Phi_2}} - \sqrt{2p}}{\sqrt{\frac{\Gamma_2}{\Phi_2}} - \sqrt{2p}}\right)^2. \tag{5.8}$$

Proof. See Appendix A.7. ■

In limiting cases, such as when $\Gamma_1/\Phi_1 \to \infty$ or $\Gamma_2/\Phi_2 \to \infty$, the theorem boils down to the single-channel condition: $\Gamma/\Phi > 2p$. Furthermore, after a simple manipulation, we can express (5.8) as

$$\left(\sqrt{\frac{\Gamma_1}{\Phi_1}} - \sqrt{2p}\right)\left(\sqrt{\frac{\Gamma_2}{\Phi_2}} - \sqrt{2p}\right) > p.$$

The difference $\sqrt{\frac{\Gamma_2}{\Phi_2}} - \sqrt{2p}$ can be considered as the extra amount of channel resources needed beyond that of one channel stabilization, and thus the product of the channel resource has to be greater than the quantity representing the degree of instability of the system.

5.4.3 Two-parameter controller

In this subsection we consider the problem of using an extra degree of freedom in designing another controller parameter to improve the performance of the system or make

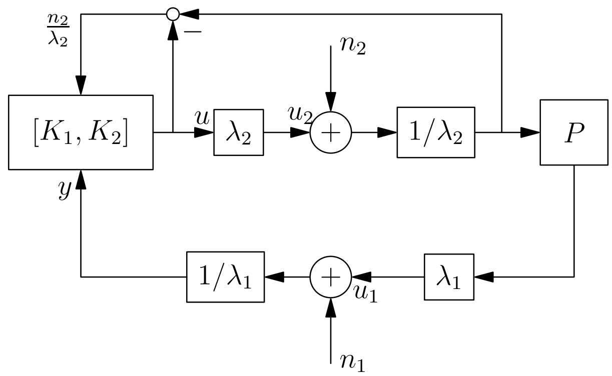

Figure 5.4: Stabilization over two channels with two-parameter controller utilizing feedback from channel.

its stabilization easier to achieve. In particular, we assume that the exact information regarding the white noise process n_2 is available at the controller. This information pattern, along with the general two-parameter controller structure, albeit idealized, gives us insight into the bound on the performance one can ever achieve. The system configuration is shown in Figure 5.4. There, the controller has a direct access of the channel noise through instant channel feedback.

Again, we study the problem (5.1). Utilizing the parameterization (2.5), if we let $Q_0 = Q + X - RN \in \mathbf{R}\mathcal{H}_\infty$, the input power at the two channels is

$$\mathcal{E}\{u_1^2\} = \|-1 + M(X - RN)\|_2^2 \,\Phi_1 + \frac{1}{\lambda^2}\,\|NQ_0\|_2^2 \,\Phi_2,$$

$$\mathcal{E}\{u_2^2\} = \lambda^2\,\|M(Y - RM)\|_2^2 \,\Phi_1 + \|-1 + MQ_0\|_2^2 \,\Phi_2.$$

As such, it has a separation property between the effect of the uplink and downlink channels.

Theorem 5.6 *Consider the system configuration in Figure 5.4. Under the assumptions of Theorem 5.5, the plant described by* (5.6) *with* $p > 0$ *is stabilizable over the channels if and*

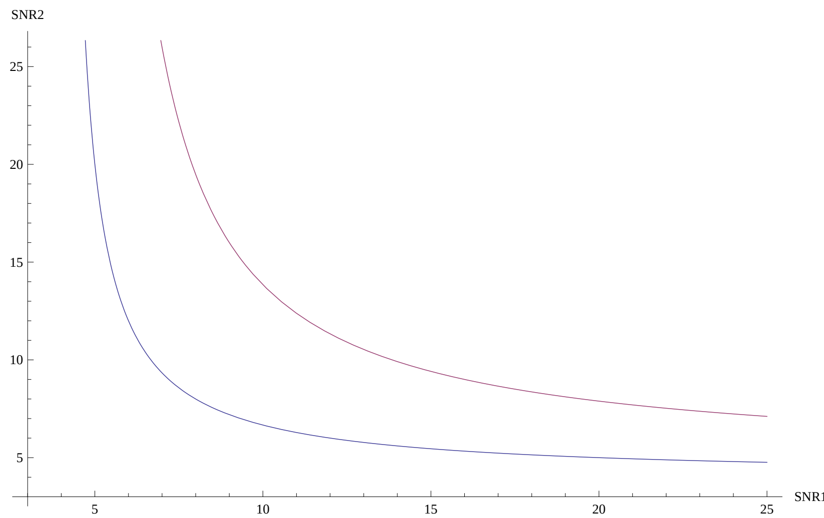

Figure 5.5: The comparison between the tradeoff of the one- and two-parameter controller for stabilization. The curve below corresponds to the two-parameter case, which has better performance. We assume $p = 2$ in this figure.

only if the following conditions hold:

$$\frac{\Gamma_2}{\Phi_2} > 2p \tag{5.9}$$

$$\frac{\Gamma_1}{\Phi_1} > 2p \frac{\frac{\Gamma_2}{\Phi_2}}{\frac{\Gamma_2}{\Phi_2} - 2p}. \tag{5.10}$$

Proof. See Appendix A.8. ■

The conditions in the theorem are equivalent to

$$\left(\frac{\Gamma_1}{\Phi_1} - 2p\right)\left(\frac{\Gamma_2}{\Phi_2} - 2p\right) > 4p^2.$$

We plot the comparison of the tradeoff curves between the original controller and two-parameter controller in Figure 5.5. The additional information and the extra parameter of the controller significantly improve the system performance, and gives a lower bound on the optimal stabilization region we can achieve over LTI controllers. The region is included in the rectangular area $\mathrm{SNR}_1 > 2p$ and $\mathrm{SNR}_2 > 2p$, which is the case if we consider only a single channel. Both curves in Figure 5.5 will approach asymptotically the single channel stabilization condition.

5.5 Summary

In this chapter, we analyzed the stabilization of linear feedback systems over both the uplink and downlink channels. The interaction of the channels with the unstable plant forms an achievable SNR region for system stabilizability. For first order LTI systems, the lower bound on the achievable SNR's exhibits a convex tradeoff that is more demanding than when there is only one channel. In addition, the use of the two-parameter controller to take advantage of the extra information from the channel feedback can better the performance significantly and expand the feasible region of SNR's.

Chapter 6

Conclusions

6.1 Overview

The thesis designs and explores a framework for the performance analysis of feedback control systems with communication constraints. We aim to gain insight into the fundamental limitations originated from the mutual impact of the communication and control. As one of the first endeavors to study performance problems in this realm, our work can possess important values in the design and synthesis of NCS's. In the thesis, analytical bounds are derived, serving as a separation line between what is achievable and what is not. Given any performance specification, we can readily pinpoint the class of channels which can satisfactorily achieve it.

In this framework, we choose the AWN channel as the communication model, focus on LTI control strategies, make use of only scaling for channel compensation, and thus keep the linearity of the closed-loop system. We characterize primarily the tracking performance and work in a full MIMO setting and parallel channels for the most part.

We have analyzed the control systems with AWN channel in the uplink. The stabilization conditions on the channel input power for a general MIMO systems depend on the unstable poles and their directions altered by the vector of noise levels of the parallel channel. If nonminimum phase zeros are present, the proximity of such zeros and unstable poles incurs stricter requirement on the channel, and that constraint on the channel input power behaves differently depending on the alignment of zero and pole directions. We derived the optimal achievable tracking performance. It depends on the unstable poles and nonminimum phase zeros of the plant, the power spectral density of the reference signal, and the power constraint and noise levels of the parallel channel. For minimum phase systems, the tracking performance exhibits a desirable property that only the power of the reference signal instead of the complete power spectral density is needed. Scaling factors across the channel are designed to always activate the channel input power constraint at optimal performance. Comparisons show apparent performance improvements and it seems unnatural to not use scaling. Under optimal tracking scheme, we have found out that the power allocations among each channel follow a "fire-quenching" policy rather than the widely-know "water-filling" solution. The power allocation of parallel channel for a fully decentralized control systems agrees with a similar policy.

The tracking performance of systems over downlink AWN channel gives rise to more interesting but harder to analyze results. In this case, the plant gain in entire frequency range plays an essential role and thus the minimum phase behaviors affect the performance. Then, certain minimum phase zeros, especially ones that are close to the imaginary axis, will greatly worsen the performance. For MIMO plants, the performance bound is related to the largest and smallest singular value of the plant transfer function matrix at the entire

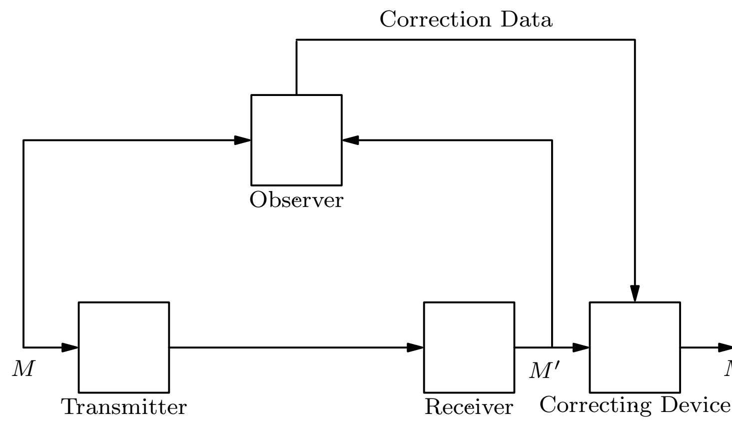

Figure 6.1: Correction Systems

frequency range.

The stabilization problem for systems over both the uplink and downlink channel through LTI control strategy is also equivalent to a constrained optimization problem. For first-order systems, we explicitly show a convex tradeoff between the SNR's of the two channels, which determines the feasible region of the SNR pair that ensures stability. If one channel becomes more reliable (has higher SNR), then the requirement on the other channel can be relaxed.

6.2 Future Work

We have illustrated in different perspectives the interaction between the communication and control in terms of performance under a linear control framework. Our work may be extended in a few directions.

As we have only analyzed scaling scheme for the channel, it is interesting and meaningful to investigate more general channel compensation strategies while staying within the same framework. A simplest extension is to consider a multi-dimension scaling that is capable of adjust each channel's input power[1], instead of the uniform scaling factor we assumed. A more general extension would be to use LTI filters in $\mathbf{R}\mathcal{H}_\infty$ across the channels. It is also important to exploit channel feedbacks or encoding/decoding schemes to possibly better the performance, for example, the correction systems shown in Figure 6.1 proposed by Shannon. In those cases, exact and analytical bounds may be hard to derive.

As for the stabilization over both uplink and downlink channels, one may consider plants with time delay, or even more general plant models. The tracking problem may also be investigated in the two channel configuration. The underlying assumption about the channels being the same type may also be dropped.

We have only focused on the AWN channel, a continuous-alphabet channel. In contrast, the performance problem with discrete-alphabet channel, which is more practical for implementation, may be considered. However, one may need to utilize appropriate information patterns and device sophisticated coding/deocoding for the channels.

[1]Similar to the one we studied in Section 3.5.1.3, but with more general assumptions on the plant and controller.

Bibliography

[1] B. D. O. Anderson and J. B. Moore. *Optimal filtering*. Prentice Hall, Englewood Cliffs, NJ, 1979.

[2] B. D. O. Anderson and J. B. Moore. *Optimal control: linear quadratic methods*. Prentice Hall, Englewood Cliffs, NJ, 1989.

[3] P. Antsaklis and J. Baillieul. Special issue on networked control systems. *IEEE Transactions on Automatic Control*, 49(9), Sept. 2004.

[4] K. J. Åström. *Introduction to Stochastic Control Theory*. Academic, New York, 1970.

[5] H. W. Bode. *Network Analysis and Feedback Amplifier Design*. Van Nostrand, Princeton, NJ, 1945.

[6] S. Boyd and C. A. Desoer. Subharmonic functions and performance bounds on linear time-invariant feedback systems. *IMA Journal of Mathematical Control and Information*, 2:153–170, 1985.

[7] S. Boyd and L. Vandenberghe. *Convex Optimization*. Cambridge University Press, New York, 2004.

[8] J. H. Braslavsky, R. H. Middleton, and J. S. Freudenberg. Feedback stabilization over signal-to-noise ratio constrained channels. In *Proc. 2004 Amer. Control Conf.*, pages 4903–4908, Boston, MA, June 2004.

[9] J. H. Braslavsky, R. H. Middleton, and J. S. Freudenberg. Feedback stabilization over signal-to-noise ratio constrained channels. *IEEE Transactions on Automatic Control*, 52(8):1391–1403, 2007.

[10] R. W. Brockett and D. Liberzon. Quantized feedback stabilization of linear systems. *IEEE Transactions on Automatic Control*, 45(7):1279–1289, Jul 2000.

[11] C. D. Charalambous, A. Farhadi, and S. Z. Denic. Control of continuous-time linear gaussian systems over additive gaussian wireles fading channels: a separation principle. *IEEE Transactions on Automatic Control*, 53(4):1013–1019, May 2008.

[12] G. Chen, J. Chen, and R. Middleton. Optimal tracking performance for SIMO systems. *IEEE Transactions on Automatic Control*, 47(10):1770–1775, Oct. 2002.

[13] J. Chen. Sensitivity integral relations and design tradeoffs in linear multivariable feedback systems. *IEEE Transactions on Automatic Control*, 40(10):1700–1716, Oct. 1995.

[14] J. Chen. Multivariable gain-phase and sensitivity integral relations and design tradeoffs. *IEEE Transactions on Automatic Control*, 43(3):373–385, Mar. 1998.

[15] J. Chen, S. Hara, and G. Chen. Best tracking and regulation performance under control energy constraint. *IEEE Transactions on Automatic Control*, 48(8):1320–1336, Aug. 2003.

[16] J. Chen and C. N. Nett. Sensitivity integrals for multivariable discrete-time systems. *Automatica*, 31(8):1113 – 1124, 1995.

[17] J. Chen, L. Qiu, and O. Toker. Limitations on maximal tracking accuracy. i. tracking step signals. In *Proc. 35th IEEE Conf. on Decision and Control*, pages 726–731, Kobe, Japan, Dec. 1996.

[18] J. Chen, L. Qiu, and O. Toker. Limitations on maximal tracking accuracy. 2. tracking sinusoidal and ramp signals. In *Proc. 1997 Amer. Control Conf.*, pages 1757–1761, Albuquerque, NM, June 1997.

[19] J. Chen, O. Toker, and L. Qiu. Limitations on maximal tracking accuracy. *IEEE Transactions on Automatic Control*, 45(2):326–331, Feb. 2000.

[20] T. M. Cover and J. A. Thomas. *Elements of Information Theory.* Wiley, New York, 1991.

[21] D. Delchamps. Stabilizing a linear system with quantized state feedback. *IEEE Transactions on Automatic Control*, 35(8):916–924, Aug. 1990.

[22] N. Elia. When Bode meets Shannon: control-oriented feedback communication schemes. *IEEE Transactions on Automatic Control*, 49(9):1477–1488, Sept. 2004.

[23] N. Elia and S. K. Mitter. Stabilization of linear systems with limited information. *IEEE Transactions on Automatic Control*, 46(9):1384–1400, Sept. 2001.

[24] B. A. Francis. *A Course in H_∞ Control Theory.* Lecture Notes in Control and Information Sciences. Springer-Verlag, Berlin, Germany, 1987.

[25] J. S. Freudenberg and D. P. Looze. Right half plane zeros and poles and design tradeoffs in feedback systems. *IEEE Transactions on Automatic Control*, 30(6):555–565, June 1985.

[26] J. S. Freudenberg, R. H. Middleton, and J. H. Braslavsky. Stabilization with disturbance attenuation over a Gaussian channel. In *Proc. 46th IEEE Conf. on Decision and Control*, pages 3958–3963, New Orleans, LA, USA, Dec. 2007.

[27] J. S. Freudenberg, R. H. Middleton, and J. H. Braslavsky. Minimum variance control over a Gaussian communication channel. In *Proc. 2008 Amer. Control Conf.*, pages 2625–2630, Seattle, WA, USA, June 2008.

[28] M. Fu and L. Xie. The sector bound approach to quantized feedback control. *IEEE Transactions on Automatic Control*, 50(11):1698–1711, Nov. 2005.

[29] A. Gersho and R. M. Gray. *Vector Quantization and Signal Compression*. Kluwer, Boston, MA, 1992.

[30] G. C. Goodwin, D. E. Quevedo, and E. I. Silva. An introduction to networked control systems. In *Proc. 6th Asian Control Conf.*, pages 50–74, Bali, Indonesia, 2006.

[31] J. P. Hespanha, P. Naghshtabrizi, and Y. Xu. A survey of recent results in networked control systems. *Proceedings of the IEEE*, 95(1):138 –162, Jan. 2007.

[32] P. P. Khargonekar and M. A. Rotea. Multiple objective optimal control of linear systems: The quadratic norm case. *IEEE Transactions on Automatic Control*, 36(1):14–24, Jan. 1991.

[33] H. Kwakernaak and R. Sivan. *Linear Optimal Control Systems*. Wiley-Interscience, New York, NY, 1972.

[34] Y. Li, E. Tuncel, and J. Chen. Optimal tracking and power allocation over an additive white noise channel. In *Proc. 2009 IEEE International Conf. on Control and Automation.*, pages 1541–1546, Christchurch, New Zealand, Dec. 2009.

[35] Y. Li, E. Tuncel, and J. Chen. Optimal tracking over an additive white gaussian noise channel. In *Proc. 2009 Amer. Control Conf.*, pages 4026–4031, Saint Louis, MO, June 2009.

[36] Y. Li, E. Tuncel, and J. Chen. Optimal tracking over an additive white noise feedback channel. In *Proc. 2009 Asian Control Conf.*, pages 501–506, Hong Kong SAR, China, Aug. 2009.

[37] Y. Li, E. Tuncel, and J. Chen. Stabilization over additive white noise forward and feedback channels. In *Proc. 8th World Congress on Intelligent Control and Automation.*, pages 1251–1256, Jinan, China, July 2010.

[38] Y. Li, E. Tuncel, J. Chen, and W. Su. Optimal tracking performance of discrete-time systems over an additive white noise channel. In *Proc. 48th IEEE Conf. on Decision and Control held jointly with 28th Chinese Control Conf.*, pages 2070–2075, Shanghai, China, Dec. 2009.

[39] D. G. Luenberger. *Optimization by Vector Space Methods*. John Wiley & Sons, New York, 1969.

[40] N. C. Martins and M. A. Dahleh. Fundamental limitations of disturbance attenuation in the presence of side information. *IEEE Transactions on Automatic Control*, 52(1):52–66, Jan. 2007.

[41] N. C. Martins and M. A. Dahleh. Feedback control in the presence of noisy channels: 'Bode-like' fundamental limitations of performance. *IEEE Transactions on Automatic Control*, 53(7):1604–1615, Aug. 2008.

[42] N. C. Martins, M. A. Dahleh, and N. Elia. Feedback stabilization of uncertain systems in the presence of a direct link. *IEEE Transactions on Automatic Control*, 51(3):438–447, Mar. 2006.

[43] M. Morari and E. Zafiriou. *Robust Process Control*. Prentice Hall, Englewood Cliffs, NJ, 1989.

[44] G. N. Nair and R. J. Evans. Stabilization with data rate limited feedback: tightest attainable bounds. *System Control Letters*, 41(1):49–56, 2000.

[45] G. N. Nair and R. J. Evans. Exponential stabilisability of finite-dimensional linear systems with limited data rates. *Automatica*, 39(4):585–593, Apr. 2003.

[46] G. N. Nair and R. J. Evans. Stabilizability of stochastic linear systems with finite feedback data rates. *SIAM J. Control Optim.*, 43(2):413–436, July 2004.

[47] G. N. Nair, F. Fagnani, S. Zampieri, and R. J. Evans. Feedback control under data rate constraints: an overview. *Proceedings of the IEEE*, 95(1):108–137, Jan. 2007.

[48] R. Nevanlinna and V. Paatero. *Introduction to Complex Analysis*. Addison-Wesley, 1969.

[49] A. Papoulis and S. U. Pillai. *Probability, Random Variables and Stochastic Processes*. McGraw Hill, New York, 4 edition, 2002.

[50] T. Qi and W. Su. Optimal tracking and tracking performance constraints from quantization. In *7th Asian Control Conference*, pages 447 –452, 2009.

[51] L. Qiu and E. J. Davison. Performance limitations of non-minimum phase systems in the servomechanism problem. *Automatica*, 29(2):337–349, Feb. 1993.

[52] L. Qiu, Z. Ren, and J. Chen. Fundamental performance limitations in estimation problems. *Communications in Information and Systems*, 2(4):371–384, Dec. 2002.

[53] A. Rojas, J. H. Braslavsky, and R. H. Middleton. Control over a bandwidth limiteed signal to noise ratio constrained communication channel. In *Proc. 44th IEEE Conf. on Decision and Control*, pages 197–202, Seville, Spain, Dec. 2005.

[54] A. Rojas, J. S. Freudenberg, J. H. Braslavsky, and R. H. Middleton. Optimal signal to noise ratio in feedback over communication channels with memory. In *Proc. 45th IEEE Conf. on Decision and Control*, pages 1129–1134, San Diego, CA, Dec. 2006.

[55] A. Saberi, P. Sannuti, and B. M. Chen. *H_2 optimal control*. Prentice Hall, Englewood Cliffs, NJ, 1995.

[56] A. Sahai and S. Mitter. The necessity and sufficiency of anytime capacity for stabilization of a linear system over a noisy communication link - Part I: Scalar systems. *IEEE Transactions on Information Theory*, 52(8):3369–3395, Aug. 2006.

[57] A. V. Savkin. Analysis and synthesis of networked control systems: Topological entropy, observability, robustness and optimal control. 42:51–62, 2006.

[58] M. M. Seron, J. H. Braslavsky, and G. C. Goodwin. *Fundamental Limitations in Filtering and Control*. Springer-Verlag, London, England, 1997.

[59] E. I. Silva, G. C. Goodwin, and D. E. Quevedo. Control system design subject to SNR constraints. *Automatica*, 46(12):428–436, Dec. 2009.

[60] S. Skogestad and I. Postlethwaite. *Multivariable Feedback Control: Analysis and Design*. John Wiley & Sons, West Sussex, England, 2 edition, 2005.

[61] T. Söderström. *Discrete-time Stochastic systems: Estimation and Control*. Advanced textbooks in control and signal processing. Springer, New York, 2 edition, 2002.

[62] W. Su, L. Qiu, and J. Chen. Fundamental limit of discrete-time systems in tracking multi-tone sinusoidal signals. *Automatica*, 43(1):15 – 30, 2007.

[63] S. Tatikonda and S. M. Mitter. Control over noisy channels. *IEEE Transactions on Automatic Control*, 49(7):1196–1201, July 2004.

[64] S. Tatikonda and S. M. Mitter. Control under communication constraints. *IEEE Transactions on Automatic Control*, 49(7):1056–1068, July 2004.

[65] O. Toker, J. Chen, and L. Qiu. Tracking performance limitations in lti multivariable discrete-time systems. *IEEE Transactions on Circuits and Systems—Part I: Fundamental Theory and Applications*, 49(5):657–670, May 2002.

[66] D. Tse and P. Viswanath. *Fundamentals of Wireless Communication*. Cambrige University Press, New York, 2005.

[67] M. Vidyasagar. *Control systems synthesis: a factorization approach*. The MIT Press, Cambridge, MA, 1985.

[68] D. Youla. On the factorization of rational matrices. *Information Theory, IRE Transactions on*, 7(3):172 –189, 1961.

[69] S. Yuksel and T. Basar. Control over noisy forward and reverse channels. *IEEE Transactions on Automatic Control*, 2011, preprint.

[70] K. Zhou, J. C. Doyle, and K. Glover. *Robust and Optimal Control*. Prentice Hall, Englewood Cliffs, NJ, 1996.

Appendix A

Proofs

A.1 Proof of Theorem 3.8

Proof. From (3.14) and the factorization (3.9), we immediately obtain

$$\begin{aligned}\mu_n &= \inf_{R\in\mathbf{R}\mathcal{H}_\infty} \left\| \Psi_n \left(F^{-1} - I\right) + \Psi_n - (X - NR)\tilde{M}_m^{(n)} \right\|_2^2 \\ &= \mu_m + \inf_{R\in\mathbf{R}\mathcal{H}_\infty} \left\| \Psi_n - (X - NR)\tilde{M}_m^{(n)} \right\|_2^2 .\end{aligned}$$

Let $H_3 \triangleq \left\| \Psi_n - (X - NR)\tilde{M}_m^{(n)} \right\|_2^2$. Since $N(s)$ can be factorized as in (2.7), we obtain that

$$H_3 = \left\| L^{-1}\left(\Psi_n - X\tilde{M}_m^{(n)}\right) + N_m R \tilde{M}_m^{(n)} \right\|_2^2 .$$

Applying (2.24) in Lemma 2.18, we obtain

$$\begin{aligned}L^{-1}\left(\Psi_n - X\tilde{M}_m^{(n)}\right) = A(s) + \sum_{i=1}^{k} \left(\prod_{j=i+1}^{k} L_j(z_i)\right)^{-1} \times \\ L_i^{-1}(s) \left(\prod_{j=1}^{i-1} L_j(z_i)\right)^{-1} \left(\Psi_n - X(z_i)\tilde{M}_m^{(n)}(z_i)\right) \quad \text{(A.1)}\end{aligned}$$

where $A(s) \in \mathbf{R}\mathcal{H}_\infty$. To proceed, we simplify the expression such that it depends on $\tilde{M}$ instead of X. And we claim that the following identity is true

$$
\begin{aligned}
&L_i^{-1}(s)\left(\prod_{j=1}^{i-1} L_j(z_i)\right)^{-1}\left(\Psi_n - X(z_i)\tilde{M}_m^{(n)}(z_i)\right) \\
&\qquad\qquad = C_i + L_i^{-1}(s)\left(\prod_{j=1}^{i-1} L_j(z_i)\right)^{-1}\Psi_n\left(I - F^{-1}(z_i)\right) \quad \text{(A.2)}
\end{aligned}
$$

where C_i is a constant matrix. Firstly, from the Bezout identity $\tilde{M}X - \tilde{N}Y = I$, we have that $X\tilde{M}\Psi_n = \Psi_n + NM^{-1}Y\tilde{M}\Psi_n$. Right-multiplying F^{-1} on both sides and taking $s = z_i$, we have

$$
\Psi_n - X(z_i)\tilde{M}_m^{(n)}(z_i) = \Psi_n\left(I - F^{-1}(z_i)\right) - E(z_i) \quad \text{(A.3)}
$$

where

$$
E(s) \triangleq P(s)Y(s)\tilde{M}_m^{(n)}(s).
$$

From (2.27), we have that

$$
L_i^{-1}(s) - I = \frac{2\mathrm{Re}\{z_i\}}{s - z_i}\boldsymbol{\eta}_i\boldsymbol{\eta}_i^H. \quad \text{(A.4)}
$$

Also, by definition of the factor (2.9), we have $\boldsymbol{\eta}_i^H L_i(z_i) = 0$. Then it follows from the factorization (2.7) that,

$$
\left(L_i^{-1}(s) - I\right)\left(\prod_{j=1}^{i-1} L_j(z_i)\right)^{-1} E(z_i) = 0.
$$

Therefore

$$
C_i = -\left(\prod_{j=1}^{i-1} L_j(z_i)\right)^{-1} E(z_i),
$$

and the claim is proved.

The next step is to decompose H_3 into parts in $\mathcal{H}_2$ and $\mathcal{H}_2^\perp$, respectively. More specifically, in light of (A.1) , (A.2) and the fact that $L_i^{-1} - I \in \mathcal{H}_2^\perp$ for $i = 1, \ldots, k$, we obtain

$$H_3 = \left\| \sum_{i=1}^{k} \left(\prod_{j=i+1}^{k} L_j(z_i) \right)^{-1} \left(L_i^{-1}(s) - I\right) \times \right.$$
$$\left. \left(\prod_{j=1}^{i-1} L_j(z_i) \right)^{-1} \Psi_n \left(I - F^{-1}(z_i)\right) \right\|_2^2 + \left\| A' - N_m R \tilde{M}_m^{(n)} \right\|_2^2,$$

where $A' \in \mathbf{R}\mathcal{H}_\infty$ and R is selected such that $A' - N_m R\tilde{M}_m^{(n)} \in \mathcal{H}_2$. It is obvious now that $\inf_{R \in \mathbf{R}\mathcal{H}_\infty} \|A' - N_m R \tilde{M}_m^{(n)}\|_2^2 = 0$. Thus we obtain

$$\begin{aligned}
\inf_{R \in \mathbf{R}\mathcal{H}_\infty} H_3 &= \left\| \sum_{i=1}^{k} \frac{2\mathrm{Re}\{z_i\}}{s - z_i} \boldsymbol{v}_i \boldsymbol{w}_i^H \right\|_2^2 \\
&= \sum_{i,j=1}^{k} 4\mathrm{Re}\{z_i\}\mathrm{Re}\{z_j\} \boldsymbol{v}_i^H \boldsymbol{v}_j \boldsymbol{w}_j^H \boldsymbol{w}_i \left\langle \frac{1}{s - z_i}, \frac{1}{s - z_j} \right\rangle.
\end{aligned}$$

A easy calculation shows $\left\langle \frac{1}{s-z_i}, \frac{1}{s-z_j} \right\rangle = 1/(\bar{z}_i + z_j)$ and the proof is complete. ■

A.2 Proof of Theorem 3.9

Proof. Lemma 3.5 shows two steps to search for the best tracking performance. We shall first derive

$$H^*(\epsilon) = \inf_{Q, R \in \mathbf{R}\mathcal{H}_\infty} H(\epsilon, Q, R, \Gamma)$$

which is defined in (3.6), and then find $H_e^*(\Gamma)$ according to (3.8).

It follows from (3.3) and the property of the $\mathcal{H}_2$ norm that

$$H^*(\epsilon) = \inf_{Q \in \mathbf{R}\mathcal{H}_\infty} \left\| \begin{bmatrix} \sqrt{1-\epsilon}(I - NQ) \\ \sqrt{\epsilon} NQ \end{bmatrix} \Psi_r \right\|_2^2 + \inf_{R \in \mathbf{R}\mathcal{H}_\infty} \left\| N(\tilde{Y} - R\tilde{M})\Psi_n \right\|_2^2 - \epsilon\Gamma. \quad \text{(A.5)}$$

For simplicity, define the following functions

$$H_1 = \left\| \begin{bmatrix} \sqrt{1-\epsilon}(I - NQ) \\ \sqrt{\epsilon} NQ \end{bmatrix} \Psi_r \right\|_2^2 ,$$

$$H_1^* = \inf_{Q \in \mathbf{R}\mathcal{H}_\infty} H_1 .$$

To search for H_1^*, we follow the techniques explainted in Section 2.3.7. It is straightforward to see that

$$H_1 = \left\| \left(\begin{bmatrix} \sqrt{1-\epsilon} I \\ 0 \end{bmatrix} + \begin{bmatrix} -\sqrt{1-\epsilon} I \\ \sqrt{\epsilon} I \end{bmatrix} NQ \right) \Psi_r \right\|_2^2 .$$

Introduce an inner matrix

$$\Delta \triangleq \begin{bmatrix} -\sqrt{1-\epsilon} I \\ \sqrt{\epsilon} I \end{bmatrix} . \tag{A.6}$$

Note that $\Delta^T \Delta = I$. According to Lemma 2.16, we are able to construct a unitary operator in $\mathcal{L}_2$ as

$$\Xi(s) \triangleq \begin{bmatrix} \Delta^T \\ I - \Delta\Delta^T \end{bmatrix} . \tag{A.7}$$

Pre-multiplying Ξ, we obtain

$$\begin{aligned} H_1^* &= \inf_{Q \epsilon \mathbf{R}\mathcal{H}_\infty} \left\| \Xi \left(\begin{bmatrix} \sqrt{1-\epsilon} I \\ 0 \end{bmatrix} + \begin{bmatrix} -\sqrt{1-\epsilon} I \\ \sqrt{\epsilon} I \end{bmatrix} NQ \right) \Psi_r \right\|_2^2 \\ &= \hat{H}_1^* + \left\| \left(I - \Delta\Delta^T \right) \begin{bmatrix} \sqrt{1-\epsilon} I \\ 0 \end{bmatrix} \Psi_r \right\|_2^2 \end{aligned} \tag{A.8}$$

where

$$\hat{H}_1^* \triangleq \inf_{Q \in \mathbf{R}\mathcal{H}_\infty} \left\| \left(\Delta^T \begin{bmatrix} \sqrt{1-\epsilon} I \\ 0 \end{bmatrix} + NQ \right) \Psi_r \right\|_2^2 .$$

As stated in Remark 3.6, the infimum $\hat{H}_1^*$ is 0 by properly choosing $Q_\theta \in \mathbf{R}\mathcal{H}_\infty$ such that

$$NQ_\theta \to (1-\epsilon)I \tag{A.9}$$

as $\theta \to 0^+$. An easy calculation of the second term of (A.8) yields

$$H_1^* = \epsilon(1-\epsilon)\|\Psi_r\|_2^2 = \epsilon(1-\epsilon)\sigma_{\boldsymbol{r}}^2.$$

From (3.13), it is now clear that

$$H^*(\epsilon) = \epsilon(1-\epsilon)\sigma_{\boldsymbol{r}}^2 + \mu_m - \epsilon\Gamma. \tag{A.10}$$

The problem is feasible if and only if $H^*(1) < 0$, which also implies $\Gamma > \mu_m$ is the lower bound on the power constraint for stabilizability of the system. Define $\alpha \triangleq \epsilon/(1-\epsilon)$. Applying Lemma 3.5, we obtain

$$H_e^*(\Gamma) = \sup_{\alpha>0}\left(\frac{\alpha}{1+\alpha}\sigma_{\boldsymbol{r}}^2 + (1+\alpha)\mu_m - \alpha\Gamma\right). \tag{A.11}$$

This function of α is concave. Thus, by setting the derivative to 0, we obtain the optimal α as

$$\alpha^* = \begin{cases} \sqrt{\frac{\sigma_{\boldsymbol{r}}^2}{\Gamma-\mu_m}} - 1, & \text{if } \mu_m < \Gamma < \mu_m + \sigma_{\boldsymbol{r}}^2, \\ 0, & \text{if } \Gamma \geq \mu_m + \sigma_{\boldsymbol{r}}^2, \end{cases} \tag{A.12}$$

which, together with (A.11), proves (3.19). ∎

A.3 Proof of Theorem 3.11

Proof. The proof is similar to and leverages the routines of that for Theorem 3.9. Since the plant has nonminimum phase zeros, the coprime factor N admits the factorization (2.7).

Then, as (A.5) indicates, we have

$$H^*(\epsilon) = H_1^* + \mu_n - \epsilon\Gamma,$$

where

$$H_1^* = \inf_{Q \in \mathbf{R}\mathcal{H}_\infty} \left\| \begin{bmatrix} \sqrt{1-\epsilon}(L^{-1} - N_m Q) \\ \sqrt{\epsilon} N_m Q \end{bmatrix} \Psi_r \right\|_2^2$$

and μ_n is given by (3.16). We decompose $L^{-1}\Psi_r$ into parts in $\mathcal{H}_2$ and $\mathcal{H}_2^\perp$. Using Lemma 2.18, we obtain that

$$L^{-1}\Psi_r = A + A_1 + A_2,$$

where A is a matrix in $\mathbf{R}\mathcal{H}_\infty$ and

$$\begin{aligned} A_1 &\triangleq \sum_{i=1}^{k} L_k^{-1}(z_i) \cdots L_{i+1}^{-1}(z_i) L_{i-1}^{-1}(z_i) \cdots L_1^{-1}(z_i)\Psi_r(z_i), \\ A_2 &\triangleq \sum_{i=1}^{k} L_k^{-1}(z_i) \cdots L_{i+1}^{-1}(z_i) \left(L_i^{-1} - I\right) L_{i-1}^{-1}(z_i) \cdots L_1^{-1}(z_i)\Psi_r(z_i) \\ &= \sum_{i=1}^{k} \frac{2\mathrm{Re}\{z_i\}}{s - z_i} \boldsymbol{a}_i \boldsymbol{b}_i^H. \end{aligned}$$

It follows that $A + A_1 = Z \in \mathbf{R}\mathcal{H}_\infty$ where Z is as defined in the theorem, and $A_2 \in \mathcal{H}_2^\perp$. Since Ψ_r is minimum phase, we can choose Q such that $(A + A_1 - N_m Q \Psi_r) \in \mathcal{H}_2$. As a result,

$$H_1 = (1-\epsilon)\left\|A_2\right\|_2^2 + \left\| \begin{bmatrix} \sqrt{1-\epsilon} Z \\ 0 \end{bmatrix} + \begin{bmatrix} -\sqrt{1-\epsilon} I \\ \sqrt{\epsilon} I \end{bmatrix} N_m Q \Psi_r \right\|_2^2 .$$

It is a straightforward calculation that $\|A_2\|_2^2 = \delta$. Then, by pre-multiplying the second term by the unitary matrix Ξ (A.7), we obtain that

$$H_1^* = (1-\epsilon)\delta + \epsilon(1-\epsilon)\|Z\|_2^2.$$

The rest of the proof consists of using Lemma 3.5 and carrying out derivations of convex optimization same as Theorem 3.9. It leads to

$$H_e^* = \sup_{\alpha>0}\left(\delta + \frac{\alpha}{1+\alpha}\|Z\|_2^2 + (1+\alpha)\mu_n - \alpha\Gamma\right)$$

and the theorem can be proved. ■

A.4 Proof of Lemma 4.5

We shall first introduce two preliminary lemmas which are necessary for the proof. The lemmas can be found in, e.g. [15]. Consider the class of functions which have limited behavior at infinity

$$\mathcal{F} \triangleq \left\{ f : \lim_{R\to\infty} \sup_{\theta\in[-\pi/2,\pi/2]} \frac{|f(Re^{\mathrm{j}\theta})|}{R} = 0 \right\}.$$

The first result is a format of Bode's attenuation integral [5], [58, p. 49] and the second result is an immediate consequence of the first.

Lemma A.1 *Suppose that $f(s)$ is analytic at $s = \infty$ and in the closed right half plane ($\mathbb{C}_+ \bigcup \mathbb{C}_0$) except for possible singularities s_0 on $\mathbb{C}_0$ that satisfy $\lim_{s\to s_0}(s-s_0)f(s) = 0$. Also suppose that $f(s)$ is conjugate symmetric. Define $f(\mathrm{j}\omega) = h_1(\omega) + \mathrm{j}h_2(\omega)$. Then,*

$$\lim_{s\to\infty} s\left[f(s) - f(\infty)\right] = \frac{1}{\pi}\int_{-\infty}^{\infty} \left[h_1(\omega) - h_1(\infty)\right] \mathrm{d}\omega. \tag{A.13}$$

Applying the above lemma on $\log f(s) \in \mathcal{F}$ yields

Lemma A.2 *Let $f(s)$ be conjugate symmetric. Suppose further that $f(s)$ is analytic and has no zeros in the closed right half plane except for possible zeros on $\mathbb{C}_0$. Also suppose that $\log f(s) \in \mathcal{F}$. Then, provided that $f(\infty) \neq 0$, we have*

$$\lim_{s\to\infty} s \log\frac{f(s)}{f(\infty)} = \frac{1}{\pi}\int_{-\infty}^{\infty} \log\left|\frac{f(\mathrm{j}\omega)}{f(\infty)}\right| \mathrm{d}\omega. \tag{A.14}$$

Proof of Lemma 4.5. Since the plant is minimum phase, we can define the free parameter in $\mathbf{R}\mathcal{H}_\infty$ as $R_0 = \tilde{X} - R\tilde{N}$. By virtue of the factorization (4.4), we obtain

$$J_2(R_0) = \left\| \frac{1}{\lambda} \begin{bmatrix} \sqrt{1-\epsilon} N R_0 \\ \lambda\sqrt{\epsilon}\left(B^{-1} - I + I - MR_0\right) \end{bmatrix} \Psi_n \right\|_2^2$$

Since $B^{-1} - I \in \mathcal{H}_2^\perp$, we have

$$J_2^* = \epsilon \left\| \left(B^{-1} - I\right) \Psi_n \right\|_2^2 + \tilde{J}_2.$$

where

$$\tilde{J}_2 = \inf_{R_0 \in \mathbf{R}\mathcal{H}_\infty} \left\| \left(\begin{bmatrix} 0 \\ \sqrt{\epsilon} I \end{bmatrix} + \frac{1}{\lambda} \Theta_i \Theta_o R_0 \right) \Psi_n \right\|_2^2$$

and

$$\begin{bmatrix} \sqrt{1-\epsilon} N \\ -\lambda\sqrt{\epsilon} M_m \end{bmatrix} = \Theta_i \Theta_o.$$

By definition of the inner-outer factorization,

$$\Theta_o^\sim \Theta_o = (1-\epsilon) N^\sim N + \lambda^2 \epsilon M_m^\sim M_m. \tag{A.15}$$

And since the P is strictly proper, we have

$$\Theta_o^\sim(\infty) \Theta_o(\infty) = \lambda^2 \epsilon M_m^\sim(\infty) M_m(\infty). \tag{A.16}$$

Construct the unitary matrix

$$\Upsilon \triangleq \begin{bmatrix} \Theta_i^\sim \\ I - \Theta_i \Theta_i^\sim \end{bmatrix}$$

and use the technique in the proof of Theorem 2.15, we have

$$\tilde{J}_2 = \inf_{R_0 \in \mathbf{R}\mathcal{H}_\infty} \left\| \Upsilon \left(\begin{bmatrix} 0 \\ \sqrt{\epsilon} I \end{bmatrix} + \frac{1}{\lambda} \Theta_i \Theta_o R_0 \right) \Psi_n \right\|_2^2.$$

We can then break $\tilde{J}_2$ into the following two parts

$$\tilde{J}_2 = \inf_{R_0 \in \mathbf{R}\mathcal{H}_\infty} J_{2a} + J_{2b},$$

in which

$$J_{2a} \triangleq \left\| \left(\Theta_i^{\sim} \begin{bmatrix} 0 \\ \sqrt{\epsilon} I \end{bmatrix} + \frac{1}{\lambda} \Theta_o R_0 \right) \Psi_n \right\|_2^2$$

and

$$J_{2b} \triangleq \left\| (I - \Theta_i \Theta_i^{\sim}) \begin{bmatrix} 0 \\ \sqrt{\epsilon} I \end{bmatrix} \Psi_n \right\|_2^2 .$$

To calculate J_{2a}, we note that

$$\Theta_i^{\sim} = (\Theta_o^{\sim})^{-1} \begin{bmatrix} \sqrt{1-\epsilon} N^{\sim} & -\lambda \sqrt{\epsilon} M_m^{\sim} \end{bmatrix}.$$

Then,

$$J_{2a} = \left\| \left[\lambda\epsilon \left((\Theta_o^{\sim})^{-1} M_m^{\sim} - (\Theta_o^{\sim})^{-1}(\infty) M_m^{\sim}(\infty) \right) + \lambda\epsilon (\Theta_o^{\sim})^{-1}(\infty) M_m^{\sim}(\infty) - \frac{1}{\lambda} \Theta_o R_0 \right] \Psi_n \right\|_2^2$$

where $(\Theta_o^{\sim})^{-1} M_m^{\sim} - (\Theta_o^{\sim})^{-1}(\infty) M_m^{\sim}(\infty) \in \mathcal{H}_2^{\perp}$ and therefore after properly choosing $R_0 \in \mathbf{R}\mathcal{H}_\infty$, we have

$$\inf_{R_0 \in \mathbf{R}\mathcal{H}_\infty} J_{2a} = \left\| \lambda\epsilon \left((\Theta_o^{\sim})^{-1} M_m^{\sim} - (\Theta_o^{\sim})^{-1}(\infty) M_m^{\sim}(\infty) \right) \Psi_n \right\|_2^2 .$$

On the other hand, after some tedious calculation, we have

$$J_{2b} = \left\| \begin{bmatrix} \lambda\epsilon\sqrt{1-\epsilon} N \Theta_o^{-1} (\Theta_o^{\sim})^{-1} M_m^{\sim} \\ \sqrt{\epsilon} \left(I - \lambda^2 \epsilon M_m \Theta_o^{-1} (\Theta_o^{\sim})^{-1} M_m^{\sim} \right) \end{bmatrix} \Psi_n \right\|_2^2 .$$

Use the definition of $\mathcal{H}_2$ norm (2.1) to expand $\tilde{J}_2$ explicitly. Then, to simplify $\tilde{J}_2$, we make use of (A.15) to cancel common terms, which yields

$$\tilde{J}_2 = \frac{1}{2\pi}\int_{-\infty}^{\infty} \mathrm{Trace}\Big\{\Big[\epsilon + \lambda^2\epsilon^2\Big(M_m(\infty)\Theta_o^{-1}(\infty)(\Theta_o^{\sim})^{-1}(\infty)M_m^{\sim}(\infty) - M_m(\infty)\Theta_o^{-1}(\infty)\Theta_o^{-H}M_m^H - M_m\Theta_o^{-1}(\Theta_o^{\sim})^{-1}(\infty)M_m^{\sim}(\infty)\Big)\Big]\Psi_n^2\Big\}\,\mathrm{d}\omega.$$

But from (A.16), we can further simplify the above and obtain the following

$$\tilde{J}_2 = -\frac{\epsilon}{\pi}\int_{-\infty}^{\infty}\sum_{i=1}^{m}\Phi_i\left(\mathrm{Re}\{g_i(\mathrm{j}\omega)\}-1\right)\mathrm{d}\omega.$$

Factorize $g_i(s)$ as

$$g_i(s) = \left(\prod_{j=1}^{N_i}\frac{s-s_j}{s+\bar{s}_j}\right)g_{im}(s) \tag{A.17}$$

where s_j, $1 \le j \le N_i$ are the nonminimum phase zeros of $g_i(s)$ and $g_{im}(s)$ is minimum phase. If we define $G(s) = \lambda^2\epsilon M_m(s)\Theta_o^{-1}(s)\Theta_o^{-T}(\infty)M_m^T(\infty)$, then by definition $G(\infty) = I$ which implies $g_i(\infty) = g_{im}(\infty) = 1$ for $1 \le i \le m$. Thus, we may invoke (A.13) and obtain

$$\begin{aligned}
&\frac{1}{\pi}\int_{-\infty}^{\infty}\Phi_i\left(\mathrm{Re}\{g_i(\mathrm{j}\omega)\}-1\right)\mathrm{d}\omega\\
&= \lim_{s\to\infty} s[g_i(s)-1]\\
&= -\lim_{s\to\infty} s^2 g_i'(s)\\
&= -\lim_{s\to\infty} s^2\sum_{j=1}^{N_i}\left(\frac{s-s_j}{s+\bar{s}_j}\right)' g_{im}(s) - \lim_{s\to\infty}s^2 g_{im}'(s)\\
&= -2\sum_{j=1}^{N_i}s_j + \lim_{s\to\infty}s\log g_{im}(s).
\end{aligned}$$

And due to Lemma A.2, we have

$$\begin{aligned}
\lim_{s\to\infty}s\log g_{im}(s) &= \frac{1}{\pi}\int_{-\infty}^{\infty}\log|g_{im}(\mathrm{j}\omega)|\,\mathrm{d}\omega\\
&= \frac{1}{\pi}\int_{-\infty}^{\infty}\log|g_i(\mathrm{j}\omega)|\,\mathrm{d}\omega.
\end{aligned} \tag{A.18}$$

Therefore,

$$\tilde{J}_2 = 2\epsilon \sum_{i=1}^{m} \Phi_i \left(\sum_{j=1}^{N_i} s_j - \frac{1}{\pi} \int_0^\infty \log |g_i(\mathrm{j}\omega)| \, \mathrm{d}\omega \right).$$

To establish the inequality (4.13b), we need

$$\begin{aligned}
|g_i(\mathrm{j}\omega)| &\leq \bar{\sigma}\left[G(\mathrm{j}\omega)\right] \\
&\leq \lambda^2 \epsilon \bar{\sigma}\left[M_m(\mathrm{j}\omega)\Theta_o^{-1}(\mathrm{j}\omega)\right] \bar{\sigma}\left[\Theta_o^{-T}(\infty) M_m^T(\infty)\right] \\
&= \bar{\lambda}^{\frac{1}{2}} \left(\left[I + \frac{1-\epsilon}{\lambda^2 \epsilon} P_m^H P_m \right]^{-1} \right) \\
&= \frac{1}{\sqrt{1 + \frac{1-\epsilon}{\lambda^2\epsilon} \underline{\sigma}^2[P(\mathrm{j}\omega)]}}.
\end{aligned}$$

The rest of the derivation is then straightforward.

In addition, for SISO systems, $G(s)$ and thus $g(s)$ are scalar minimum phase transfer functions. Specifically,

$$g(s) = \lambda \sqrt{\epsilon} M_m(s) \Theta_o^{-1}(s).$$

It follows that

$$\begin{aligned}
|g(\mathrm{j}\omega)|^2 &= \lambda^2 \epsilon \left| \frac{M_m(\mathrm{j}\omega)}{\Theta_o(\mathrm{j}\omega)} \right| \\
&= \left[1 + \frac{1-\epsilon}{\lambda^2 \epsilon} \left| P(\mathrm{j}\omega) \right|^2 \right]^{-1}.
\end{aligned}$$

We can then apply (A.18) and complete the proof. ■

A.5 Proof of Lemma 4.7

Two preliminary results that are variants of Lemma A.1 and A.2 shall be needed for the derivations of the lemma. The first result can be found in, e.g. [58, p. 50] and [15].

Lemma A.3 *Suppose that $f(s)$ is conjugate symmetric and analytic at $s = \infty$ and in the closed right half plane except for possible singularities s_0 on $\mathbb{C}_0$ that satisfy $\lim_{s \to s_0}(s - s_0)f(s) = 0$. Denote $f(\mathrm{j}\omega) = h_1(\omega) + \mathrm{j}h_2(\omega)$. Then,*

$$f'(0) = \frac{1}{\pi} \int_{-\infty}^{\infty} \frac{h_1(\omega) - h_1(0)}{\omega^2} \, \mathrm{d}\omega. \tag{A.19}$$

An application of Lemma A.3 on $\log f(s)$ implies the following lemma:

Lemma A.4 *Consider a conjugate symmetric function $f(s)$. Suppose it is analytic and has no zeros in the closed right half plane except for possible zeros on $\mathbb{C}_0$. Suppose also that $\log f(s) \in \mathcal{F}$. Then, provided that $f(0) \neq 0$,*

$$\frac{f'(0)}{f(0)} = \frac{1}{\pi} \int_{-\infty}^{\infty} \frac{1}{\omega^2} \log \left| \frac{f(\mathrm{j}\omega)}{f(0)} \right| \mathrm{d}\omega. \tag{A.20}$$

Proof of Lemma 4.7. The entire proof amounts to the calculation of J_1^*. We start with

$$J_1(Q) = \left\| \left(\begin{bmatrix} \sqrt{1-\epsilon} I \\ 0 \end{bmatrix} - \Theta_i \Theta_o Q \right) \Psi_r \right\|_2^2$$

where we applied the inner-outer factorization (4.11). Then, as in the proof of Lemma 4.5, we make use of the unitary matrix Υ and obtain

$$J_1^* = \inf_{Q \in \mathbf{R}\mathcal{H}_\infty} J_{1a} + J_{1b},$$

where

$$J_{1a} \triangleq \left\| \left(\Theta_i^\sim \begin{bmatrix} \sqrt{1-\epsilon} I \\ 0 \end{bmatrix} - \Theta_o Q \right) \Psi_r \right\|_2^2$$

and

$$J_{1b} \triangleq \left\| (I - \Theta_i \Theta_i^\sim) \begin{bmatrix} \sqrt{1-\epsilon} I \\ 0 \end{bmatrix} \Psi_r \right\|_2^2.$$

Following an orthogonal decomposition of J_{1a} in $\mathcal{L}_2$, we may then eliminate the $\mathcal{H}_2$ part by properly choosing Q and have

$$\inf_{Q \in \mathbf{R}\mathcal{H}_\infty} J_{1a} = \left\| (1-\epsilon) \left[(\Theta_o^\sim)^{-1} N^\sim - (\Theta_o^\sim)^{-1}(0) N^\sim(0) \right] \Psi_r \right\|_2^2 .$$

On the other hand, after some involved calculations,

$$J_{1b} = \left\| \begin{bmatrix} \sqrt{1-\epsilon}\left(I - (1-\epsilon) N \Theta_o^{-1} (\Theta_o^\sim)^{-1} N^\sim\right) \\ \lambda(1-\epsilon)\sqrt{\epsilon} M_m \Theta_o^{-1} (\Theta_o^\sim)^{-1} N^\sim \end{bmatrix} \Psi_r \right\|_2^2 .$$

Since the plant P has at least a pole at $s = 0$, the relation (A.15) gives rise to

$$\Theta^T(0)\Theta(0) = (1-\epsilon) N^T(0) N(0). \tag{A.21}$$

The above equation can be used to simplify J_1^*. After a long derivation, we obtain

$$J_1^* = \frac{1-\epsilon}{2\pi} \int_{-\infty}^{\infty} \mathrm{Trace}\Big\{ \Big[2I - (1-\epsilon)\Big(N \Theta_o^{-1} \Theta^{-H}(0) N^H(0) + N(0) \Theta^{-1}(0) \Theta_o^{-H} N^H \Big) \Big] G_r(\mathrm{j}\omega) \Big\} \, \mathrm{d}\omega.$$

It is then straightforward to see that

$$J_1^* = \frac{1-\epsilon}{\pi} \int_{-\infty}^{\infty} \sum_{i=1}^{n} \sigma_{ri}^2 \frac{1 - \mathrm{Re}\{f_i(\mathrm{j}\omega)\}}{\omega^2} \, \mathrm{d}\omega$$

where $f_i(s)$ is defined by (4.14). From (A.21) we know that $f_i(0) = 1$ for $1 \le i \le n$. We may also directly verify that $f_i(s) \in \mathcal{F}$. Then, applying Lemma A.3 gives rise to

$$J_1^* = -(1-\epsilon) \sum_{i=1}^{n} \sigma_{ri}^2 f_i'(0).$$

We may factorize $f_i(s)$ as

$$f_i(s) = \left(\prod_{j=1}^{N_i} \frac{\bar{s}_j (s - s_j)}{s_j (s + \bar{s}_j)} \right) f_{im}(s) \tag{A.22}$$

where s_j, $1 \leq j \leq N_i$ are the nonminimum phase zeros of $f_i(s)$ and $f_{im}(s)$ is minimum phase. In light of the factorization above, we have

$$f_i'(0) = \left.\frac{\mathrm{d}\,\log f_i(s)}{\mathrm{d}\,s}\right|_{s=0} = -2\sum_{j=1}^{N_i}\frac{1}{s_j} + f_{im}'(0).$$

We may apply Lemma A.4 and obtain

$$\begin{aligned} f_{im}'(0) &= \frac{1}{\pi}\int_{-\infty}^{\infty}\frac{\log|f_{im}(\mathrm{j}\omega)|}{\omega^2}\,\mathrm{d}\omega \\ &= \frac{1}{\pi}\int_{-\infty}^{\infty}\frac{\log|f_i(\mathrm{j}\omega)|}{\omega^2}\,\mathrm{d}\omega. \end{aligned}$$

As a result,

$$J_1^* = 2(1-\epsilon)\sum_{i=1}^{n}\sigma_{ri}^2\left(\sum_{j=1}^{N_i}\frac{1}{s_j} - \frac{1}{\pi}\int_0^{\infty}\frac{\log|f_i(\mathrm{j}\omega)|}{\omega^2}\,\mathrm{d}\omega\right).$$

However,

$$\begin{aligned} |f_i(\mathrm{j}\omega)| &\leq (1-\epsilon)\overline{\sigma}\left(N(\mathrm{j}\omega)\Theta_o^{-1}(\mathrm{j}\omega)\Theta_o^{-T}(0)N^T(0)\right) \\ &\leq (1-\epsilon)\overline{\sigma}\left(N(\mathrm{j}\omega)\Theta_o^{-1}(\mathrm{j}\omega)\right)\overline{\sigma}\left((\Theta_o^{-T}(0)N^T(0))\right) \\ &= \sqrt{1-\epsilon}\,\bar{\lambda}^{\frac{1}{2}}\left(\Theta_o^{-H}(\mathrm{j}\omega)N^H(\mathrm{j}\omega)N(\mathrm{j}\omega)\Theta_o^{-1}(\mathrm{j}\omega)\right) \end{aligned}$$

where the last equality follows from (A.21). Then, in light of (A.15), we may further simplify the above as

$$\begin{aligned} |f_i(\mathrm{j}\omega)| &\leq \bar{\lambda}^{\frac{1}{2}}\left(\left[I + \frac{\lambda^2\epsilon}{1-\epsilon}\left(P_m(\mathrm{j}\omega)P_m^H(\mathrm{j}\omega)\right)^{-1}\right]^{-1}\right) \\ &= \frac{1}{\sqrt{1+\frac{\lambda^2\epsilon}{(1-\epsilon)\overline{\sigma}^2(P_m(\mathrm{j}\omega))}}} \end{aligned}$$

which can be used to prove the inequality (4.15b).

For SISO systems, the equality is true since the scalar function

$$f(s) = \sqrt{1-\epsilon}N(\mathrm{j}\omega)\Theta_o^{-1}(\mathrm{j}\omega)$$

is minimum phase. ■

A.6 Proof of Theorem 5.2

Proof. To solve (5.3), we form the Lagrangian

$$H(k, \lambda, \epsilon) = (1-\epsilon)\mathcal{E}\{u_1^2\} + \epsilon(\mathcal{E}\{u_2^2\} - \Gamma_2) \tag{A.23}$$

with $0 \le \epsilon \le 1$. Plugging (5.2) in H, we obtain

$$H(k, \lambda, \epsilon) = \frac{\left[(1-\epsilon) + \frac{\epsilon}{\lambda}\left(1-\alpha^2-2\alpha k\right)\right] k^2 \Phi_1}{1-(\alpha+k)^2} + \frac{(1-\epsilon)\lambda\Phi_2 + \epsilon k^2 \Phi_2}{1-(\alpha+k)^2} - \epsilon\Gamma_2.$$

It is straightforward to see that for fixed k and ϵ, the optimal λ that minimizes H satisfies

$$\lambda^* = \frac{\sqrt{\epsilon\left(1-\alpha^2-2\alpha k\right) k^2 \Phi_1}}{\sqrt{\Phi_2(1-\epsilon)}}.$$

It follows that

$$H(k, \lambda^*, \epsilon) = \frac{2\sqrt{\epsilon(1-\epsilon)\left(1-\alpha^2-2\alpha k\right) k^2 \Phi_1 \Phi_2}}{1-(\alpha+k)^2} + \frac{k^2\left((1-\epsilon)\Phi_1 + \epsilon\Phi_2\right)}{1-(\alpha+k)^2} - \epsilon\Gamma_2.$$

The next step is to find the optimal controller k. To this end, we calculate the partial derivative of $H(k, \lambda^*, \epsilon)$ with respect to k as

$$\frac{\partial H(k, \lambda^*, \epsilon)}{\partial k} = \frac{2k(1-\alpha^2-\alpha k)}{(1-(\alpha+k)^2)^2} f(k) \triangleq g(k) \tag{A.24}$$

where

$$f(k) \triangleq -\epsilon\left(1 - \frac{\sqrt{\Phi_2(1-\epsilon)}\left(1-\alpha^2-2\alpha k+k^2\right)}{\sqrt{\Phi_1\epsilon}\sqrt{\left(1-\alpha^2-2\alpha k\right)k^2}}\right)\Phi_1 + \Phi_1 + \epsilon\Phi_2.$$

It is easy to verify that, for $\forall\, k$ that satisfies $(\alpha+k)^2 < 1$, we have $f(k) > 0$. Then, $k^* = 1/\alpha - \alpha$ is the only solution of $g(k) = 0$ that stabilizes the system. Moreover, after some tedious calculation, we can show that

$$\frac{\partial^2 H(k, \lambda^*, \epsilon)}{\partial k^2}\Big|_{k=1/\alpha-\alpha} > 0,$$

which then implies that k^* is indeed the optimal state feedback gain. The last step is to find the optimal Lagrange multiplier.

Define the multiplier $\theta = \epsilon/(1-\epsilon)$, and

$$\begin{aligned}\varphi(\theta) &= \frac{H(k^*, \lambda^*, \epsilon)}{1-\epsilon} \\ &= (\alpha^2 - 1)\Phi_1 + (\alpha^2 - 1)\Phi_2\theta + 2\alpha\sqrt{(\alpha^2 - 1)\Phi_1\Phi_2\theta} - \theta\Gamma_2.\end{aligned}$$

Because of the convexity, and from Theorem 2.19, the optimization problem (5.3) can be solved by $\max \varphi(\theta)$. Taking the derivative on $\varphi(\theta)$, we have

$$\frac{\mathrm{d}\,\varphi(\theta)}{\mathrm{d}\theta} = (\alpha^2 - 1)\Phi_2 - \Gamma_2 + \frac{\alpha\sqrt{(\alpha^2 - 1)\Phi_1\Phi_2}}{\sqrt{\theta}}.$$

It is a monotonically decreasing function and it implies that a necessary condition on Γ_2 for stabilizability is

$$\Gamma_2 > \left(\alpha^2 - 1\right)\Phi_2 \tag{A.25}$$

since otherwise $\max \varphi(\theta) \to \infty$. Under this condition, the optimal θ is

$$\theta^* = \frac{\alpha^2(\alpha^2 - 1)\Phi_1\Phi_2}{(\Gamma_2 - (\alpha^2 - 1)\Phi_2)^2},$$

and thus the lower bound for stabilizability on the input power of uplink channel is

$$\mathcal{E}\{u_1^2\}^* = \frac{(\alpha^2 - 1)\Phi_1(\Gamma_2 + \Phi_2)}{\Gamma_2 - (\alpha^2 - 1)\Phi_2},$$

and the proof is complete. ■

A.7 Proof of Theorem 5.5

Proof. We shall need the factorization (cf. Section 2.3.5)

$$M(s) = B(s)M_m(s),$$

where $M_m(s)$ is minimum phase, and $B(s)$ is all-pass.

Define

$$J^*(\epsilon,\lambda) \triangleq \inf_{Q\in RH_\infty} J(Q,\epsilon,\lambda).$$

Introduce two inner-outer factorizations (cf. Section 2.3.6)

$$\begin{bmatrix} \sqrt{\epsilon}M_m \\ \frac{\sqrt{1-\epsilon}}{\lambda}N \end{bmatrix} = \Theta_i\Theta_o$$

and

$$\begin{bmatrix} \lambda\sqrt{\Phi_2}M_m \\ \sqrt{\Phi_1}N \end{bmatrix} = \Delta_i\Delta_o. \tag{A.26}$$

The optimization of J over Q can be separated into two parts: define

$$\begin{aligned} H_1 &\triangleq \left(\epsilon\lambda^2 \left\|(Y-MQ)M\right\|_2^2 + (1-\epsilon)\left\|(Y-MQ)N\right\|_2^2\right)\Phi_1, \\ H_2 &\triangleq \left(\epsilon\left\|(Y-MQ)N\right\|_2^2 + \frac{(1-\epsilon)}{\lambda^2}\left\|(X-NQ)N\right\|_2^2\right)\Phi_2. \end{aligned}$$

In the following derivations, we need the partial fraction expansions

$$B^{-1}YN = -(B^{-1}-1) - 1 + M_mX$$

and

$$B^{-1}YM_m = -(B^{-1}-1)\frac{M_m(p)}{N(p)} - \frac{M_m(p)}{N(p)} + R_m$$

in which $-M_m(p)/N(p) + R_m \in \mathbf{R}\mathcal{H}_\infty$. We can then transform H_1 to

$$\frac{H_1}{\Phi_1} = \left(\epsilon\lambda^2\left(\frac{M_m(p)}{N(p)}\right)^2 + 1 - \epsilon\right)\left\|B^{-1}-1\right\|_2^2 + \left\|A_1 + \begin{bmatrix} \sqrt{\epsilon}\lambda M_m \\ \sqrt{1-\epsilon}N \end{bmatrix} QN\right\|_2^2$$

where

$$A_1 = \begin{bmatrix} \sqrt{\epsilon}\lambda\left(\frac{M_m(p)}{N(p)} - R_m\right) \\ \sqrt{1-\epsilon}\,(1-M_mX) \end{bmatrix}.$$

With aid of the inner-outer factorization[1], the second term can be expressed as

$$\|(I - \Theta_i \Theta_i^{\sim})\, A_1\|_2^2 + \|\Theta_i^{\sim} A_1 + \lambda \Theta_o Q M_m\|_2^2 .$$

Following a similar procedure, we have

$$\frac{H_2}{\Phi_2} = \epsilon \left\|B^{-1} - 1\right\|_2^2 + \|(I - \Theta_i \Theta_i^{\sim})\, A_2\|_2^2 + \|\Theta_i^{\sim} A_2 + \Theta_o Q N\|_2^2$$

where

$$A_2 = \begin{bmatrix} \sqrt{\epsilon}\,(1 - M_m X) \\ -\frac{\sqrt{1-\epsilon}}{\lambda} N X \end{bmatrix} .$$

To proceed, we decompose $\Theta_i^{\sim} A_1$ and $\Theta_i^{\sim} A_2$ into parts in $\mathcal{H}_2$ and $\mathcal{H}_2^{\perp}$, respectively. Then we add the remaining two parts involving Q, make use of the factorization (A.26) and follow Section 2.3.7. In the end, we obtain the following expression[2] for J^*

$$J^*(\epsilon, \lambda) = J_1 + J_2 + J_3 \tag{A.27}$$

where

$$J_1 = \epsilon \left(\left\|B^{-1} - 1\right\|_2^2 + \frac{1}{\pi} \int_{-\infty}^{\infty} \left(1 - \sqrt{\epsilon} \mathrm{Re}\left(\frac{M_m(j\omega)}{\Theta_o(j\omega)}\right)\right) \mathrm{d}\omega \right) \Phi_2,$$

$$\begin{aligned} J_2 = \Bigg[& \left(\epsilon \lambda^2 \left(\frac{M_m(p)}{N(p)}\right)^2 + 1 - \epsilon\right) \left\|B^{-1} - 1\right\|_2^2 \\ & + \lambda^2 \left\| \left((\Theta_o^{\sim})^{-1} \left(\epsilon M_m^{\sim} \frac{M_m(p)}{N(p)} + \frac{1-\epsilon}{\lambda^2} N^{\sim} \right) - \frac{\Theta_o(p)}{N(p)} \right) (B^{-1} - 1) \right\|_2^2 \\ & + \epsilon(1-\epsilon) \left\| \Theta_o^{-1} \left(M_m - N \frac{M_m(p)}{N(p)} \right) (B^{-1} - 1) \right\|_2^2 \Bigg] \Phi_1, \end{aligned}$$

[1]See Section 2.3.7

[2]the details of this lengthy derivation are omitted.

and

$$J_3 = \lambda^2 \Phi_1 \Phi_2 \left\| \Delta_o^{-1} \left(M_m \left(\Theta_o M^{-1} - \sqrt{\epsilon} \right) - N \left(B^{-1} - 1 \right) \frac{\Theta_o(p)}{N(p)} \right) \right\|_2^2$$

$$+ \left\| (\Delta_o^{\sim})^{-1} \left(\lambda^2 \Phi_1 M_m^{\sim} \frac{\Theta_o(p)}{N(p)} \left(B^{-1} - 1 \right) + \Phi_2 N^{\sim} \left(\Theta_o M^{-1} - \sqrt{\epsilon} \right) \right) - \left(B^{-1} - 1 \right) \frac{\Delta_o(p)\Theta_o(p)}{M_m(p)N(p)} \right\|_2^2 .$$

The fundamental bound on the channel input power over any LTI controllers is given by

$$\Gamma_1 > \inf_{\lambda, Q \in \mathbf{R}\mathcal{H}_\infty} \mathcal{E}\{u_1^2\} = \inf_{\lambda>0} \sup_{\epsilon>0} \frac{1}{1-\epsilon} J^*(\epsilon, \lambda),$$

where the equality holds according to Theorem 2.19.

As the system equation is (5.6), the transfer function is given by $P(s) = 1/(s-p)$. The coprime factorization of the plant yields

$$N = \frac{1}{s+1}, \qquad M = \frac{s-p}{s+1}, \qquad B = \frac{s-p}{s+p}, \qquad M_m = \frac{s+p}{s+1}.$$

The inner outer factorizations are given by

$$\Theta_o = \sqrt{\epsilon} \frac{s + \sqrt{p^2 + \frac{1-\epsilon}{\lambda^2 \epsilon}}}{s+1},$$

and

$$\Delta_o = \lambda \sqrt{\Phi_1} \frac{s + \sqrt{p^2 + \frac{\Phi_2}{\lambda^2 \Phi_1}}}{s+1}.$$

After a cumbersome calculations, we have

$$\begin{aligned} J_\theta(\theta, \lambda) &\triangleq \frac{1}{1-\epsilon} J^*(\epsilon, \lambda) \\ &= \left(p + \sqrt{p^2 + \frac{\Phi_2}{\lambda^2 \Phi_1}} \right) \Phi_1 \\ &\quad + \theta \left(p + \sqrt{p^2 + \frac{1}{\theta \lambda^2}} \right) \left(\Phi_2 + 2p\lambda^2 \left(p + \sqrt{p^2 + \frac{\Phi_2}{\lambda^2 \Phi_1}} \right) \Phi_1 \right) - \theta \Gamma_2 \end{aligned}$$

where $\theta \triangleq \frac{\epsilon}{1-\epsilon}$.

Setting the derivative of J_θ with respect to θ to 0, we obtain the optimal Lagrangian multiplier as

$$\theta^* = \frac{1}{2p^2\lambda^2}\left(\frac{l}{\sqrt{l^2-p^2}}-1\right)$$

where

$$l = \frac{\Gamma_2}{\Phi_2 + 2p\lambda^2\left(p+\sqrt{p^2+\frac{\Phi_2}{\lambda^2 Phi_1}}\right)\Phi_1} - p.$$

Further simplifications yield the optimum as

$$J_\theta^*(\lambda) = \frac{1}{2p\lambda^2}\left(\Gamma_2 - p\Phi_2 - \sqrt{\Gamma_2\left(\Gamma_2 - 2p\left(\Phi_2 + 2p\lambda^2\left(p+\sqrt{p^2+\frac{\Phi_2}{\lambda^2\Phi_1}}\right)\Phi_1\right)\right)}\right).$$

The final step is to search for the optimal scaling factor λ. In fact, using the same elementary calculus argument, we have

$$\inf_{\lambda>0} J_\theta^*(\lambda) = \frac{p}{2}\left(\frac{2\sqrt{\frac{\Gamma_2}{\Phi_2}}-\sqrt{2p}}{\sqrt{\frac{\Gamma_2}{\Phi_2}}-\sqrt{2p}}\right)^2$$

when the scaling factor is

$$\lambda^* = \frac{\sqrt{2\Phi_2\Gamma_2}}{4p^2}\frac{\left(\frac{1}{\sqrt{p}}-\sqrt{\frac{2\Phi_2}{\Gamma_2}}\right)^2}{\frac{1}{\sqrt{p}}-\sqrt{\frac{\Phi_2}{2\Gamma_2}}}$$

and the proof is complete. ■

A.8 Proof of Theorem 5.6

Proof. The proof is similar to Appendix A.7. As (A.27), the Lagrangian optimized over all stabilizing two-parameter controllers Q_0 and R yields

$$J^*(\epsilon, \lambda) = J_1 + J_2.$$

Thus, the cross term J_3 is eliminated by the use of the additional controller parameter. We can then obtain

$$J^*(\epsilon, \lambda) = \epsilon \left(p + \sqrt{p^2 + \frac{1-\epsilon}{\epsilon\lambda^2}} \right) \Phi_2 + 2p \left(1 + \epsilon \left(-1 + 2p \left(p + \sqrt{p^2 + \frac{1-\epsilon}{\epsilon\lambda^2}} \right) \lambda^2 \right) \right) \Phi_1 - \epsilon\Gamma_2.$$

The optimal Lagrange multiplier θ is

$$\theta^* = \frac{1}{2p^2\lambda^2} \left(\frac{r}{\sqrt{r^2 - p^2}} - 1 \right)$$

where

$$r = \frac{\Gamma_2}{\Phi_2 + 4p^2\lambda^2\Phi_1} - p.$$

Therefore, we have

$$J^*_\theta(\lambda) = \Gamma_2 - p\Phi_2 + \sqrt{\Gamma_2 \left(\Gamma_2 - 2p\Phi_2 - 8p^3\lambda^2\Phi_1\right)}.$$

The optimization over the scaling factor λ gives rise to (5.10) when

$$\lambda^* = \frac{\Gamma_1\Phi_2 - 2p\Phi_2^2}{4\Gamma_2 p^2 \Phi_1}.$$

■